Addis Ababa University

Addis Ababa Institute of Technology

School of Civil and Environmental Engineering

Evaluation of the Impact of Land Use/Land Cover Changes on Flood Hazard and Risk Prone Areas Using Multicriteria Decision Making Techniques: The Case of Akaki Watershed, Ethiopia

By

Seid Ali Shifaw

Feburary, 2021

Addis Ababa, Ethiopia

Addis Ababa University

Addis Ababa Institute of Technology

School of Civil and Environmental Engineering

A thesis submitted to

School of Civil and Environmental Engineering in partial fulfillment of the

Requirements for the Degree of Master of Science in Geodesy and Geomatics,

Specialization in Geomatics Engineering

Feburary, 2021

Addis Ababa, Ethiopia

The undersigned have examined the thesis entitled Evaluation of the impact of Land Use Land /Cover Changes on Flood Hazard and Risk Prone Areas Using Multicriteria Decision Making Technique: The Case of Akaki Watershed, Ethiopia presented by **Seid Ali.** A candidate for the degree of **Master of Science in Geodesy and Geomatics program** and hereby certifies that it is worthy of acceptance.

Dr. Berhan Gessesse	_____	_____
Advisor	Signature	Date
Dr. Worku Zewude	_____	_____
Internal Examiner	Signature	Date
Dr. Tulu Busha Bedada	_____	_____
External Examiner	Signature	Date
Mebruk Mohammed (Dr-Ing)	_____	_____
Chairperson	Signature	Date

Undertaking

I certify that research work titled Evaluation of the Impact of Land Use/Land Cover Changes on Flood Hazard and Risk Prone Areas Using Multicriteria Decision techniques: The Case of Akaki Watershed, Ethiopia is my work. The work has not been presented elsewhere for assessment. Where material has been used from other sources it has been properly acknowledged/referred.

_____

Seid Ali

Acknowledgments

I would like to express my enormous gratitude to *almighty Allah.* No success would have been achieved without his grace and mercy. It is my great pleasure to thank all the individuals and organizations that supported me during this study. First and foremost, I would like to express my sincere gratitude to *Dr. Berhan Gessese,* my supervisor, for his excellent guidance, supervision, and invaluable suggestions, and critical comment on this thesis. He has taught me the methodology to carry out the research and to present the research works as clearly as possible. I would like to thank the Ethiopian governmental institutions such as the Ministry of Water, Irrigation, and Electricity; the National Metrological Agency, and the Central Statistical Agency for their support concerning the data required for the present study. Last but not the least, I would like to thanks and give my appreciation to all of my parents and my friends who were supporting and motivating me in the achievement of this study. Special thanks to my friend Mohamed Melese Hussein he supported me throughout the study period.

Table of Contents

List of Tables

List of Figures

Abbreviation and Acronyms

AHP	Analytic Hierarchy Process
AL	Radiance Additive Scaling Factor for The Band
ALOS	The Advanced Land Observing Satellite
AMC	Antecedent Moisture Condition
$A\rho$	Reflectance Additive Scaling for The Band
CHIRPS	Climate Hazards Center Infrared Precipitation with Station Data
CI	Consistency Index
CN	Curve Number
CR	Consistency Ratio
DEM	Digital Elevation Model
DN	Digital Number
ESUN	Mean Solar Exoatmospheric Irradiance
ETM^+	Enhanced Thematic Mapper
HSG	Hydrological Soil Group
LULC	Land use/land cover
$L\lambda$	Spectral Radiance
MCDM	Multiple-Criteria Decision-Making
ML	Radiance Multiplicative Scaling Factor for The Band
$M\rho$	Reflectance Multiplicative Scaling Factor for The Band
NEH-4	National Engineering Handbook
NMA	National Meteorological Agency
OLI	Operational Land Imagery
P	The Depth of The Precipitation
Q	Depth of Direct Runoff
QGIS	Quantum Geographic Information System
RI	Random Index
S	Maximum Potential Retention
TM	Thematic Mapper
TOA	Top of The Atmosphere
TWI	Topographic Wetness Index
USDA	United States Department of Agriculture
Θ	Solar Angle

Abstract

The change in land use/land cover leads to a wide range of environmental impacts and degradation such as flooding, landslide, peak runoff, climate change, and loss of biodiversity around the world. The overall objective of the present study was evaluation of the impact of spatial and temporal variation of land use/land cover change on flood hazard and risk prone area of the Akaki Watershed using multicriteria decision making techniques. To achieve the objective of this study different flood hazard and risk causative factors were used such as elevation, slope, rainfall, drainage density, soil type, surface runoff and topographic wetness index (TWI) were integrated with different land use scenario in Analytical hierarchical process (AHP). Furthermore, the LULC change had been computed using post classification methods and the surface runoff also estimated using the SCS CN method for the three-land use scenario. As the result of the LULC revealed that urbanization was significantly increased. Consequently, the agricultural and forest-land was decreased, whereas the waterbodies were increased from 1988 to 2003 and then decreased from 2003 to 2018. Due to the expansion of built environment and the decline of forestland, the amount of surface runoff increased throughout the study period. in which the runoff increases in the LULC of 2003 from the LULC of 1988 by 17.27mm and the runoff increases in the LULC of 2018 from the LULC of 2003 by 24.85mm. Besides of this the flood hazard, risk and Vulnerability also increased throughout the study period in each land use scenario such as in the land use of 1988 the flood hazard level were estimated to 29.68, 274.53, 961.25 ,513.16, 8.92 km^2 in the land use of 1988, 24.83,274.81, 915.62,562.63,9.65 km^2 in the land use of 2003 and 17.12, 233.28, 698.21, 827.38, 11.56 km^2.Which is subjected to Very low, low, moderate, high and very high respectively. and the flood risk also estimated to 481.68, 532.81 km^2 which is subjected to high and very high, 786.83, 39.30 which is subjected to high and very high, and 40.87, 43.87 km^2 also subjected to high to very high in the LULC of 1988, 2003 and 2018 respectively. The major findings of the present study revealed that the agricultural land and the built-up area were the most affected by flood hazard land-use class and the downstream of the present study was highly affected by flood hazard and near riverside and high populated areas of the watershed were faced with flood risk. To reduce the effect of flood hazard and risk proper land use management, afforestation, relocation of a house near riverside plays a significant role, specifically for the downstream or the low -lying flood hazard zone.

Keywords: *Flood hazard, Flood risk, Vulnerability, LULC, Runoff, CN, Multicriteria analysis*

CHAPTER 1: INTRODUCTION

1.1 Background of the Study

The terms Land use/Land cover are not synonymous and they have a different meaning, Land cover refers to the spatial distribution of soil, water, vegetation, and anthropogenic activities on the surface of the Earth, or it is the observed bio-physical cover on the earth surface whereas land use refers to the way humans manage or modify land to use it (Prasad and Ramesh, 2019). Another researcher also defines the term land cover as land cover refers to the type of feature which is present on the surface of the earth such as Forest, lakes, soil, While land use refers to the human activity associated with a specific piece of land (Thapa and Murayama, 2011). The land use/land cover has been used to drive different biophysical parameters such as vegetation index, biomass, and carbon content (Lam, 2008).

LULC change is the modification of the earth's terrestrial surface through human activity such as deforestation, overgrazing, and urban expansion. The change in land use/land cover encompasses the greatest environmental change at the local. regional and global scale, it causes global warming, climate change, biodiversity loss, increase the amount of surface runoff cause flooding pollution of water, soil, and air (Ellis, 2007). Many factors drive the change in land use/land covers such as, the rapid expansion of cultivated land, and settlements, population growth, and deforestation is the main driving force of the change in land use/land cover (Kindu *et al.*, 2015). The change in land use/land cover (LULCC) is among the major factors that affect environmental degradation such as the productivity of land, biodiversity, land degradation, hydrological cycle, and environmental conditions (Betru *et al.*, 2019).

Generally, the change in land use /land cover resulted from a wide range of environmental impacts or degradation such as flooding, landslide, climate change, and biodiversity loss across the globe. Among these impacts increase in the amount of surface runoff and flooding was the major concern of the present study. Runoff is the flowing of precipitated water in the catchment area through a channel after satisfying all surface and sub-surface losses (Ningaraju, B and Surendra, 2016).

Several studies show that surface runoff can be estimated through the GIS and SCS CN method and it can be estimated using different input parameters such as hydrological soil group, *LULC, precipitation, CN lookup table, and the weighted curve* number(Gebresamuel, Singh and Dick, 2010; Laura, Keri, and Rusu, 2011; Nagarajan and Poongothai, 2012; Williams *et al.*, 2012; R. Viji, P. Rajesh Prasanna, 2015; Ningaraju, B and Surendra, 2016; Kannan, 2017; Pani and Chakrabarty, 2017).

Among all-natural hazards such as landslide, floods drought, and earthquake. Floods are the most common natural hazard that occurs all over the world including Ethiopia. It causes damage and destruction. It kills thousands of lives and destructs properties costing billions birr. According to FDRE National Disaster Risk Management, Flood Alert # 3, (2019) 20% of the total death of life and 33% of destruction in terms of global economic loss is accounted for flood as compared to another natural disaster. Generally, there are four types of floods such as riverine flood, coastal flood, urban flood, and flash flood. Among all types of flooding, Ethiopia experienced two types of floods such as the flash flood and riverine flood. Flash floods are the worst kinds of flood hazard, which is characterized by small scale, excess rainfall, heavy peak discharge and it is unpredictable and fastest flood types (Ali, Bajracharyar and Raut, 2017).

The flood hazard mapping can be obtained using GIS and remote sensing through the integration of different factors such as hydrological, topographical, ecological, and environmental in multicriteria decision-making techniques. Flood hazard mapping can be mapped using different thematic layers such as absolute height, slope, landform, river buffer, rainfall, and confluence buffer through the analytical hierarchical process (AHP)(Ghosh and Kar, 2018).

Flood vulnerability mapping can be mapped using various vulnerability indexes such as population density, land use, road network density, distance to flood shelter, and distance to hospital in analytical hierarchical process and spatial multicriteria analysis(Chakraborty and Mukhopadhyay, 2019). Similarly, flood vulnerability can be mapped using different parameters such as population density, urban structure, and drainage density(Danumah *et al.*, 2016).

The final flood risk mapping is the product of flood hazard and flood vulnerability, the vulnerability index such as population, roads, and infrastructure or other civil engineering works (Ouma and Tateishi, 2014). According to (Klijn *et al.*, 2015), flood risk mapping is the product of the probability of flooding and the consequence of flooding or it is the product of flood hazard and flood vulnerability.

According to the report of FDRE National Disaster Risk Management Commission, (2006) Ethiopia is both a highland/mountainous and lowland country and divided into nine major river basins and 12 lakes. The Abay, Baro Akobo, Tekeze, Mereb, Awash river basin, the Omo, and the Shebelle River basin. Due to the topography of the country, the drainage system originates from centrally situated highlands and flows to the lowlands (Bishaw, 2012). Flood plains are a vital part of the river or stream ecosystem. They are important because, they act as flood buffers, water filters, and are major centers of biological life in the river or stream ecosystem(Ejenma, and E.Sunday, 2014).

. The rate, pattern, and magnitude of land use/land cover change were determined after performing post-classification and surface runoff was computed using the SCS CN method. Finally, the flood hazard and risk of the Akaki Watershed were evaluated by using multicriteria decision-making techniques based on the different factors that govern flood hazards such as elevation, slope, precipitation, land use, soil type, surface runoff, TWI, and drainage density. Therefore, this study is an attempt to contribute to a better understanding of the pattern of the spatial and temporal variation of land use and land cover change, runoff change, flood hazard, and risk in the Akaki Watershed.

This study aims to evaluate the impact of LULC Changes on flood hazards and risk-prone areas using multicriteria decision-making techniques. The rapid urbanization of Addis Ababa city and the surrounding LULC change of the Study area plays the increase in impervious surface leads to an increase in the amount of surface runoff and flooding.

1.2 Statement of the problem

The change in LULC leads to a wide range of environmental impacts/ degradation such as flooding, landslide, peak runoff climate change, and loss of biodiversity around the world. The change in LULC is caused by different factors such as the rapid expansion of urbanization, expansion of diversified agricultural activities, wood extraction infrastructure extension are clusters of direct causes of LULC changes(Gessesse and Bewket, 2014). The LULC change associated with human activities may change the hydrological processes and increase flood hazards and risks(Zhang, Ma, and Wang, 2008). The flood hazard is the most destructive natural hazard affecting the social, economic, and ecological aspects of the world, it claims more lives than any other natural hazard (Rosser, Leibovici, and Jackson, 2017). According to the UN report (2016), around 117 million people around the world are affected by natural disasters per year. Flooding shows an increasing trend around the world, especially in developing countries due to climate change, rapid urbanization, excess rainfall, deforestation, and the existence of some closed drainage systems. According to WHO (August 2018), reports more than 2 billion people worldwide from 1998-2017 were affected by flood.

In Ethiopia, the flood hazard is frequently occurred in many parts of the country, mainly in the low-lying area of the watershed and near the riverside. The most common flood hazard in Ethiopia was caused by a rapid and excessive amount of rainfall that rises the amount of water, rivers, streams, and channels. According to the report of the flash flood appeal, (2006) flood Disaster in Ethiopia, about 517, 400 people were vulnerable to flooding from the total population,19,9900 were affected and 639 were dead. Several flood incidences have been already reported in Oromia, Afar, SNNP and Somali regions since 15 April 2018, displacing thousands and causing loss of property and livelihoods. In the rainy season, the Akaki Watershed also flooded (National Meteorology Agency (NMA), 2018). The Akaki Watershed is one of the most environmentally affected areas in the Awash River basin. In which the Addis Ababa city is located at the center of the watershed, due to a large number of populations the Addis Ababa city experienced rapid urbanization in history and environmentally affected.

The change in LULC could alert the amount of peak runoff as well as flood hazard and risk zone, as regards of these the rapid urbanization and deforestation are the main causes of the increase in peak runoff and decline of infiltration rate. Furthermore, the change in LULC could affect the flood hazard and risk. The Akaki Watershed has experienced rapid LULC change that could cause flooding, peak runoff, and loss of environmental services. Some studies were conducted on LULC dynamics, surface runoff, and flood hazard and risk in the Akaki Watershed and Addis Ababa city(Birhanu *et al.*, 2016; Worako, 2016; Desta, Goitom and Aregay, 2019; Shawul and Chakma, 2019; Zeberie, 2019). However, a study on the impact of land use/land cover changes on flood hazard and risk using multicriteria decision-making techniques is not yet conducted at the Akaki Watershed. Therefore, evaluating the impact of land use/land cover change on flood hazard and risk-prone area, as well as the pattern, rate, and magnitude of land-use change using remote sensing data and multicriteria decision-making techniques through a scientific approach is necessary to conduct a better solution.

1.3 Objectives

1.3.1 General Objective

The general objective of the study was to evaluate the impact LULC change on flood hazards and risk-prone areas in the case of Akaki Watershed using Multi-criteria decision-making techniques.

1.3.2 Specific Objectives

- ✓ To evaluate the spatial and temporal variation of the LULC change of the study area between 1988 and 2018.
- ✓ To evaluate the impact of LULC change on surface runoff and flooding in the study area.
- ✓ To investigate and map the flood hazard, flood risk, and flood vulnerability hotspot sites in the Study area.

1.4 Research Questions

To achieve the stated problem and objectives, the study attempted to answer the following scientific questions:

- ✓ Which LULC class is highly changed since 1988?
- ✓ What is the impact of LULC change over the surface runoff and flooding in the Akaki Watershed? and
- ✓ Which area of the watershed is affected by flood hazards and what percentage of the area is highly affected?

1.5 Significance of the Study

The study on evaluation of the impact of LULC change on flood hazard and risk-prone area has a significant role for researchers, Addis Ababa City Fire Emergency Prevention and Rescue Agency, Addis Ababa city environmental protection authority (AAEPA), and for the national metrological Agency (NMA). The significance of the present study for the researcher will be used as Literature and will have a better understanding of the way of flood zonation, computation of runoff based on the SCS curve number models, and Evaluation of LULC change and its impact on surface runoff. For Addis Ababa City Fire, Emergency Prevention and Rescue Agency, Addis Ababa city environmental protection authority (AAEPA) and the national metrological agency will help them as an input to have an overview of the spatial location of flood hot spot site.

1.6 Scope of the Study

This research covers the Akaki Watershed with a total area of 1787.5 sq. km. Moreover, the study evaluates the impact of LULC change on flood hazard and risk using multicriteria decision-making techniques. The study uses the AHP methods with pairwise comparison, and factors of flooding such as slope, elevation, drainage density, rainfall, TWI, runoff, soil type, and LULC of the Akaki Watershed. Also, it mainly covers the computation and mapping of CN and runoff, assessment of LULC change, and its impact on surface runoff and flooding in the Akaki Watershed.

1.7 Limitation of the study

The limitation of the present study was the lack of evenly distributed ground rain gage stations data in the study area and the unavailability of those data. In the study area, there is a large number of missing precipitation data. Due to such a problem, the researcher was adopted to use satellite precipitation data. The precipitation data, which is used to compensate for the limitation was Chirps v2.0 satellite estimate precipitation (CHIRPS V2.0). Which have a spatial resolution of 5km*5km (0.05 degree*0.05 degree).

1.8 Thesis Organization

The present thesis is organized into five (5) chapters, which are stated as follows. Chapter 1 contains the background of the study and provides a brief overview of the overall study undertaken. It also provides information on the study and gives a highlight of the significance of the study as well as the goals and scope of the study. Chapter 2 emphasizes the historical background of land use/land cover change, runoff, flood hazard, and risk and also states the application of the multicriteria decision-making techniques. the third chapter deals with the material and method, the data source, and the data used in the present study, and the fourth chapter describes the data analysis, result, and discussion. The last chapter i.e., chapter five contains the conclusion, recommendation, and suggestion for feature works for the researcher.

CHAPTER 2 : LITERATURE REVIEW

2.1 Introduction

2.2 Land use/land cover Change

The term land use and land cover change (LULCC) identifies all kinds of human modification of the Earth's surface (Jokar Arsanjani, 2012). Land cover refers to the spatial distribution of soil, water, vegetation. Whereas land use refers to the means humans manage or modify land to use it (Prasad and Ramesh, 2019). Another researcher also defines the term land cover as follows land cover refers to the type of feature which is present on the surface of the earth such as Forest, lakes, soil, While land use refers to the human activity associated with a specific piece of land (Thapa and Murayama, 2011). The LULC has been used to drive different biophysical parameters such as the Vegetation index, biomass, and carbon content (Lam, 2008). The LULC change is a dynamic and complex process that can be caused by different factors of the interacting process such as deforestation, urbanization, and socioeconomic dynamics (Humagain, 2012; Prasad and Ramesh, 2019). Changes in land use range from the modification of the landscape to extreme cases, modification refers to anthropogenic i.e. deforestation for agricultural expansion it causes flooding, wildfire, disease, and epidemics (Nicole molders, 2012). The land cover is affected by the local weather and depends on the local climate. Consequently, the land cover may change naturally in response to extreme weather conditions which causes wildfires, flooding, drought, and land cover change in response to climate change causes sea-level rise, volcanic eruption earthquake, and landslide (Nicole molders, 2012). The previous study conducted in the Akaki Watershed shows the land use/land cover had been classified into four major groups of land use namely water bodies, forest land, built up and agricultural land, as the result revealed that the built-up area raised from 25.71% in 1985 to 31.51% in 2015 with the expense of agricultural land reduction from 64.27% in 1985 to 56.28% in 2015 as the study indicates there is a rapid expansion of built-up area and reduction of agricultural land ,the expansion rate of urbanization has great impact on the socio-economic conditions of the surrounding semi-urban community (Worako, 2016).

2.2.1 Image Classification Techniques

Image classification is important for the generation of thematic maps from remotely sensed images. The generated maps represent different objects on the Earth's surface like vegetation, buildings, and roads. Different satellite sensor produces different quality images. Accuracy of classification depends on satellite image quality (Jog and Dixit, 2016). There are different principles of image classification techniques such as pattern recognition principles, Artificial Neural Networks principles, super vector machine, Methods based on Fuzzy Set theory, and Decision Trees principles (Mather and Tso, 2010). However there two broad types of image classification methods such as supervised image classification, and unsupervised image classification methods. For the present study, the supervised image classification method was used in image classification techniques.

2.3 Drivers of Land use/land cover Change

Understanding the driving force of LULC change is important for future dynamics and development of management policies (Kindu *et al.*, 2015). The land use/land cover change generated by different factors such as social, economic, environmental, institutional, and technological factors, more specifically the driving force of the LULC change is expansion of cultivated lands and settlements, population growth, the expansion of diversified agriculture, and cutting of woody species for fuelwood, , LULC conversion, soil erosion, landslides, and natural fires factors are a major cause of land use/land cover changes (Gessesse and Bewket, 2014; Kindu *et al.*, 2015). LULC can occur through the direct and indirect consequences of human activities to secure essential resources (Jokar Arsanjani, 2012). The LULC change may result in loss of biodiversity, climate change, Pollution (Jokar Arsanjani, 2012). The change in LULC plays a significant role in climate change on a different scale such as regional scale, local scale, and global scale(Jokar Arsanjani, 2012). On a global scale, the LULC change is accountable for the releasing of greenhouse gases into the atmosphere resulted in global warming, and the land use/land cover plays a significant role in Pollution such as air pollution, water pollution, etc.

2.4 Estimation of Runoff Using SCS-CN Method

Runoff is one of the most important hydrologic variables used in most water resource applications(Kumar *et al.*, 2010). Rainfall is the primary source of water for runoff generation over the land surface. The runoff curve number is an empirical parameter, which is extensively used in hydrology to estimate the direct runoff or infiltration rate from the rainfall excess, which is also called the curve number or simply CN. The USDA Natural Resources Conservation Service, formerly known as the Soil Conservation Service or SCS, developed the curve number system. The number of works of literature is now widely referred to as the "SCS runoff curve number." From an empirical study of runoff from small catchment(Pani and Chakrabarty, 2017). Originally, the NRSCS method was developed in 1954 and documented in national engineering handbook (NEH-4) by the soil conservation service now called the SCS -CN. The document has also been revised in different years, i.e. 1964, 1965, 1971, 1972, 1985, and 1993(Williams *et al.*, 2012).

There are different methods available to compute the surface runoff in an ungauged river catchment these are the Artificial Neural Network (ANN), SCS Curve number model, Geomorphological Instantaneous unit hydrograph (Rajbanshi, 2016). Among these methods, the SCS method is the most widely used method due to its simplicity(Rajbanshi, 2016). The SCS -CN method is a simple and efficient method for computing the approximate amount of surface runoff from excess rainfall events in a specific area and it can be scaled to find the average annual runoff values from the daily and monthly values of runoff (Askar, 2014). Also, the SCS curve number method is computed based on different factors such as hydrological soil group, LULC, digital elevation model (DEM), and the CN look Up table.

2.5 Flood hazard Mapping

Hazard is defined as a threatening event, or the possibility of occurrence of a potentially damaging phenomenon within a given period and area (Alaghmand *et al.*, 2010). In other literature, the hazard is a potentially harmful physical event, phenomenon, and/or human activity that may cause loss of life or injury, damage to property, social and economic disturbance, or degradation of the environment (Schneiderbauer and Ehrlich, 2004).

There are different types of hazards such as geological, meteorological, oceanographic, hydrological, biological, and money more, among all the above-listed hazard types the present study focused on the hydrological hazard, which is flood hazard. Floods are among the most common and destructive types of disasters, causing massive harm and affecting livelihoods around the world. There is a wide variety of flood risk management approaches that can minimize this damage, and flood risk management requires an assessment of the flood hazards and causative factors (Bank, 2016). Most causes of flooding are closely related to topographical, meteorological, climatic, biological, and hydrological factors. Flood hazard is a natural disaster that happens mainly in response to heavy rainfall and river discharge and becomes a disaster when it causes heavy loss of life and infrastructure and property damage. Among all kinds of natural hazards, the flood hazard is one of the most devastating, widespread, and frequent in the monsoon-dominated tropical and subtropical regions of the planet (Ghosh and Kar, 2018). According to (Chakraborty and Mukhopadhyay, 2019), the flood hazard assessment mapping is done with the help of an analytical hierarchal process (AHP) by integrating and weighing the elevation, surface runoff, slope, drainage density, distance to the river, rainfall, proximity to a stream, geomorphic features and distance to the embankment. There are many flood-generating factors needed to consider for delineate flood hazard zones. According to Assefa et al. (2011), slope, soil type, elevation, Land use/ Land cover, Drainage density, Rainfall, and population were rated and combined to delineate flood hazard zones in GIS using the multi-criteria evaluation technique. For the final weighted overlay analysis, the weight of each flood-generating factor was computed. Also, by pairing all factors flood hazard map is produced.

2.6 Flood hazard Vulnerability Mapping

The term vulnerability is defined as the degree to which an area, infrastructures or economic assets, population are exposed to loss, injury (damage) caused by the impact of a hazard (Dandapat and Panda, 2017). According to different works of literature such as (Balica, Wright, and van der Meulen, 2012; Bhuiyan and Dutta, 2012; Buldakova, Zaikanov, and Minakova, 2016; Dandapat and Panda, 2017; López-Valencia, 2019; Baky, Islam and Paul, 2020; De Risi *et al.*, 2020), Flood vulnerability assessment defined in terms of different level of Vulnerability indexes such as physical, social index, economic index, and ecological aspects. Although, Physical vulnerability is related to building, livelihood-related infrastructures, agriculture, hospitals, roads, communications system, and many other functioning of a society. Social vulnerability includes women, children, mentally and physically handicapped persons, elderly persons, poor people, and refugees. Whereas, an economic vulnerability assessment is related to the risk of the hazard and its impact on economic assets and processes (Ali, Bajracharyar, and Raut, 2017). Evaluation of vulnerability to natural hazards such as flood, drought, flash flood, and landslide is a critical starting point to minimize disaster-related damage to society. for the evaluation of flood risk vulnerability of communities has done by integrating different vulnerability index such as physical, social (population), economic and environmental factors through the spatial multicriteria techniques (Dewan and Corner, 2014).

2.7 Flood Risk Mapping

Risk is defined as the possibility of occurrence or the degree of loss of a specified element expected from a specific hazard and Risk is the overlapping areas of three factors- hazard, exposure, and vulnerability (Dandapat and Panda, 2017). In other literature, the risk is defined as it is the possibility of harmful consequences or expected losses resulting from a given hazard to a given element at danger over a specified time (Schneiderbauer and Ehrlich, 2004).

Many models are used to analysis hazard -related risk and vulnerability such as the pressure and release model (PAR) model, hazards-of-place (HOP) model, regions of risk model, the disaster resilience of place model (Dewan and Corner, 2014).

2.7.1 Pressure and Risk (PAR) Model

The pressure and risk (PAR) model are one of the best-known models that define vulnerability as' characteristics of an individual or community and their situation that influence their capacity to anticipate, cope with, resist and recover from the impact of a natural hazard and approach sees disaster risk as to the product of hazard and vulnerability (Wisner *et al.*, 2014). The PAR model approach evaluates the disaster (risk) as the product of hazard and Vulnerability and the PAR model is valuable for descriptive analysis rather than empirical testing (Dewan and Corner, 2014).

2.7.2 The hazard of place (HOP) Model

The basic concept of this model is that vulnerability is connected to interactive elements, such as the location and people living there, and to the interaction and intersection of social and biophysical elements. Vulnerability is characterized as a combination of social structures (social vulnerability) and biophysical conditions (potential exposure) in a spatial context (Dewan and Corner, 2014). The place of hazard model was developed by cutter (1996) and the model integrates biophysical and social characteristics relating to the causal process of hazard (Dewan and Corner, 2014). The HOP model of disaster or risk assessment is operational in geospatial technologies (Dewan and Corner, 2014).

2.7.3 Urban Vulnerability Framework

Dewan (2013) developed an urban vulnerability framework, which is primarily based on the HOP model, but also borrowed elements from others. This model incorporates a coping capacity indicator in the estimation of vulnerability to the natural hazard (Dewan and Corner, 2014). Other literature also defined the risk assessment in the same fashion, Flood risk assessment expressed as the product of hazard, and Vulnerability (Dandapat and Panda, 2017).

2.8 Flooding in Ethiopia

Flooding in Ethiopia is one of the major causes of natural hazards that causes significant damage to lives and livelihoods in the part of the country. Flooding in the country is mainly associated with heavy rainfall and the topography of the highland mountains and lowland plains with natural drainage systems formed by the principal river basins, in most cases, flooding occurs in the country as a result of prolonged heavy rainfall causing rivers to overflow and inundate areas along the river banks in lowland plains.

According to the national disaster risk management commission, early warning and emergency response report of flood alert,(2018) the major river flood-prone areas of the country including parts of Oromia and Afar regions lying along the upper, middle, and down-stream plains of the Awash River; parts of Somali region along the Wabe Shebelle, Genale, and Dawa Rivers; low-lying areas of Gambella along the Baro, Gilo, Alwero and Akobo Rivers; down-stream areas along the Omo and Bilate Rivers in SNNPR and the extensive floodplains surrounding Lake Tana and the banks of Gumera, Rib and Megech Rivers in Amhara region (National Disaster Risk Management Commission, 2018).

According to the FDRE National Disaster Risk Management Commission (2018) some areas have been recognized as flood risk areas across all region of the country such as Addis Ababa, Afar, Oromia, Tigray, SNNP, Amhara, Dire Dawa, and Harari the detail and summary of flood risk areas in Ethiopia are presented in **Table 2. 1**.

Table 2. 1 Summary of flood risk affected area in Ethiopia,

No	Region	Flood risk areas
1	Addis Ababa	Addis Ababa city
2	Afar	Zone 1: (Dubti, Afambo, Elidaar, Asayita, Mille and Chifra) Zone 2: (Ab'ala, Berhale, Megale, Dalule and Koneba Zone3: (Amibara, Dulecha, Gewane, Awash Fentale and Buremudaytu) Zone 4: (Teru, Yalo and Gulina) Zone 5: (Dalifege, Arthuma, Dewe, and Semurubi)
3	Amhara	North Shewa zone (AntsokiyaGemza, EfrataGidm, Kewet, and TarmaBer). Waghimra zone: (Dehnan, Sekota, GazGibla, Ziquala) North Gondar: (Dembia, GonderZuria, Matema and Chelga) South Gondar (LiboKemkem, Fogera, Dera, Simada, and TacheGaint) West Gojjam (Semen achefer, Debubeachefer, Baher Dar Zuria, Mecha and Degadamot
4	Benishangul Gumuz	Assossa and Metekel (Debate)
5	Dire Dawa	Dire Dawa city and Kaka
6	SNNP	South Omo (Dasenech, Gnangatom, Hammer, BenaTsemay, Jinka town, Selamago, Debub Are and Semen Are) Hadiya (Shashogo, MirabBadewacho and Limu)

7	Oromia	East Showa (Dugda, Bora, Adama, Boset, Fentale, Wonji and Ziekula) Southwest Shoa (Illu, Becho and Sebeta Awas) West Shoa (Wolmera Dendi and Ejere) Borena (Moyale, Abaya, Dugda Dawa, Melka Soda, Dire, Miyo, Gelana, and Boku) W. Hararge zone (Habro, HawiGudina, Oda Buletuma and Mieso) West Wollega (MeneSibu, Gimbi, Yebdo, Kondal, Babogambel and Jaros) West Arsi (Shala and Siraro) Arsi (Hitosa, Chole, OnkoloWabe, Jeju, Merti, Ziway Dugda, Gololcha, Seru and Dodota) East Hararge zone (Bedeno, GoroGutu, Jarso, Gursum, Dadar, Kumbi, Haromaya, Girawa, Meta, Gola Oda, Kersa and Kombolcha).
8	Gambella	Etang special woreda (Etang), Nuer (Lare, Jikawo, Akobo, Mackoye, and Wanthewa) and Anuak (Gambella town, Gambella zuria, Jor, Gog, and Dimma)

As the report of the national meteorological agency (NMA), (2018), several flash flood incidents have already been reported in Somali, Afar, Oromia, and SNNP regions since 15 April 2018, which causes displacing thousands of peoples and causing loss of property and livelihoods. According to the Somali Regional Disaster Prevention and Preparedness Bureau (RDPPB) report the flooding in the Somali region had been affected 43,887 families/households 263,322 people), of which, 25,238 households/151,428 people were displaced, the floods in the Somalia region also destroyed 12,911 hectares of farmland,76 health facilities, 123 schools, and more than 15,643 houses were destroyed during the time of flooding According to DPPC (then DPPA) of 1978, some areas have been recognized as flood-prone areas: In Gondar Administrative Region immediately East of Lake Tana where River Ribb, and Gumara enter the Lake; In Hararghe Administrative Region on the Wabe Shebelle River from Imi to Mustahil; In Illubabor Administrative Region on the Baro River from the town of Gambella to the border town of Jakao; In Wollo Administrative Region on the Awash River around Assayita In Shewa Administrative Region around Tefki in the Teji Depression. Areas and Population Affected/under Threat by Flood Disaster in the 2006 main Rainy Season (Assefa, 2018).

Table 2. 2 summaries of flood risk and vulnerability in a different region of Ethiopia

No	Region	Vulnerable	Affected
1	Afar	28000	4600
2	SNNP	106300	44000
3	Amhara	47100	47100
4	Oromia	61300	21900
5	Tigray	122300	2600
6	Dire-Dawa	10400	10400
7	Somali	87000	43200
8	Gambella	62000	26100
Total		524400	199900

Source: (Assefa, 2018).

2.9 Impacts of Land use/land cover change on Surface runoff and Flood.

The land use/land cover change affects the surface runoff as the runoff increased with increased rainfall between the year 1970 and 1980 about 88% of the runoff increases due to the rainfall increase and the runoff decreased and increased by the land use/land cover change (LULC), it contributed about 44% of the surface runoff changes in between the 1980 and 1990 and later the runoff changes to 71% from 1990 to 2000 (Yin *et al.*, 2017). The reduction of forestland and agriculturally used land to the newly built environments such as residential sites, industrial sites, and commercial centers can reduce the availability of retention areas to manage surface runoff during and after rainfall events (Khare *et al.*, 2017). As the study conducted in East Africa shows that due to the loss of forest cover there is an increase in annual discharge and surface runoff by 16 ± 5.5% and 45 ± 14% respectively, an increase of forest covers may lead to the decreases in discharge and surface runoff (Guzha *et al.*, 2018). The study conducted in Kenya the result shows that the LULC cover change has a direct impact on the runoff process, as the agricultural land increased from 39.6% to 64.3% between the year 1973 to 2001, although the forest cover decreased from 12.3 to 7% the change in LULC accounted for a difference in runoff from 55 to 68% (Githui, Mutua and Bauwens, 2009).

The LULC change in the process of urbanization affects the hydrological process such as surface runoff, and flooding (Hu, Fan, and Zhang, 2020). The LULC changes such as the natural land of forests, rangelands, and bare land have been decreased from 1990 to 2002 as a result of these the intensity of peak flood discharge increased from 1990 to 2002 which is 10 times that of the initial period (Panahi, Alijani and Mohammadi, 2010). The LULC change such as the built-up area and the open space area had been increased by 59.66% and decreased by 39.47% respectively between 1966 to 2009, which leads to the increase in surface runoff and flood hazard (Zope, Eldho and Jothiprakash, 2015).

2.10 GIS and Multicriteria Decision Making Techniques for Flood Hazard Mapping

Multicriteria decision-making is a very important problem-solving technique in any field of study. According to (Saaty, 2001) decision-makers could study and understand the problems through multi-criteria analysis methods such as AHP which solves complex problems by structuring the factors into a hierarchical framework. In today's world the integration of GIS with multicriteria decision-making techniques playing a very critical role in every aspect of risk assessment and hazard mitigation tasks. It makes the analysis easier and more efficient and reduces time wasted. Not only this, helps to study areas that are thought too inaccessible before. Many studies were conducted on flood risk zonation and mitigation measures with the help of multicriteria and geospatial approach such as (Ouma and Tateishi, 2014; Atta-Ur-Rahman and Shaw, 2015; Wu *et al.*, 2015; Fang, Li and Shi, 2015; Klijn *et al.*, 2015; Lollino *et al.*, 2015; Bracken *et al.*, 2016; Werren *et al.*, 2016; Danumah *et al.*, 2016; Demir and Kisi, 2016; Koch *et al.*, 2016; Rosser, Leibovici and Jackson, 2017; Hu *et al.*, 2017; Lian *et al.*, 2017). The spatial data stored in the digital database of the GIS, like DEM, slope with other factor can be used to predict the future flood-prone area. The GIS database may also contain agriculture, socio-economic, communication, population, and infrastructural data as spatial vector format (point, line, and polygon) or as attribute (tabular) information for spatial data. This can be used, in combination with the flooding data to adopt an evacuation strategy, rehabilitation planning, and damage assessment in case of a critical flood situation.

There are many reasons for most of the frequent choice should be the protection from the flood through physical control of the river but it also needs a comprehensive and wide-ranging program for managing flood hazards in the study area. ArcGIS was useful as a

tool as a result; detailed mapping was drawn for the flood hazard assessment Nawaz (2006). They have applied one of the multi-criteria decision-making techniques, Analytical Hierarchical Process (AHP) which provides a systematic approach for assessing and integrating the impact of various factors, involving several levels of dependent and independent, qualitative and quantitative information. Also, present a novel methodology for computing a composite index of flood hazard derived from topographical, land cover, geomorphic, and population-related data.

CHAPTER 3: MATERIALS AND METHODS

3.1 Description of the Case Study Area

3.1.1 Location

The Akaki Watershed is geographically located between 8°46´–9°14´N and 38°34´–39°04´E and covers a total area of 1787.5 Km.$^{2.}$ The Akaki Watershed is one of the sub-watersheds of the upper Awash River basin and the city of Addis Ababa is located at the center of the Akaki Watershed.

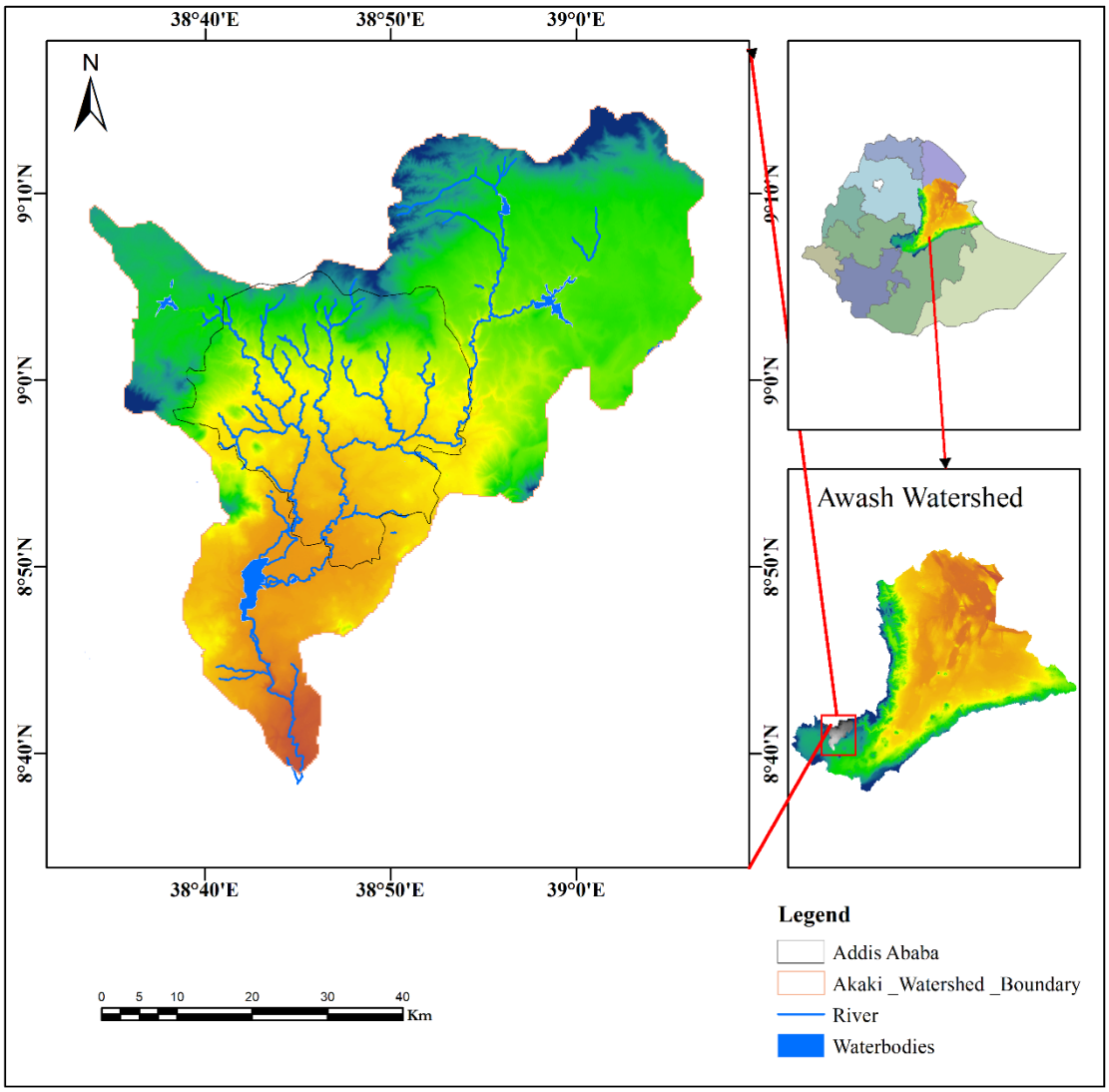

-

Figure 3. 1 Location of Akaki Watershed.

Generally, the main water bodies found in the Akaki Watershed are the Akaki River, and a four-water reservoir namely Legedadi, Geferssa, Dire, and Lake Aba-Samuel. All the above-listed reservoirs and water bodies are the major water supply source of Addis Ababa city. Akaki River has two main branches. Which are the great Akaki River and the Little Akaki River. The drainage area of the Little Akaki River basin covers the western part of Addis Ababa city. However, the eastern part of the study area is covered with the Big Akakai River drainage areas and it consists of the main tributaries of the Big Akaki River are Kebena, Kechene, Ginfle, Kurtume, and Yeka rivers (Tamru, 2001).

3.1.2 Land use/land cover

Four LULC types, such as agricultural land, built-up (such as residential, commercial/industry/transport), water bodies, and forest (Worako, 2016). Most of the catchment area is covered by agricultural land and built-up area with residential, commercial, industrial, and transportation

3.1.3 Topography and Elevation

The topography of the Great Akaki River basin is rugged and steep mostly between Enttoto and Filwoha but it is gentle and flat-lying in the south and southwest parts of the basin (Feyera Asfaw, 2007). The Akaki Watershed laying between 1810 to 3382 above mean sea level (MSL).

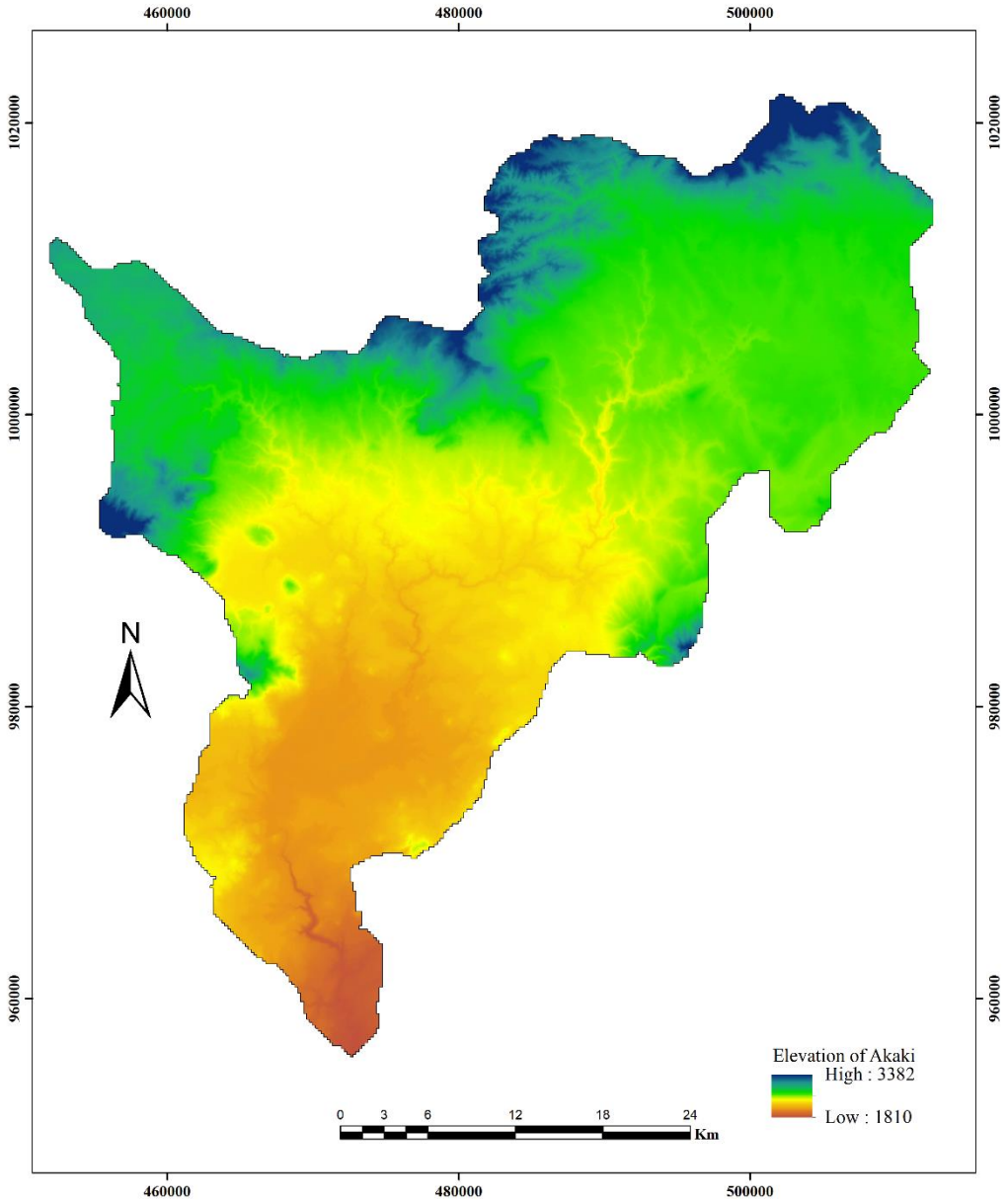

Figure 3. 2 Elevation Map of Akaki Watershed extracted from ALOS PALSAR DEM

3.1.4 Drainage density

The drainage network is basic information for developing applications involving surface and underground water resources. The determination of good quality drainage network can be extracted from altimetry grids with a high or at least medium resolution digital elevation model. In this study, the drainage density was extracted from the high-resolution ALOS DEM.

3.1.5 Soil Type

The soil data used for the present study is obtained from the Ministry of Agriculture. Based on a given soil data, the study area has a total of five soil types excluding the waterbodies these are Chromic Luvisols, Eutric Vertosols, Humic Nitisols, Lithic Latosols, Water bodies, and Vertic Cambisols, which have an area coverage of 388.17 Km^2, 112.26 Km^2, 1039.91 Km^2, 220.03 Km^2, 10.43 Km^2, and 16.3 Km^2 and have a percentage coverage of 21.72 %, 6.28 %, 58.19 %, 12.31 %, 0.6%, and 1% from the total area of the study area, respectively.

The most dominant soil type in the study area is Eutric vertisols which cover an area of 1039.91 Km2 have a percentage of 58% from a total soil type in study area .and the least dominant soil type is Lithic Leptosols, which have an area coverage of 16.16 Km^2 it is 0.6% of total soil type of the study area. Based on their texture the Akaki Watershed contains three types of soil texture these are the clay, sandy loam, and loam. Also, the study area is covered by three hydrological soil groups such as “A”, “B” and “D”. Soil group “D” is the dominant soil group of the study area, which covers 65% of the total study area. The second dominant soil group is soil group “B” which covers 34 % of the total area and then the least is soil group “A” which have an area coverage of 10.43 km^2 from a total area of the hydrological soil group, soil group “A” covers only 1 % of the study area.

Table 3. 1 Summary of soil texture and their area coverage

Soil texture type	Area coverage (km^2)	Percent coverage (%)
Clay	608.2	34.03
Sandy loam	1152.17	64.47
Loam	10.43	0.6
Water	16.36	1

Table 3. 2 Summary of Hydrological Soil Group and their area coverage

HSG	Area coverage(km^2)	Percent Coverage (%)
D	1161.9	65%
B	607.75	34%
A	16.16	1%

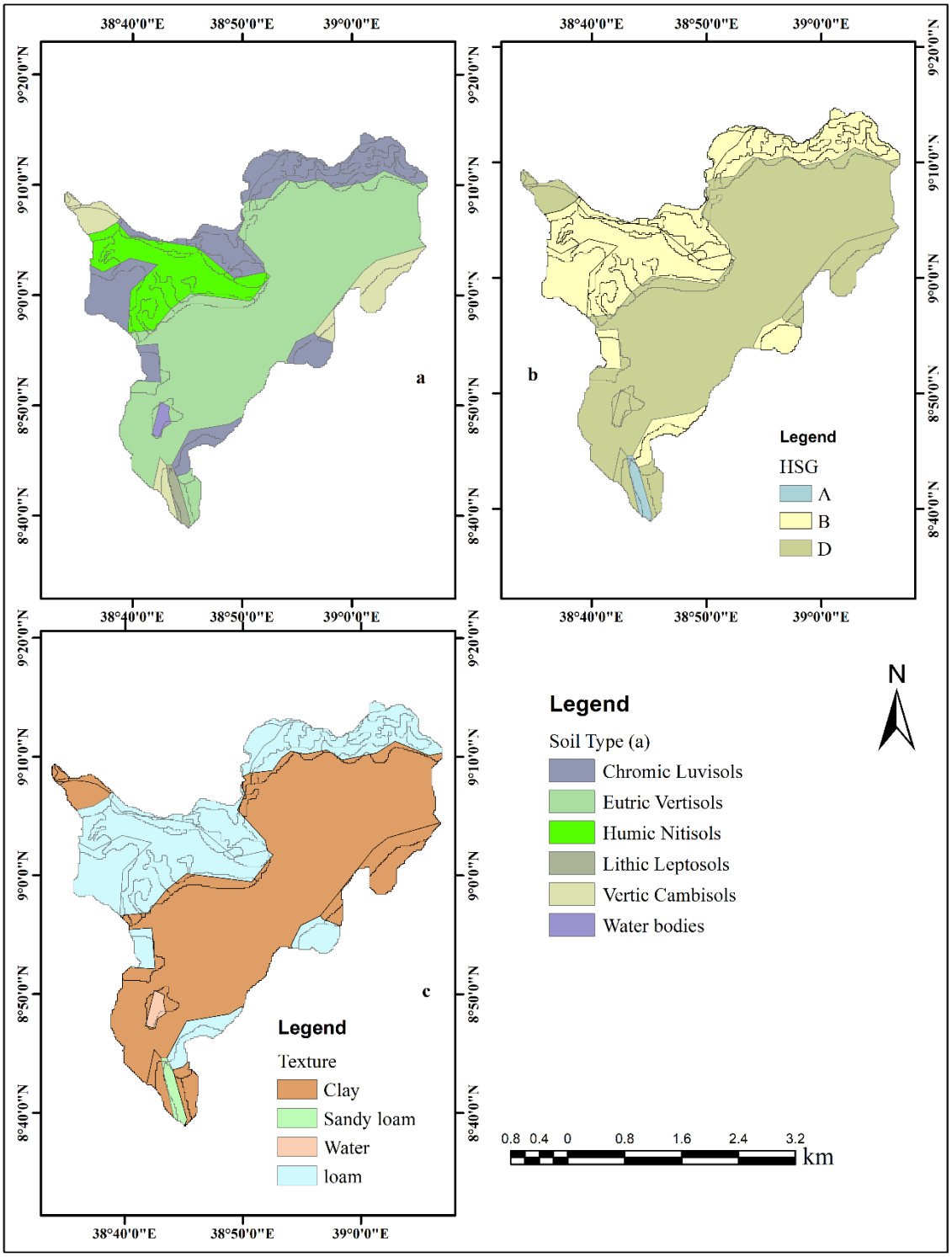

Figure 3. 3 Soil Map of Akaki Watershed, a (soil type), b (hydrological soil group), and ''c'' Soil texture.

3.1.6 Climate

3.1.6.1 Temperature

Geographically the Akaki Watershed is found near the equator due to this, the temperature is very constant from month to month. The mean monthly minimum and maximum temperatures vary from 7-11 ºC and 21-25 ºC, respectively. The lowest temperature of the project area is 7ºC which is registered in November and December, and the maximum temperature is 25ºC registered in March and May(*World Weather Information Service*).

Table 3. 3 Mean daily minimum and maximum temperatures

Month	Mean daily Minimum Temperature(°C)	Mean daily Maximum Temperature(°C)	Mean total Rainfall (mm)	Mean Number of Rain Days
Jan	8	24	13	3
Feb	9	24	50	5
Mar	10	25	58	7
Apr	11	24	82	10
May	11	25	84	10
Jun	10	23	138	20
Jul	10	21	280	27
Aug	10	21	290	26
Sep	10	22	149	18
Oct	9	23	27	4
Nov	7	23	7	1
Dec	7	23	7	1

Source:(*World Weather Information Service*)

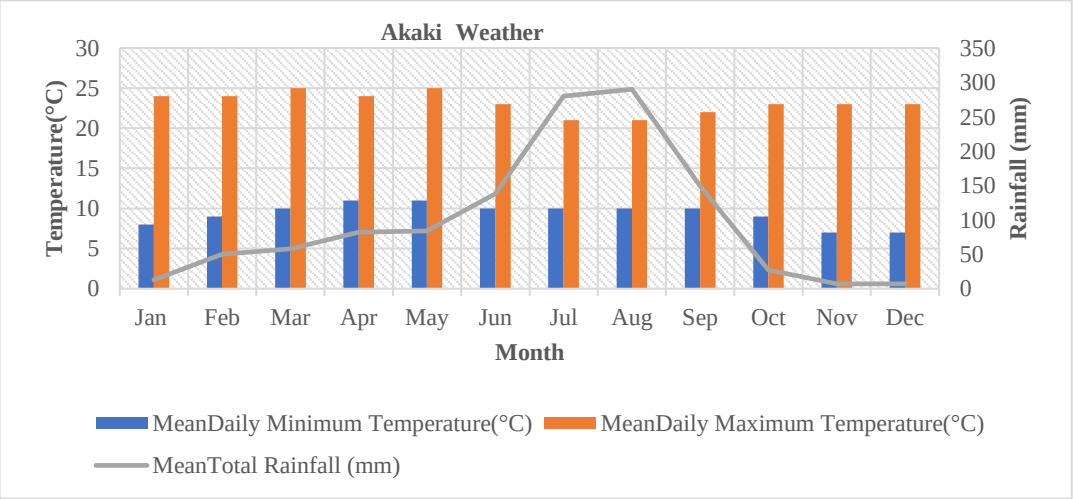

Figure 3. 4 Mean daily minimum and maximum temperatures, Rainfall

3.1.6.2 Rainfall

The dataset available for the extraction of rainfall data was the remotely sensed climate data, which is the Climate Hazards Group Infrared Precipitation with Stations (CHIRPS) from 1981 to the present, which is available in hourly, daily, monthly, two monthly, pentad, and yearly scales. The main rainy season of the Akaki Watershed is late June to early September also characterized by dry winter, which is the dry season of the area. Generally, the watershed area has an annual precipitation of 1165mm/year.

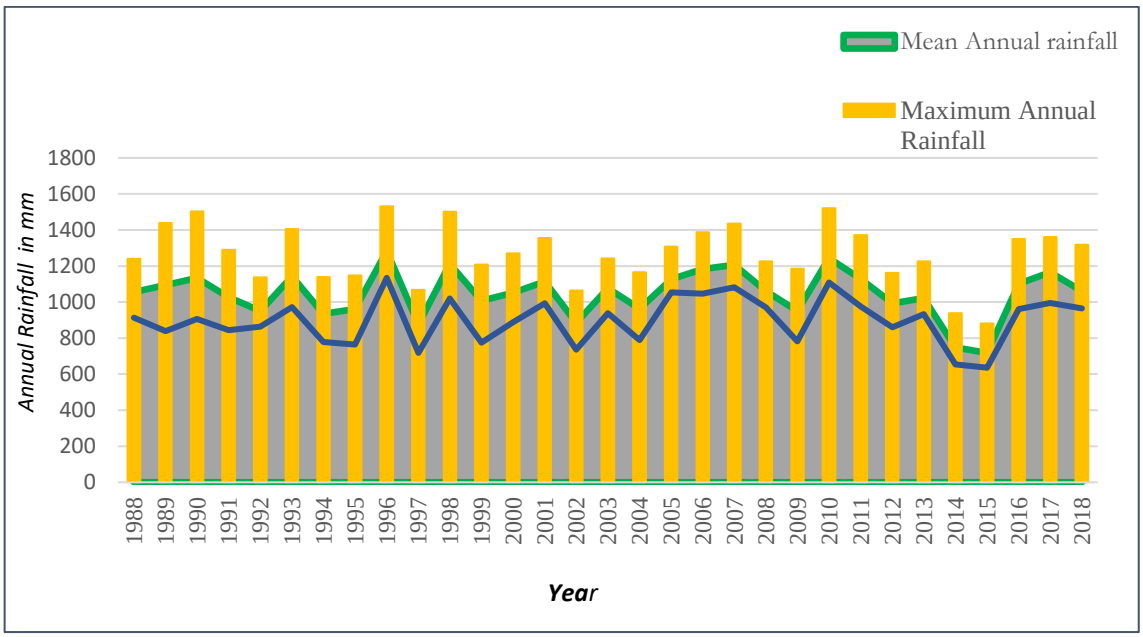

Figure 3. 5 Graph shows the Annual rainfall of (1988-2018)

3.1.7 Population

According to CSA, (2018), the watershed has a population projection value of *4254559* and the population density ranges from 138.573757 to 43336.39301 per square kilometer (population/Km^2). The lowest and the highest population density exist in the watershed is Walmara and Addis Ketema respectively.

3.2 Data Source and Materials Used

3.2.1 Data Source

The overall work of any scientific study result or findings depends on the quality of the input data, based on this assumption in the present study a series of multi-temporal satellite imageries such as Landsat 5, Landsat 7, and Landsat 8[1]and also other satellite imagery product and data collected from a different organization such as ALOS DEM[2], Chirps V2.0 (Precipitation)[3] , rainfall data[4], soil data[5] and both published and unpublished resource (such as books, journal articles, reports, and case study) were used.

3.2.1.1 Satellite Imagery (Landsat 5,7,8)

In the present study, a series of multi-temporal satellite imageries such as Landsat 5 Thematic Mapper, Landsat 7 Enhanced Thematic Mapper, and Landsat 8 Operational Land imagery- thermal infrared sensor (OLI-TIRS) were used, which is acquired from the United States Geological Survey (USGS). The imageries were selected at an interval of 15 years from 1988 to 2018, for estimation of CN, surface runoff, LULC change detection (rate, pattern, and magnitude of the land use/land cover), and the impact of LULC change on flood hazard and risk prone area.

3.2.1.2 Chirps Satellite Estimate Precipitation

The Climate Hazards Group InfraRed Precipitation with Station data (CHIRPS) is a 39-year quasi-global satellite estimate precipitation data set. Spanning 50°S-50°N (and all longitudes) and ranging from 1981 to near-present. chirps have a resolution of 0.05° satellite imagery, and in-situ station data to create gridded rainfall time series for trend analysis (Climate Hazard Center, 2019). which was used for rainfall-runoff generation and used as a flood hazard index.

3.2.1.3 ALOS PALSAR DEM

ALOS is one of the largest earth observation satellites in the world. Its purposes are global monitoring, cartography, regional observation, disaster monitoring, resources surveying,

[1](www.earthexplorer.usgs.gov/)
[2] www.Alaskasatelite facility
[3] www.chrips portal V2.0/p05
[4] National metrological Agency
[5] Ethiopian ministry of Agriculture

and technology development by collecting globally land observation data with high resolution. ALOS DEM has a spatial resolution of 12.5*12.5m.

In this study ALOS DEM was used to extract elevation, slope, drainage density, TWI, and for the delineation of the watershed.

Table 3. 4 Satellite data and other auxiliary data used for the present study

Satellite	Acquisitions Date	WRS_Path	WRS_Row	Resolution (m)
Landsat 5	1988- 03-31	168	054	30*30
Landsat 7	2003-01-12	168	054	30*30
Landsat 8	2018-01-13	168	054	30*30
DEM	2006 to 2011	Elevation TWI Slope Drainage density Watershed delineation		12.5*12.5
Chirps V2.0	1988-2018	Precipitation Runoff		0.05°*0.05°
Rainfall Data	1988 – 2018	For Validation of chirps		
Soil Map		Used as flood hazard index		
Google Earth & GPS Point	For Validation and verification of LULC			
River network [6]	For vulnerability Analysis			
Road [7]				
Population density [8]				

[6] From ministry of water, irrigation and electricity
[7] www.osm.com
[8] From projected value of 2018 CSA data

3.2.2 Material and software

To achieve the designed objective of the present study the following hardware and software were used.

3.2.2.1 Software Used in the present Study

The software used in this study was selected based on the ability to work on the existing problems for accomplishing the predetermined objectives. To achieve these objectives the following software was used, such as HEC-GeoHMS, ArcGIS 10.8, ERDAS Imagine 2015, QGIS, Microsoft office 2019, and L-THIA toolbox.

Table 3. 5 Software used for the present Study

Software used	Function
ArcGIS	Data analysis, thematic Map preparation, weighted overlay analysis and zonal statics
HEC-GeoHMS	Runoff curve number generation. delineation of Watershed
QGIS	Atmospheric correction of satellite imageries Image classification of satellite images

3.3 Methodology

In the present study, the researcher explains the detail and the necessary framework and methods in data acquisition, data creation, data processing, and manipulation involved in the determination of LULC change, estimation of runoff using SCS CN method, and evaluation of the impact of LULC cover change on surface runoff and flooding.

3.3.1 Method of Image Processing

In image processing, the following processing and conversion step was done to enhance the visibility and clarity of the satellite image, such as radiometric correction including DN to Radiance, Radiance to reflectance /Atmospheric correction.

3.3.1.1 Radiometric Correction

Radiometric correction is done to reduce errors in the DN of images. the radiometric correction used to improve the interpretability and quality of remotely sensed data. Radiometric calibration and correction are particularly important when comparing data sets over multiple periods (Khanna *et al.*, 2017). Like change detection of time series data

for this study, the researcher has applied a radiometric correction for the image of TM, ETM+, and OLI for the respective year of 1988,2003, and 2018.

3.3.1.1.1 Conversion of DN to Radiance for TM /ETM^{+}

According to the handbook of Landsat 5, 7, and 8 (TM, ETM+, and OLI), the following correction was applied to each Landsat product. There are two methods of converting DN to radiance which is, the gain and bias or offset and the spectral radiance scaling method (USGS, 2011). The conversion depends on the availability of the metadata(header) file exist. for this study, the researcher was used the spectral radiance scaling method to convert the DN value to radiance value which is stated in equation (3.1) given by (USGS, 2011).

$$L\lambda = \left(\frac{LMAX\lambda - LMIN\lambda}{QCALMAX - QCALMIN}\right) * (QCAL - QCALMIN) + LMIN\lambda \dots\dots\dots\dots\dots\dots 3.1$$

where Lλ is the spectral radiance at the sensor's aperture in mW/ (cm2·sr·µm); DN is the digital number of the quantized calibrated pixel value; Lλmax is the maximum spectral radiance that is scaled to QCALλmax; Lλmin is the minimum spectral radiance that is scaled to QCALλmin; QCALλmax is the maximum quantized calibrated pixel value in DN (corresponding to Lλmax), and QCALλmin is the minimum quantized calibrated pixel value in DN (corresponding to Lλmin). Once we convert the digital number to radiance value, the next step is converted into top-of-atmosphere (TOA) reflectance using Equation.

3.3.1.1.2 Conversion of Radiance to Reflectance for TM /ETM+

For relatively clear Landsat scenes, a reduction in between-scene variability can be achieved through a normalization for solar irradiance by converting spectral radiance to spectral reflectance (TOA)(USGS, 2011). In the present study, conversion of radiance to reflectance was applied using the equation (3.2) given by (USGS, 2011).

$$p = \left(\frac{\pi * L * d2}{ESUN * \cos(SZ)}\right) \quad \dots\dots\dots\dots\dots\dots\dots\dots\dots\dots\dots\dots\dots\dots\dots\dots\dots\dots (3.2)$$

Where p = Unitless planetary reflectance, L= Spectral radiance at sensor aperture in mW cm^{-2} ster^{-1} □m^{-1}, d = the square of the Earth-Sun distance in astronomical units (1 - 0.01674 cos (0.9856 (JD-4)))^2 where JD is the Julian Day (day number of the year) of the image acquisition. [Note: the units for the argument of the cosine function of 0.9856 x (JD-4)

will be in degrees; if your cosine function (e.g., the cos function in Excel is expecting the argument in radians, multiply by p/180 before taking the cosine)]. ESUN= Mean solar Exoatmospheric irradiance in mW cm-2 mm-1, SZ= sun zenith angle in radians when the scene was recorded.

3.3.1.2 Conversion of DN to Radiance for Landsat 8(OLI)

Originally, images are acquired in the form of DN value. These values can then be converted to spectral radiance using the radiance scaling factors. In the present study, conversion of DN to radiance was applied using the equation (3.3) given by (USGS, 2018).

$$L\lambda = ML * Qcal + AL \quad \text{..... (3.3).}$$

where: Lλ = Spectral radiance (W/ (m2 * sr * μm)), ML= Radiance multiplicative scaling factor for the band (RADIANCE_MULT_BAND_n from the metadata), AL = Radiance additive scaling factor for the band (RADIANCE_ADD_BAND_n from the metadata). Qcal = L1 pixel value in DN

3.3.1.3 Conversion of Radiance to Reflectance for Landsat 8(OLI)

Similar to the conversion of DN to radiance, the 16-bit integer values in the L1 product can also be converted to TOA reflectance. The following equation is used to convert Level 1 radiance values to TOA reflectance (*USGS, "Landsat 8 Science Data Users Handbook*, 2016).

$$\rho\lambda = \frac{M\rho * Qcal + A\rho}{sin(\theta)} \quad \text{..... (3.4)}$$

Where ρλ= TOA Planetary Reflectance (Unitless), Mρ= Reflectance multiplicative scaling factor for the band (REFLECTANCE_MULT_BAND_n from the metadata),

Aρ=Reflectance additive scaling for the band, Θ = Solar Elevation Angle (from the metadata).

3.3.1.4 Supervised Image Classification

Classification of satellite imagery is necessary to extract information about an object. In the present study, supervised Image classification was carried out using the maximum likelihood classifier. Supervised image classification had been done for the Landsat image of 1988, 2003and 2018 or TM, ETM+, and OLI respectively.

3.3.2 Accuracy Assessment Method

Assessing the thematic accuracy of maps or other spatial data requires sampling to determine the accuracy of the classified map because it is not economically feasible to visit the whole study area. The accuracy of classified satellite imagery was evaluated based on the following statistical parameters (Kappa Index) such as user accuracy, producer accuracy, omission error, commission error, and overall accuracy. The reference data used for map accuracy assessment were collected from field surveys and high-resolution google earth Image. The google earth image was used for the LULC of 1988 and 2003. The google earth image is at the same period as the satellite imagery date. For the LULC of 2018 field survey and high-resolution google earth image were used to validate the classification result(Tilahun, 2015; Rwanga and Ndambuki, 2017; Hoang, Nasahara and Katagi, 2018; Hu *et al.*, 2019; Prasad and Ramesh, 2019; Yesuph and Dagnew, 2019). Google earth image was used as a reference with other supplementary data for validation and verification of the classified LULC map. The sampling technique used in the present study was the stratified random sampling design and the kappa statistics were computed using the following equation as given by (Maiti and Bidinger, 1981).

$$\text{User Accuracy} = \frac{\text{Number of correctly classified Pixels}}{\text{total Classified Pixels}} * 100 \quad \text{(3.5).}$$

$$\text{Producer Accuracy} = \frac{\text{Number of correctly classified Pixels}}{\text{total reference Pixels}} * 100 \quad \text{(3.6).}$$

$$\text{overall Accuracy} = \frac{\text{Sum of correctly classified Pixels}}{\text{total number of reference pixels}} * 100 \quad \text{(3.7).}$$

$$\text{Kappa coefficient} = \frac{N \sum_{i=1}^{r} Xii - \sum_{i=1}^{r} (X_{i+} * X_{+i})}{N^2 - \sum_{i=1}^{r} Xii - \sum_{i=1}^{r} (X_{i+} * X_{+i}} \quad \text{(3.8).}$$

Where N is the total samples; r is the number of rows in the error matrix; X_{ii} is the total corrected samples in the i^{th} row, and column; N^2 is the square of total samples; X_{i+} is the column total, and X_{+i} is the row total.

Table 3. 6 Kappa index classification and explanation

Kappa Index (%)	Quality of estimation
80 to 100	Excellent
60 to 80	Very good
40 to 60	Good
20 to 40	Reasonable
0 to 20	Bad
< 0	Very Bad

source:(De Oliveira Duarte *et al.*, 2016).

3.3.3 Land use/ Land cover Change Analysis

There are different types of change detection techniques in LULC change detection Analysis such as image differencing, Principal component analysis, Image rationing, image regression, and post-classification comparison. In this study, post-classification comparison techniques were used. The percent change, the annual rate of change, and the magnitude of the change were also estimated using the following equation as given by (Michael, 2017; Joseph Asen, Godwin Nnaemeka, and Ashetu, 2020).

$$\% \text{ change} = \frac{At_2 - At_1}{At_1} * 100 \quad \text{(3.9)}.$$

$$\text{The annual rate of change} = \frac{At2 - At1 * 100}{n * At1} \quad \text{(3.10)}.$$

$$\text{The magnitude of change } = At_2 - At_1 \quad \text{(3.11)}.$$

Where At_2 = the area of final land use /land cover class, $At_{1=}$the area of initial land use /land cover and n is the number of years.

3.3.4 Surface Runoff Generation Method

The soil conservation service curve numbers (SCS-CN) model was developed by the United States Department of Agriculture (USDA) for the computation of the direct runoff through an empirical formula as a function of rainfall and the curve number. The curve number is the combination of the LULC and the HSG. The SCS CN model involves the relationship between the LULC, HSG, and the curve number(Mishra and Singh, 2006). Normally the SCS model computes direct runoff with the help of the following relationship as given by (Kumar *et al.*, 2010; Nagarajan and Poongothai, 2012; Williams *et al.*, 2012; Kannan, 2017).

$$Q = \frac{(P-Ia)^2}{P-Ia+S} \qquad (3.12).$$

$$S = 254\left(\frac{100}{CN} - 1\right) \qquad (3.13).$$

$$Ia = 0.2S \qquad (3.14).$$

$$Q = \frac{(P-0.2S)^2}{P-0.8S} \qquad (3.15).$$

Where, P is the depth of precipitation, mm S = maximum potential retention, (mm), Q = depth of direct runoff, (mm), CN = index that represents the combination of a hydrologic soil group and land use and treatment class which was used to generate the weighted curve number. Ia = initial abstraction

3.3.5 Antecedent Moisture Condition

Antecedent Moisture Condition (AMC) is based on the five-day antecedent Rainfall related to soil moisture conditions (Jae, Sun, and Shik, 2018). The curve number (CN) grid was computed by using HEC-GeoHMS. Which is termed CN II on AMC II representing average soil moisture condition. The AMCI, AMCII, and AMC III are assigned for CNI, CNII, and CNIII respectively. The conversion was computed using equations (3.16 and 3.17) as given by (R.Viji, P. Rajesh Prasanna, 2015).

$$CNI = \frac{CNII}{2.281-0.0128 \times CNII} \qquad (3.16)$$

$$CNIII = \frac{CNII}{0.427+0.0057 \times CNII} \qquad (3.17)$$

Table 3. 7 Classification of AMC Condition

AMC	Description	Sum of Antecedent 5-days Precipitation	
		Growing season	Dormant season
AMC I	Soils are dry	P5 < 35 mm	P5 < 12 mm
AMCII	Average Condition	35 mm ≤ P5 ≤ 53 mm	12 mm ≤ P5 ≤ 28 mm
AMCIII	Soils are wet	53 mm < P5	28 mm < P5

Source: USDA (1984).

3.3.6 Flood Hazard Prone Area Computation Method

The computation of flood hazard-prone area of the Akaki Watershed was done using multicriteria decision-making techniques by considering different causative factors such as elevation, slope, Drainage density, TWI, Surface runoff, Soil type, LULC, and rainfall data. These causative factors have a different spatial resolution, to compute the flood hazard-prone area the spatial resolution should have the same, to do that resampling technique was used. the resampling technique was done from finer-resolution to coarser resolution.

3.3.6.1 Multicriteria Decision Making Techniques

In the present study, the multicriteria decision-making techniques were used for the computation of flood hazard mapping by considering different causative factors of flooding. Once the pairwise comparison matrix had been computed, the next step is to normalize the matrix by summing up the numbers in each column of the matrix. Each entry in the column is then divided by the column sum to yield the normalized matrix. The normalized matrix for the element $a_{jk.}$ computed by using equation (3.18) as given (Hillier *et al.*, 2012).

$$\overline{ajk} = \frac{\boldsymbol{ajk}}{\sum_{i=1}^{n} \boldsymbol{aik}} \text{……………………………………………………… (3.18)}$$

Where $\overline{ajk}$ is normalized Matrix, a_{jk} is each entry in the column and $\sum_{i=1}^{n} aik$ is the sum of the element in the column. and Finally, the *criteria weight vector w* (that is an *n*-dimensional column vector) is built by averaging the entries on each row of the normalized matrix as given by (Saaty, 2001; Hillier *et al.*, 2012).

$$w\bar{J} = \frac{\sum_{i=1}^{n} \text{aji}}{\text{n}} \text{………………………………………………..…… (3.19)}$$

$$\lambda\text{max} = \frac{w}{n} \text{……………………………………………………..…… (3.20)}$$

After computing **Lλmax,** the consistency index (CI) was calculated using equations (3.22) and (3.23) as given by (Saaty, 2001; Hillier *et al.*, 2012).

$$Consistency\ index\ (CI) = \frac{\lambda max - n}{(\text{n}-1)} \quad \text{……………………………… (3.22)}$$

the consistency ratio (CR) = CI/RI ………………………………. (3.23)

3.3.7 Flood Vulnerability prone Area Computation Method

The flood risk Vulnerability was computed using a spatial multicriteria weight system by considering different vulnerability indexes such as social Vulnerability (population), socioeconomic (land use). ecological (distance from the river) and infrastructure (road density). The final vulnerability index was computed by integrating the individual vulnerability index.

3.3.8 Flood Risk Prone areas computation Method

The flood risk-prone area of the Akaki Watershed was obtained herein using the integration of flood hazard and flood vulnerability. According to (Dewan and Corner, 2014; V *et al.*, 2017; Vishwanath and Tomaszewski, 2018; Baky, Islam, and Paul, 2020), the flood risk is the product of hazard and vulnerability, in this study the hazard of place (HOP) model were applied to produce the flood risk map of the Akaki Watershed. The hazard of place (HOP) model allows computing risk in geospatial technology. The final flood risk of the study was computed by equation (3.24) as given by (Dewan and Corner, 2014).

$$Risk = hazard * Vulnerability \ldots\ldots\ldots\ldots\ldots\ldots\ldots\ldots\ldots\ldots \quad (3.24).$$

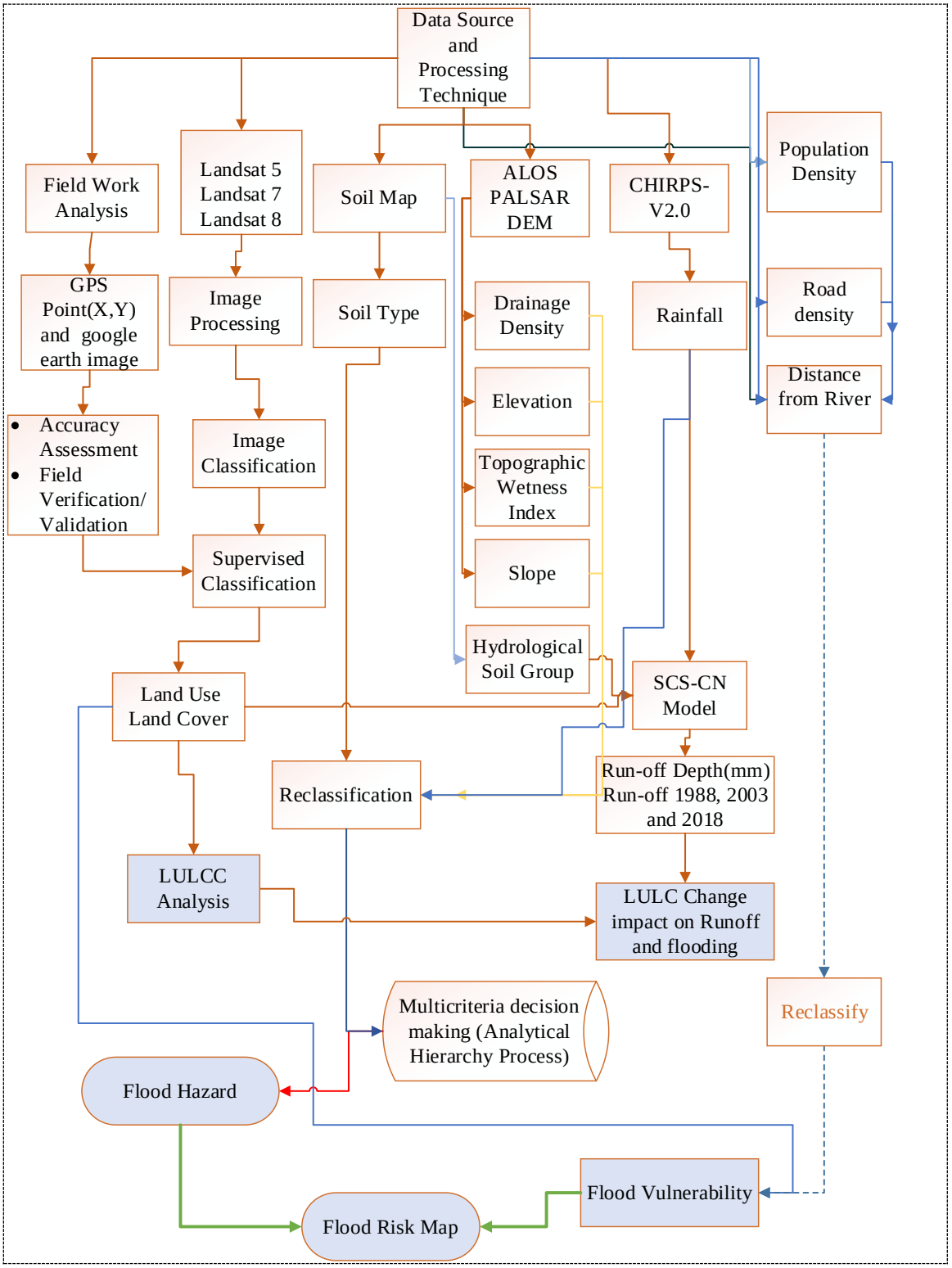

Figure 3. 6 General Frame Work of Data processing techniques and Methodology

CHAPTER 4: DATA ANALYSIS, RESULTS, AND DISCUSSION

4.1 DATA ANALYSIS AND RESULT

4.2 Land use/land cover mapping

According to the first Level classification system of Anderson, the Land use /land cover of the Akaki Watershed was classified into four land use categories, namely: (1) Built-up, (2) Forest, (3) water bodies, and (4) Agriculture.

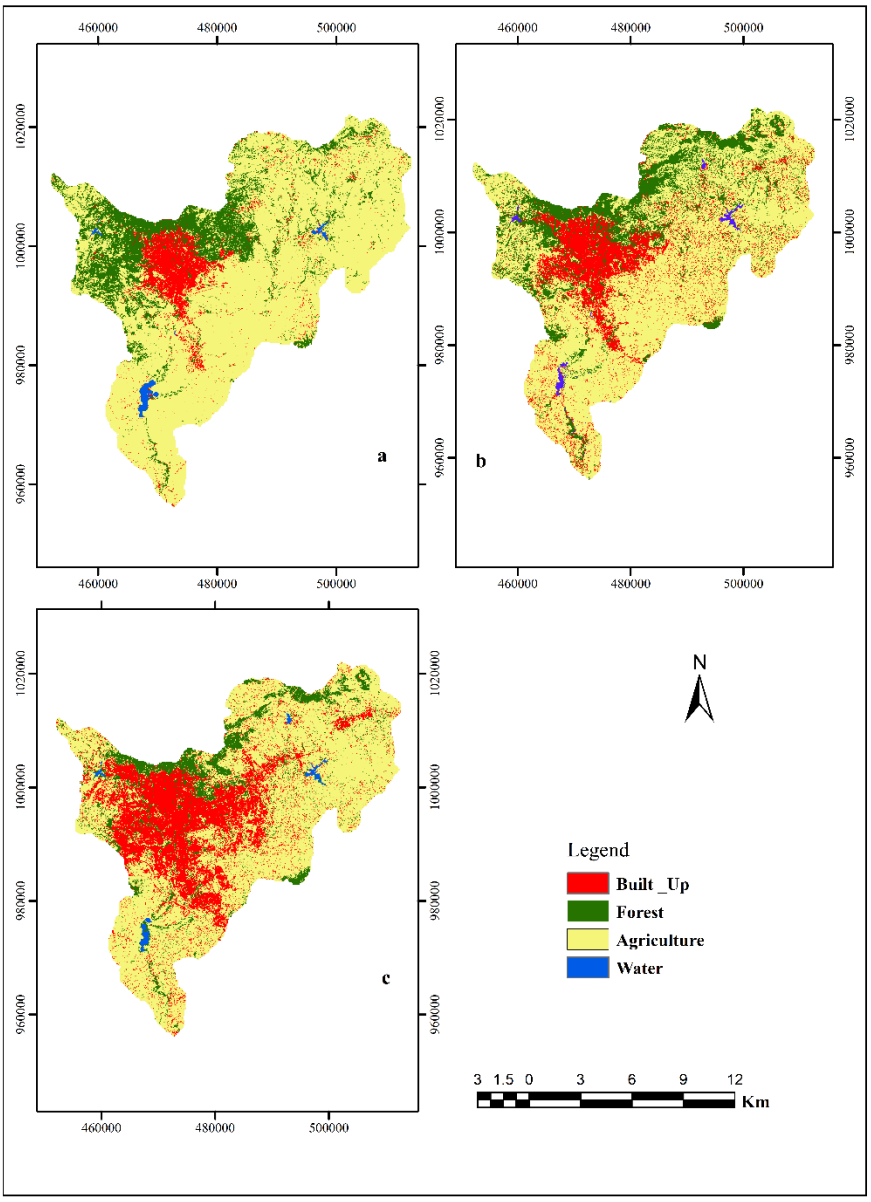

Figure 4. 1 Land use/land cover map of 1988(a), 2003 (b), and 2018 (c).

The accuracy of the LULC classification in the present study was estimated by using the kappa statistics, as the result revealed that 78.5 % and 83.9 %, 86.5 % and 90.04%, 86.4% and 90% of the kappa coefficient and the overall accuracy in the land use of 1988, 2003, and 2018 respectively.

4.3 LULC Change of Akaki Watershed

The percentage changes of the LULC class, from 1988 to 2018 had been estimated. As the result shown in Table 4. 1. it is clear that the built-up area in the Akaki Watershed was highly increased, simultaneously the agricultural and the forestland were reduced in their distribution from 1988 to 2018 within the watershed.

Table 4. 1 Land use/land cover coverage and percent share of Akaki Watershed

LULC	Land use/land cover area coverage (km2) & % share					
	1988		2003		2018	
	Area (km2)	%	Area (km2)	%	Area (km2)	%
Built	112.54	6.29	209.60	11.73	461.34	25.81
Forest	315.71	17.66	338.69	18.95	189.35	10.59
Agri	1346.77	75.34	1224.16	68.48	1125.48	62.96
Water	12.53	0.70	15.09	0.84	11.39	0.64
Total	1787.55	100	1787.55	100	1787.55	100

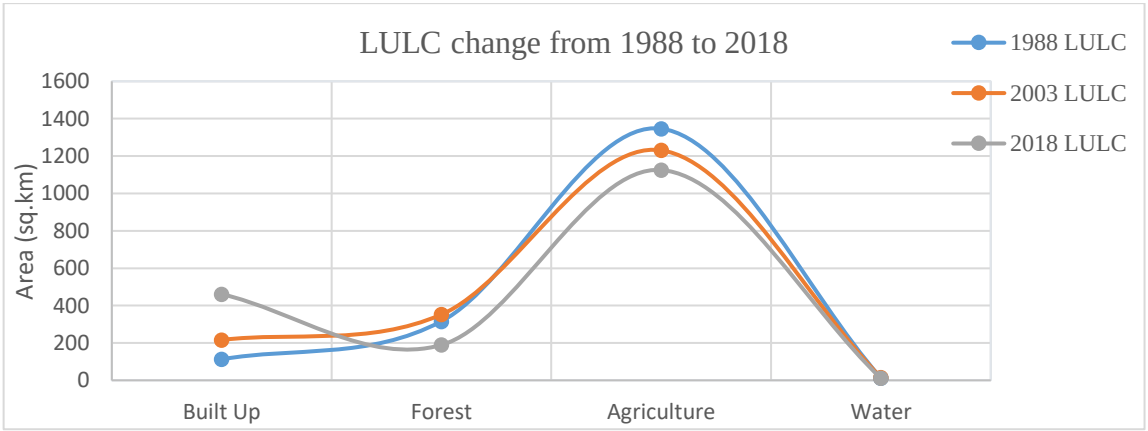

Figure 4. 2 Trend of LULC change between 1988 and 2018.

In terms of area coverage and percentage share of the agricultural land was the dominant land use class in 1988, which covers 75.34 % (1346.77km^2) of the total study area, in the land-use class of 2003 and 2018 the agricultural land was reduced to 68.48 % (1224.16 km^2), 62.96% (1125.48 km^2) respectively. The built-up LULC classes also rapidly increase through the entire study period. 6.29 % (112.54 km^2), 11.73 % (209.60km^2), and 25.81% (461.34km^2) were a percentage share of the LULC class of 1988, 2003, and 2018 respectively.

Table 4. 2 rates of change, % change, and pattern of LULC change of the study area

	LULCC (a-b) 1988 -2003		Annual	LULCC (b-c) 2003-2018		Annual	LULCC (a-c) (1988 -2018)		Annual
	Magnitude (km^2)	% change	Rate change	Magnitude (km^2)	% change	Rate change	Magnitude (km^2)	% change	Rate change
Built up	(+) 97.06	(+) 86.24	(+) 5.74	(+) 251.74	(+) 120.1	(+) 8.01	(+) 348.79	(+)309.9	(+) 10.33
Forest	(+) 22.98	(+) 7.28	(+) 0.49	(-) 149.34	(-) 44.09	(-) 2.94	(-) 126.36	(-) 40.02	(-)1.33
Agricul	(-) 122.61	(-) 9.10	(-) 0.61	(-) 98.68	(-) 8.06	(-) 0.54	(-) 221.29	(-) 16.43	(-)0.55
Water	(+) 2.57	(+) 20.48	(+) 1.36	(-) 3.71	(-) 24.58	(-) 1.63	(-) 1.14	(-) 9.13	(-) 0.30

Note: the (+) denotes the increase magnitude, % change and annual rate of change, & (-) sign denotes a decrease of magnitude, % change, and rate of change of LULC category at a different time.

The percentage change of the LULC analysis of the Akaki Watershed which was presented in Table 4. 5 showed that in 2003 LULC, the built-up area had been increased by 86.24 % (+97.06 km^2) and simultaneously, the agricultural area had reduced by 9.1% (-122.61km^2) as compared to the land use of the year 1988. In the LULC of 2018, the built-up area had been increased by 120 % (251.74 km^2), and the forestland, agricultural land had been reduced by 44.09%, (-149.34 km^2), and 8.06% (98.68 km^2) respectively. As compared with the land use of 2003. Through the entire study period (1988 -2018) the built environment had been increased by 309.93% (+348.79 km^2) and simultaneously, the forest, agricultural, and water land had been decreased by -40 % (-126.36 km2), -16.43 % (-221.29 km^2) and -9 % (-1.14 km^2) respectively. During the entire study period, the major LULC changes had been observed the rapid expansion of urban cover and the gradual decline of agricultural and forest lands.

The urban area expanded nearly by 310 %, from 112.54 km^2 in 1988 to 461.34km^2 in 2018, with an average annual growth rate of 10.33 %. The loss of forest-land cover leads to an increase in the amount of peak runoff and flood hazards. The study conducted in Birendra agar, Surkhet (Nepal) confirms the result of the present study, the study estimated the land-use change of different period, and the observed land-use change had been the rapid expansion of urban cover and the decline of cultivated lands, the urban expansion was expanded by 700% through the entire study area (Rijal, Rimal, and Sloan, 2018).

The study conducted in the lake Ziway (Ethiopia) watershed by (Desta and Fetene, 2020) as the result revealed that cultivated and settlement areas have consistently increased from 1973 to 2018 Settlement areas increased by 12% during the first period and further increased (116%) during the second period. In Ethiopia, the majority of LULC changes are mostly driven by demands for more agricultural lands, building materials, and fuelwood cited in (Desta and Fetene, 2020).

The study conducted in India by (Prasad and Ramesh, 2019), as the result states that the built-up area had been increased by 6.59 % to 18.16 % from 1973 to 2017, this is due to the demographic growth of the study area. The same is true for the present study as the population growth increase the built environment were increased so the result of the present study completely agrees with all the above-listed study.

4.4 Surface Runoff Mapping

Based on SCS CN methods the daily, monthly, and annual runoff were estimated for the year 1988, 2003, and 2018. The computed runoff values were presented in the form of a graph, maps, and tables.

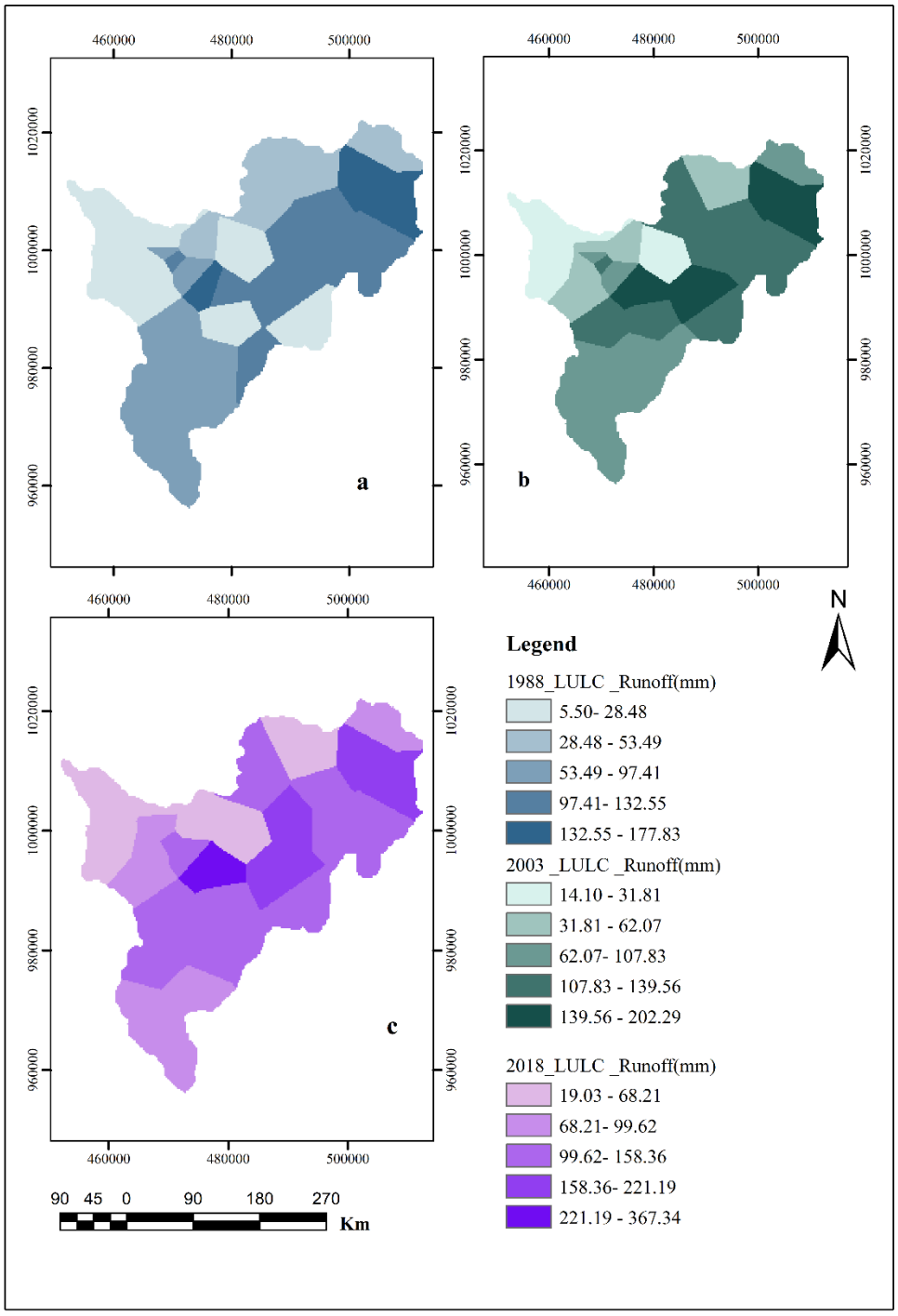

Figure 4. 3 Runoff Map a (1988 LULC runoff), b (2003 LULC runoff), and c (2018LULC runoff)

4.4.1 Analysis of Monthly and Annual Runoff

The monthly runoff was computed from the daily surface runoff; originally, the daily runoff values used in the analysis were converted from daily values, which were computed based on the SCS curve number method. Details of the daily runoff available in appendix A. as the figure shown in **Figure** 4. **4**. The average monthly runoff was estimated for different LULC scenarios such as 1988,2003, and 2018.as the result revealed that the maximum peak runoff occurred in June, July, August, September, and October which is 154mm,296.3mm,425.44mm,288.8mm, and 160.6mm respectively.

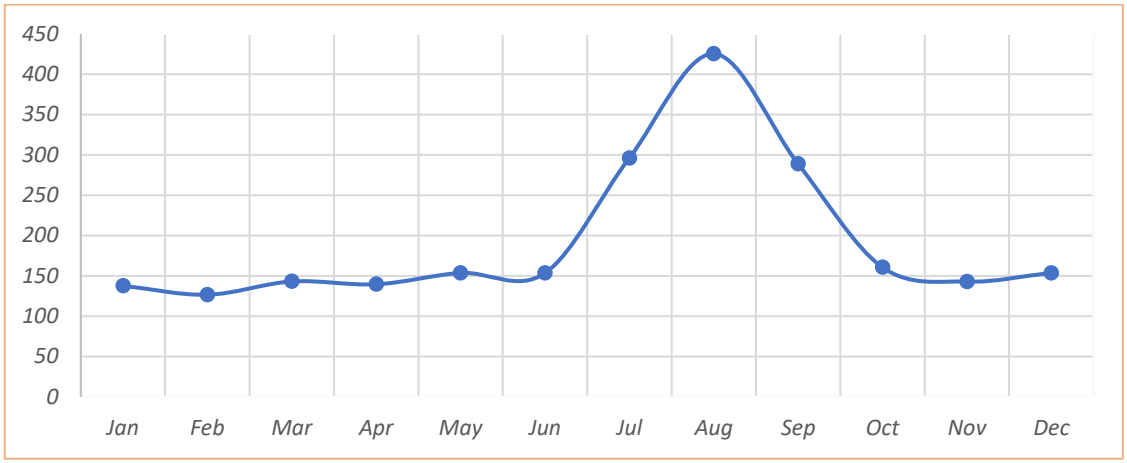

Figure 4. 4 Average Monthly Runoff (mm)

The analysis of annual runoff of the Akaki Watershed was estimated in different LULC scenarios, as the result revealed that 260.0, 278.27, and 303.1 mm runoff were estimated in each LULC scenario such as 1988, 2003, and 2018 respectively. The change in land use/land cover such as the expansion of the built-up areas, and the reduction of forestland may affect the hydrology of the watershed and it leads to an increase in runoff and reduce the amount of infiltration rate. The increase in surface runoff and decrease in the infiltration rate leads to an increasing in flooding.

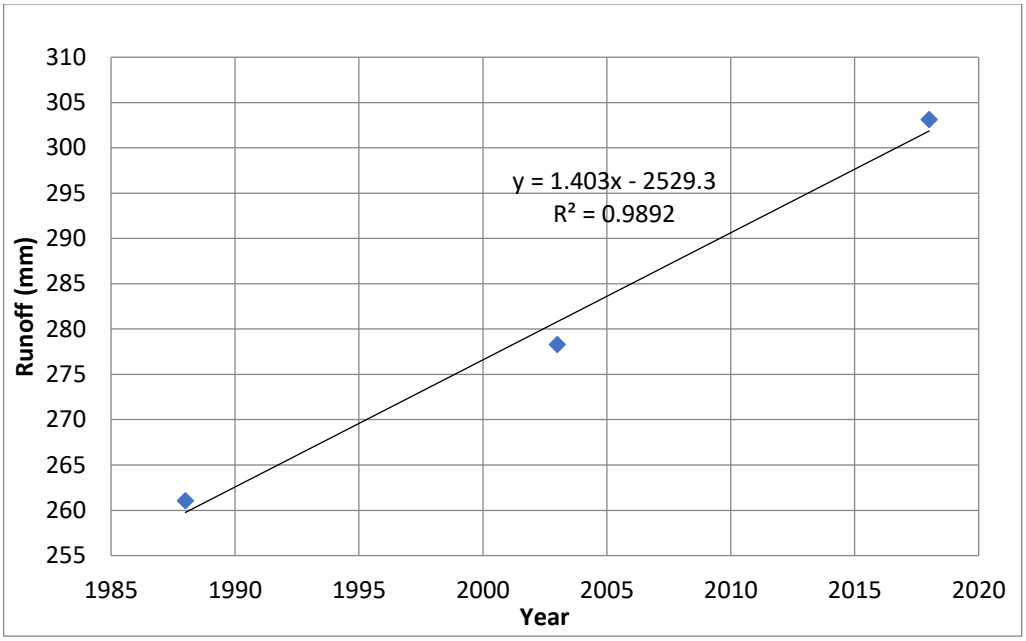

Figure 4. 5 Runoff Trend Line for the three LULC scenario

4.5 The Impact of Land use/land cover Change on Surface Runoff

The change in LULC may affect the hydrology of the watershed, such as runoff, soil erosion, flood hazard, groundwater, and surface water. In the present study the change in the impervious (built-up) area, forestland, and agricultural land increase the runoff process in the watershed. The amount of runoff increases during the rainy season (June-September) in the 2003 LULC from the 1988 LULC by 17.27 mm. Which is 261.03mm in the LULC of 1988 and 278.27mm in the LULC of 2003. Consequently, in the LULC of 2018, the runoff rapidly increased from 278.27 to 303.12 mm in the watershed. This is due to the rapid urbanization and decrement of forestland in the Akaki Watershed. The LULC analysis of the Akaki Watershed, which was presented in Table 4. 1 showed that in 2003 LULC, the built-up area had been increased by 86.24 % (+97.06 km^2) and simultaneously, the agricultural area had been reduced by 9.1 % (-122.61 km^2) as compared to the land use of the year 1988. In the LULC of 2018, the built-up area had been increased by 120 % (251.74 km^2). Also, the forest land and agricultural land had been reduced by 44.09 %, (-149.34 km^2) and 8.06% (98.68 km^2) respectively. As compared with the land use of 2003. Through the entire study period (1988 -2018) the built environment had been increased by 309.93 % (+348.79 km^2) and simultaneously, the agricultural, forest, and water bodies had been decreased by -40 % (-126.36 km^2), -16.43 % (-221.29 km^2) and -9 % (1.14 km^2) respectively.

The increase in the built environment and the decrease in agricultural, and forest leads to an increase in peak runoff and flooding in Akaki Watershed. in the present study, the runoff had been increased from 260.0 mm to 278.27mm, and 303.12 mm in the land use/land cover of 1988,2003, and 2018 respectively. The runoff increases due to reduction of the forest, and the increment of farmland and settlement(Berhanu, 2018). The increase or decrease of the surface runoff depends on the amount of built-up area (Younis and Ammar, 2017). The study conducted in Beijing (China) shows urbanization leads to the increased impervious surface which results in increases in surface runoff (Hu, Fan, and Zhang, 2020). The study conducted in East Africa completely agrees with the present study, forest cover loss leads to increases in surface runoff (4–90%). Results from case studies with forest cover increase scenarios show that surface runoff decreased with forest cover gain(Guha, 2018).as the vegetative area decreased by 7.81% from the 1980s to the 1990s, and the percentages of cropland, barren areas, and urban and built-up areas increased by 2.39, 5.43, and 0.11 %, respectively, the surface runoff also increases by 54.25% due to the increased human activities (Yin *et al.*, 2017). The increase of deforestation and urbanization increases surface runoff (Gebresamuel, Singh and Dick, 2010). All of the above-cited studies agree with the present study, which is conducted in the Akaki Watershed.

4.6 CHIRPS Validation Result

The Pearson Correlation coefficient is used to evaluate the strength of the linear relationship between the satellite rainfall and the reference ground station rainfall (Ayehu *et al.*, 2018). The value of negative results shows the two products have negatively correlated whereas a value of positive results shows that the two products have positively correlated. The minimum time scale used in the validation of chirps by the reference ground station was the monthly and yearly time scale. There were found good agreement between the ground rain gage station and CHIRPS rainfall product over the study area with a correlation coefficient of ($r^2 = 0.92$).

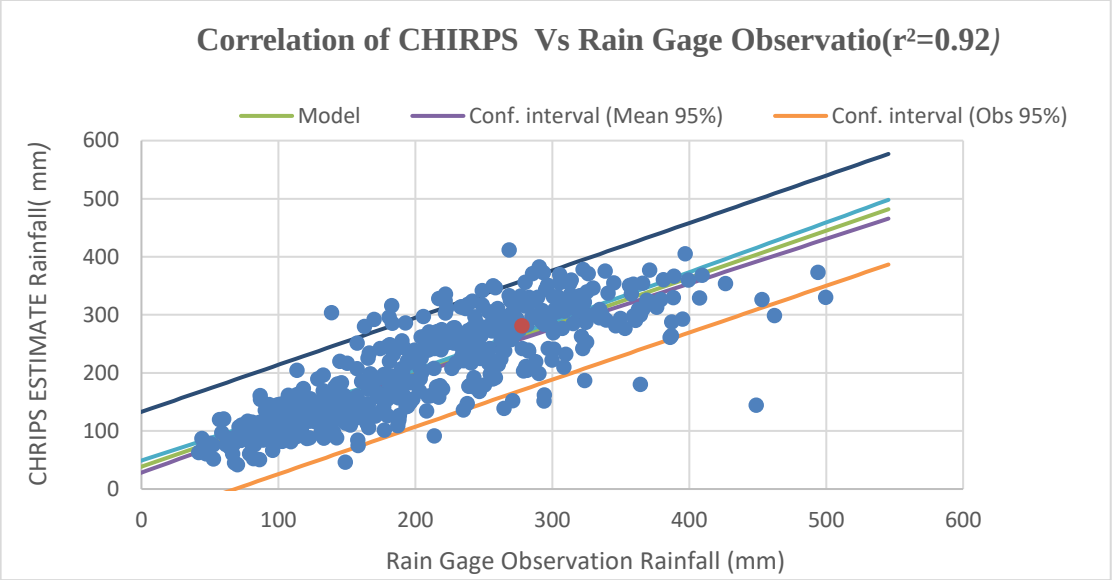

Figure 4. 6 Scatter plot shows Correlation of CHIRPS Estimate Rainfall Vs Ground Rain Gage Observation Rainfall Values

4.7 Flood Hazard Prone Areas Based on Different Causative Factors

The flood hazard-prone area was computed using the multi-criteria decision-making techniques, by integrating different causative factors such as elevation, slope, drainage density, rainfall, runoff, land use, and TWI, using the analytic hierarchy process (AHP) The method was developed by Satty (1980). The delineation of flood hazard mapping in the present study mainly passes four main steps, such as forming pairwise comparison, standardization of the criteria weight, estimation of each criterion rank, and summation of the causative factors.

In the present study, the pairwise comparison was framing by comparing each pair of criteria with the goal of the problem (flood hazard mapping), the weight of each criterion was given based on Satty nine-point scale by looking at real problems, considering the role of each criterion for flood hazard and risk susceptibility, researchers knowledge of view, related research works, and different local expert knowledge of the view. The framing pairwise comparison is shown in Table 4. 3.

Factors	Elevation	Slope	LULC	Rainfall	Drainage density	Soil Type	Runoff	TWI
Elevation	1.00	1.00	3.00	5.00	6.00	7.00	5.00	8.00
Slope	1.00	1.00	3.00	5.00	6.00	7.00	7.00	8.00

LULC	0.33	0.33	1.00	3.00	3.00	4.00	5.00	7.00
Rainfall	0.20	0.20	0.33	1.00	2.00	3.00	3.00	5.00
Drainage density	0.17	0.17	0.33	0.50	1.00	3.00	3.00	5.00
Soil Type	0.14	0.14	0.25	0.33	0.33	1.00	3.00	3.00
Runoff	0.20	0.14	0.20	0.33	0.33	0.33	1.00	3.00
TWI	0.13	0.13	0.14	0.20	0.20	0.33	0.33	1.00

Table 4. 3 Pairwise Comparison Matrix for Flood Hazard delineation

Table 4. 4 Computed Normalized Matrix and Criteria Weight Vector

	Elevation	Slope	LULC	Rainfall	Drainage density	Soil Type	Runoff	TWI	Weight
Elevation	0.316	0.321	0.363	0.325	0.318	0.273	0.183	0.200	0.287
Slope	0.316	0.321	0.363	0.325	0.318	0.273	0.256	0.200	0.297
LULC	0.105	0.107	0.121	0.195	0.159	0.156	0.183	0.175	0.150
Rainfall	0.063	0.064	0.040	0.065	0.106	0.117	0.110	0.125	0.086
Drainage density	0.053	0.054	0.040	0.033	0.053	0.117	0.110	0.125	0.073
Soil Type	0.045	0.046	0.030	0.022	0.018	0.039	0.110	0.075	0.048
Runoff	0.063	0.046	0.024	0.022	0.018	0.013	0.037	0.075	0.037
TWI	0.039	0.040	0.017	0.013	0.011	0.013	0.012	0.025	0.021
									1.000

In pairwise comparison, some of the decision-makers fall with the matrix inconsistency when they evaluate the given criteria. To overcome the problem of inconsistency the AHP incorporates an effective method for checking the consistency of the evaluations made by the decision-makers.

Table 4. 5 Values of the Random Index (RI)

n	2	3	4	5	6	7	8	9	10
RI	0	0.58	0.90	1.12	1.24	1.32	1.41	1.45	1.51

Table 4. 6 computation of consistency index and consistency ratio

	Elevation	Slope	LULC	Rainfall	Drainage density	Soil Type	Runoff	TWI	SUM	SUM/Weight
Elevation	0.287	0.297	0.451	0.432	0.438	0.336	0.186	0.171	2.597	9.034
Slope	0.287	0.297	0.451	0.432	0.438	0.336	0.260	0.171	2.671	9.006
LULC	0.096	0.099	0.150	0.259	0.219	0.192	0.186	0.149	1.350	8.989
Rainfall	0.057	0.059	0.050	0.086	0.146	0.144	0.111	0.107	0.761	8.821
Drainage density	0.048	0.049	0.050	0.043	0.073	0.144	0.111	0.107	0.626	8.577
Soil Type	0.041	0.042	0.038	0.029	0.024	0.048	0.111	0.064	0.398	8.275
Runoff	0.057	0.042	0.030	0.029	0.024	0.016	0.037	0.064	0.300	8.080
TWI	0.036	0.037	0.021	0.017	0.015	0.016	0.012	0.021	0.176	8.249
Sum weight										69.032
lambda max										8.63
CI										0.09
CR										0.06

A perfectly consistent decision-maker should always obtain *CI*=0, but a small amount of inconsistency may be tolerated. A minimum value of tolerated CR< 0.1 (Hillier *et al.*, 2012). The CR value was estimated to 0.06 since it is accepted. Now we can continue the process of decision-making using AHP. Finally, the final computed weight vector values were used as the coefficient for the respective flood hazard factors such as elevation, slope, TWI, runoff, land use, rainfall, drainage density, and soil type layers to be combined in the weighted overlay in ArcGIS to generate the final flood hazard map of the Akaki Watershed using the following equation.

Table 4. 7 Computed weight vectors of each factors

Factors	Elevation	Slope	LULC	Rainfall	Drainage density	Soil type	Runoff	TWI
Weight	0.287	0.297	0.150	0.086	0.073	0.048	0.037	0.021

4.7.1 Topographic Wetness Index

The Topographic Wetness Index (TWI) is the most commonly used hydrologically-based topographic index that describes the tendency of a cell to accumulate water and is used to identify the flood-prone areas (Mattivi *et al.*, 2019). The wetness index is one of the flood causative factors and is commonly used to quantify topographic control on hydrological processes. The index is a function of both the slope and the upstream contributing area per unit width orthogonal to the flow direction (Abuzied and Mansour, 2018). The Methods

of computing this index differ primarily in the way the upslope contributing area is calculated by the following formula(Abuzied and Mansour, 2018).

$$TWI = \ln\left(\frac{a}{tan(\beta)}\right) \quad \text{(4.0)}$$

Where a is the specific catchment area [a=A/L, catchment area (A) divided by contour length (L)] and tan B is the slope.

In the present study, the topographic wetness index was derived from ALOS DEM. with a spatial resolution of 12.5 m, which was downloaded from the Alaska satellite facility and reclassify into five classes as per flood susceptibility. The area of the watershed having higher values of TWI are more vulnerable to flood inundation and the lower value of the TWI are less vulnerable to flood inundation map(Shafizadeh-Moghadam *et al.*, 2018).

Table 4. 8 Topographic Wetness index suitability for Flood Hazard Zonation

TWI	Description	Ranking	Classification
1.28- 4.8	Very high Dry	1	Very Low
4.8 -7.1	High Dry	2	Low
7.1 – 8.7	Moderately Dry	3	Moderate
8.7 – 10.8	High wet	4	High
10.8 – 19.1	Very high Wet	5	Very High

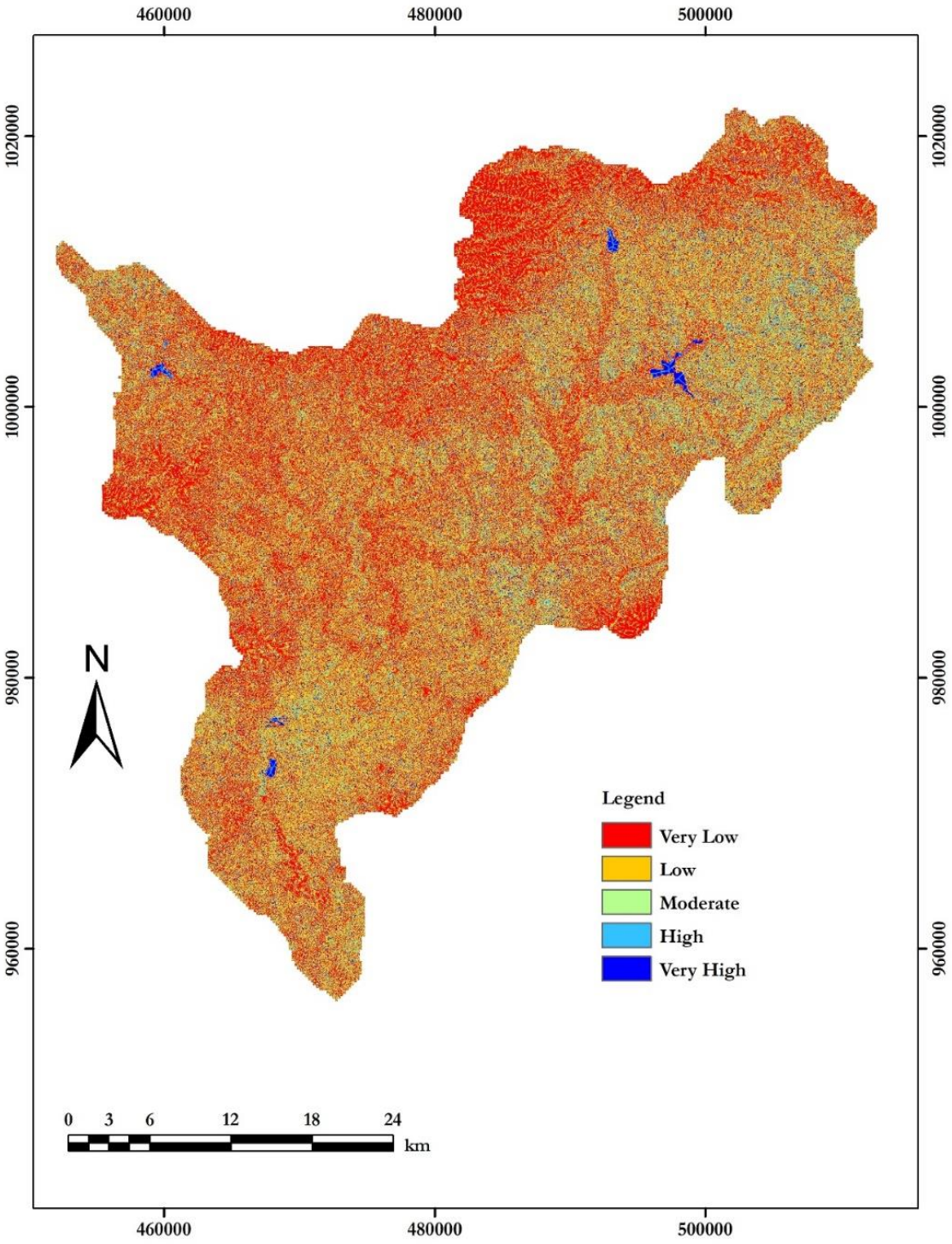

Figure 4. 7 Reclassified TWI suitability for flood hazard delineation.

4.7.2 Elevation Factor

In the present study, the elevation is the main flood-generating factor; the elevation map of the study area was extracted from ALOS PALSAR DEM. The value of elevation ranges from (1810 m to 3382m) and then elevation was classified into five classes and ranked as per flood hazard susceptibility. An area having the lowest elevation is highly affected by flood and an area having the highest elevation lowly affected by the flood, this is due to water flows from a higher elevation to the lowest elevation. The elevation was classified and ranked based on different works of literature such as (Gashaw and Legesse, 2011; Gebre SL, 2015; Assefa, 2018).

Table 4. 9 Summary of Elevation Classification and Ranking for flood hazard delineation.

Elevation (m)	Ranking	Classification
1,810 - 2,161.39	5	Very High
2,161.4 -2,377.15	4	High
2,377.15-2,574.4	3	Moderate
2,574.42-2,802.52	2	Low
12,802.52 - 3,382	1	Very Low

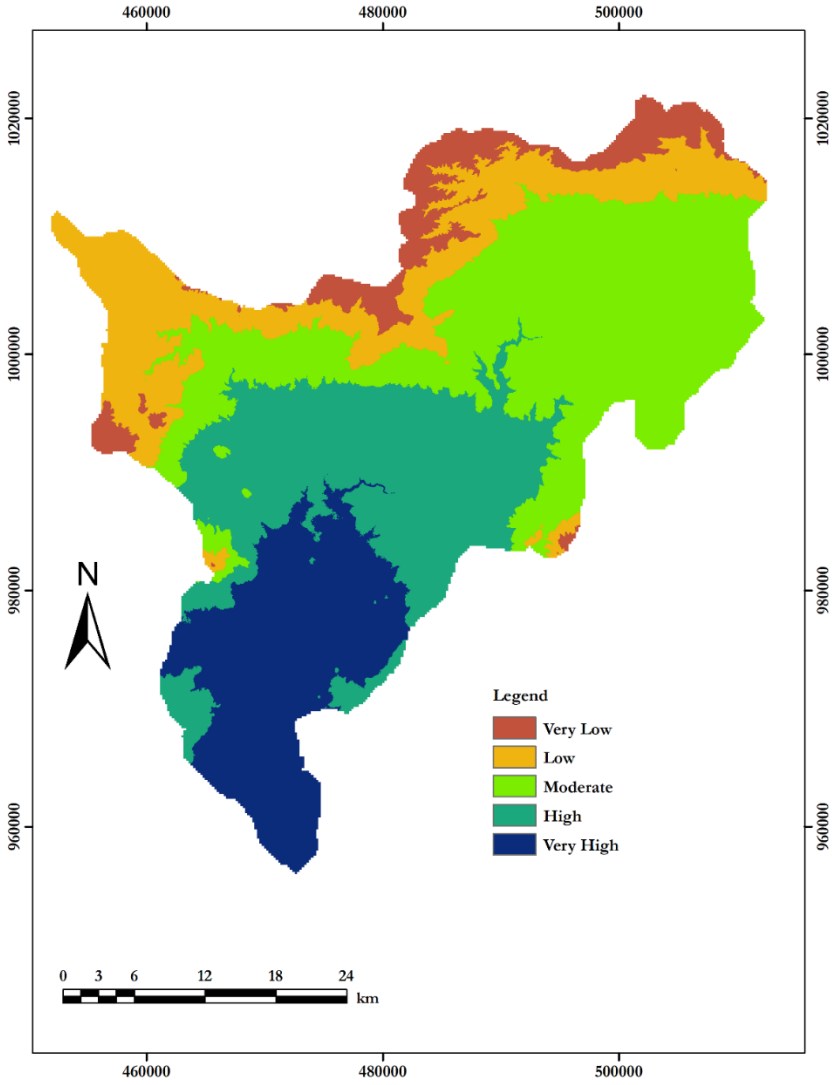

Figure 4. 8 Reclassified Elevation suitability for flood hazard delineation

4.7.3 Soil Type

In the present study, five main soil classes were distinguished based on the hydrologic soil grouping system of the Ministry of agriculture, *Chromic Luvisols, Eutric Vertosols, Humic Nitisols, Lithic Latosols, Water bodies, and Vertic Cambisols.* The most dominant soil type in the study area is Eutric vertisols which cover an area of 1039.91 Km^2 have a percentage of 58% from a total soil type in the study area. These five groups of soil types were converted into raster and reclassified based on the rate of flood generating capacity. The soil type that has a very high capacity to generate a very high flood rate is ranked as class 5, high ranked as class 4, Moderate ranked as 3, low ranked as 2, very low ranked as 1, the classification of soil type as per the suitability of flood hazard vulnerability (Gebre SL, 2015).

Table 4. 10 summaries of soil type classification and ranking for flood hazard mapping

Soil Type	Ranking	Classification
Lithic Leptosols	1	Very Low
Chromic Luvisols	2	Low
Humic Nitisols	3	Moderate
Vertic Cambisols	4	High
Eutric Vertisols	5	Very High

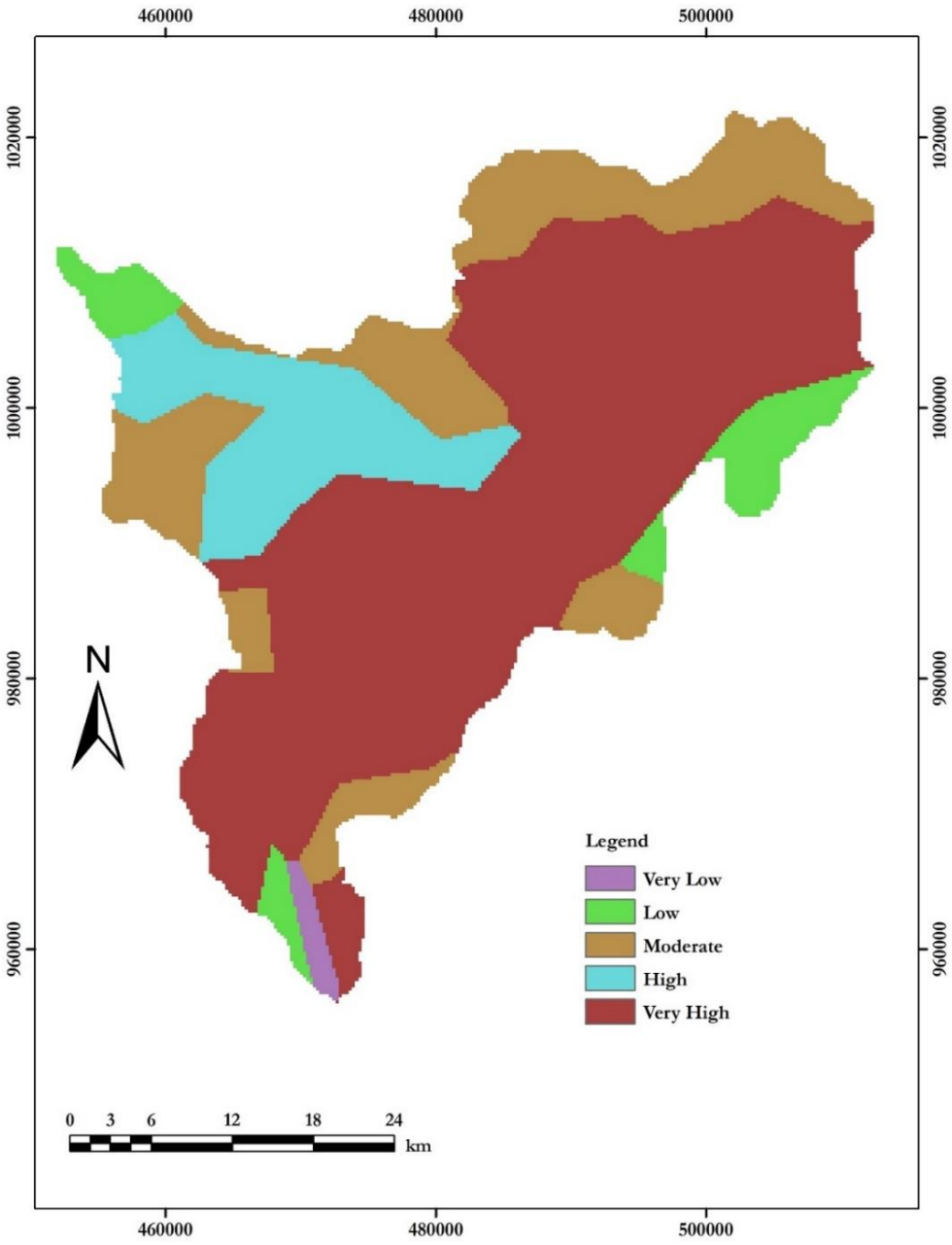

Figure 4. 9 Reclassified Soil Map for flood hazard delineation

4.7.4 Rainfall Factor

In the present study, the rainfall data for the Akaki Watershed was collected from the CHIRPS data portal from the year *(1988-2018)* and the annual average value of the rainfall was generated. Based on the importance of flood hazard delineation the average annual rainfall was reclassified into five categories, which are shown in Table 4. 11.Based on flood hazard susceptibility the rainfall was classified and ranked into five classes Such as class (1,152.48 -1,264.93mm), (1,084.77-1,152.48mm), (1,032.38 - 1,084.77mm) (986.38-1,032.38mm) and (939.11-986.38 mm) rated and ranked 5 to 1 (Very high to very low) respectively. The classification of rainfall for flood hazard delineation was based on different works of literature such as (Alemu, 2008; Gebre SL, 2015; Ogato *et al.*, 2020).

Table 4. 11 Rainfall suitability for Flood Hazard Zonation.

Factor	Class(mm)	Rank	Classification
Rainfall (mm)	939.11-986.38	1	Very low
	986.38 -1,032.38	2	Low
	1,032.38 - 1,084.77	3	Moderate
	1,084.77 - 1,152.48	4	High
	1,152.48 - 1,264.93	5	Very high

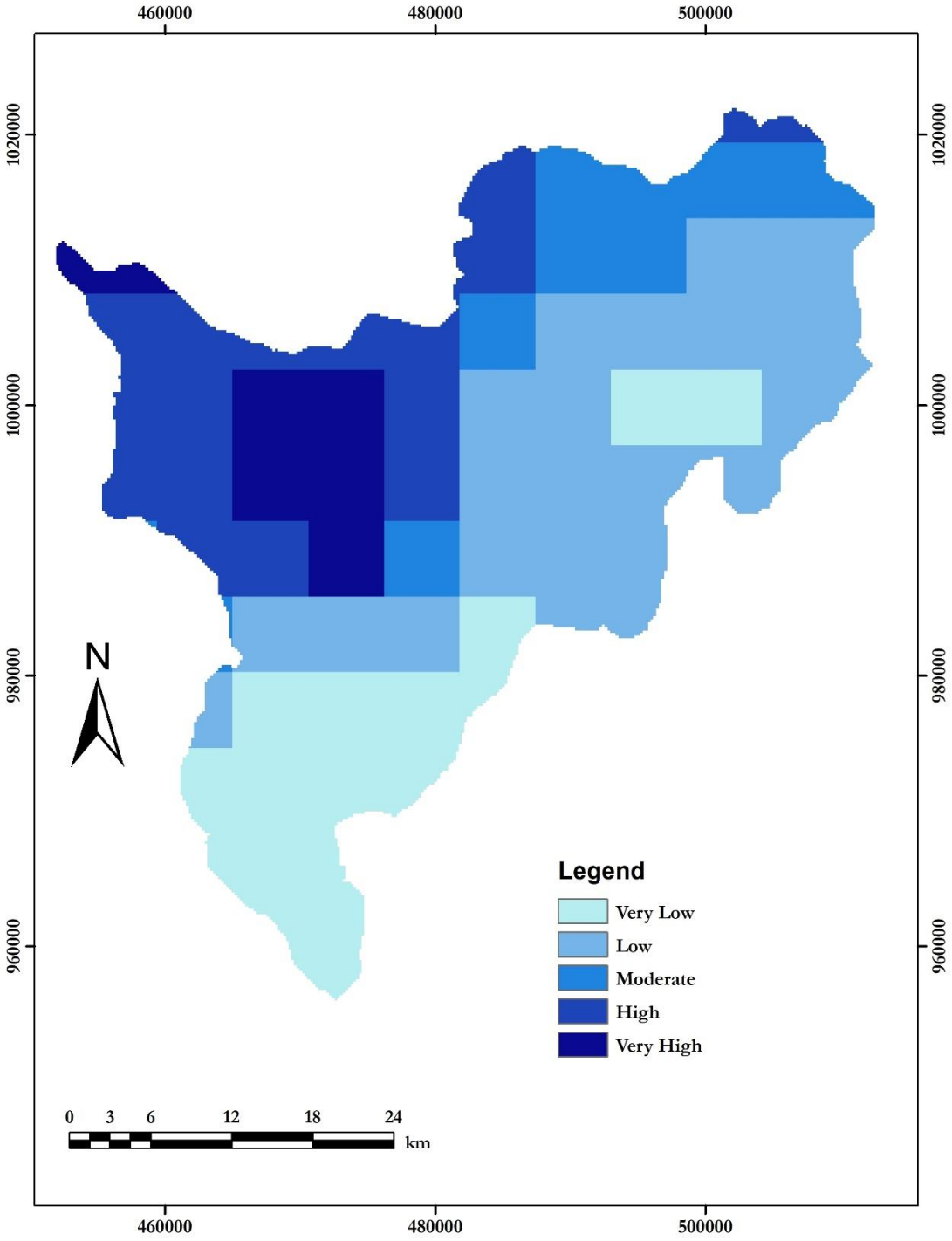

Figure 4. 10 Rainfall suitability for flood hazard delineation

4.7.5 Slope Factor

The slope was derived from ALOS DEM with a spatial resolution of 12.5m×12.5m in ArcMap using Slope tools in Spatial Analyst. According to FAO, the 2006 slope classification system, the slope was classified into five categories from gently sloping to a steep slope. Further, it was reclassified into five classes based on a 1 to 5 scale, where the lower value of the slope was assigned as a value of 5 and the higher value of the slope was assigned as a lower slope value. This means the lower value of slope has the probability of flood hazard occurrence and vice versa.

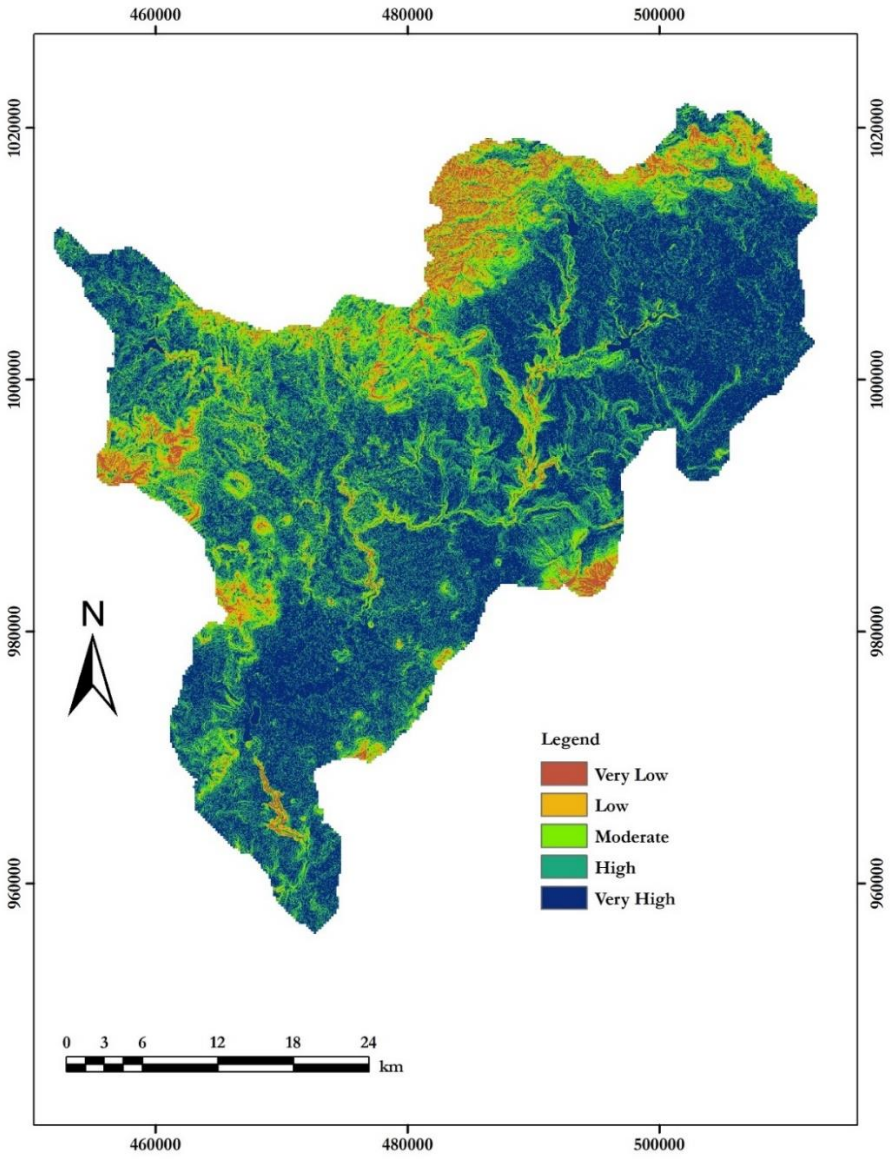

Figure 4. 11 Reclassified Slope suitability for flood hazard delineation

Table 4. 12 Slope Suitability for Flood Hazard

Slope (degree)	Classification	Ranking
0-5	Very highly vulnerable	5
5.1-10	Highly vulnerable	4
10.1-15	Medium vulnerable	3
15.1-25	Low vulnerable	2
>25	Very low vulnerable	1

4.7.6 Drainage Density Factor

The extraction of drainage networks from the DEM in the Akaki Watershed was carried out using the Arc Hydro tools, which is the extension of ArcGIS. Arc Hydro tools are based on the most commonly used methods of flow direction determination which is the D8 algorithm(Liu and Zhang, 2010). For accurate delineation of the drainage network, high-resolution DEM or hydrologically sound DEM is necessary (Liu and Zhang, 2010). According to Horton (1945), the drainage density was determined by the ratio of the total length of the stream segments in the given watershed to the total area of the given watershed. The resulted in drainage density of the study area ranges from 0 to 3.67 km/km^2. The area of high drainage density indicates high runoff potential and low infiltration rate so flood hazard has more chance to occur in the area of high drainage density and has a low chance in the area of low drainage density (Gebre SL, 2015).

Table 4. 13 ranked and classified Drainage density for flood hazard delineation

Drainage Density (km/km^2)	Description	Ranking	Classification
0- 0.46	Very low density	1	Very low flood
0.46-0.98	Low density	2	Low flood
0.98 – 1.57	Moderate density	3	Moderate Flood
1.57 - 2.20	High density	4	High flood
2.20 -3.67	Very high density	5	Very high Flood

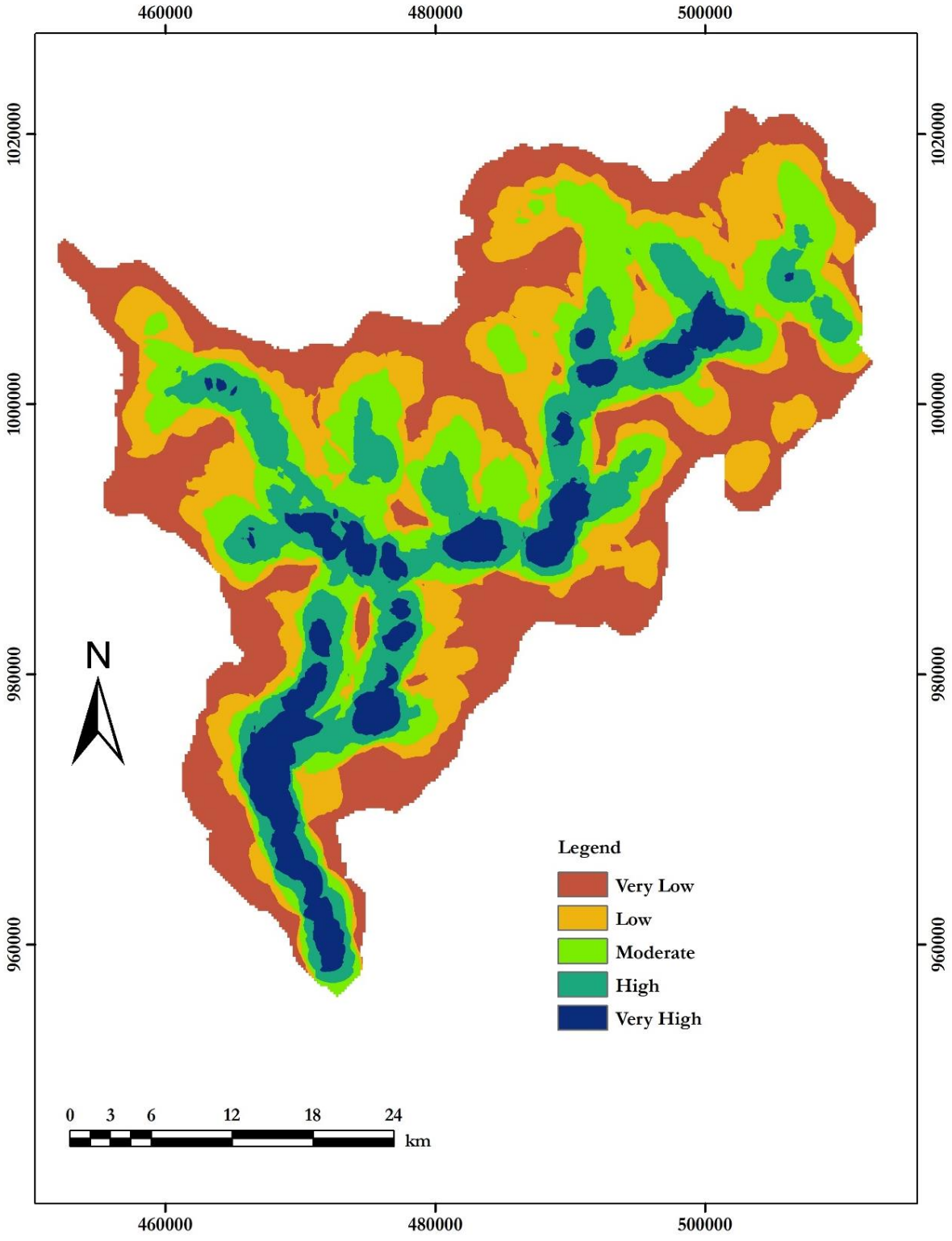

Figure 4. 12 Drainage Density suitability Map for delineation of flood hazard.

4.7.7 Runoff Map Factor

The runoff was computed using the SCS CN method, the runoff value ranges from (19.2-367.3 mm), the runoff was classified into five class and ranked as per flood hazard susceptibility. An area having high runoff is highly affected by flood and an area having low runoff lowly affected by the flood. The runoff was classified and ranked into the following five classes as per vulnerability of flood hazard and the classification was based on the work of different kinds of literature such as (Abuzied and Mansour, 2018; Talisay, Puno, and Amper, 2019; Morea and Samanta, 2020).

Table 4. 14 Runoff suitability for Flood Hazard Zonation

Runoff (mm)	Ranking	Classification
19.2- 68.2	1	Very low
68.2 - 99.6	2	Low
99.6 - 158.4	3	Moderate
158.4 - 221.2	4	High
221.2 - 367.3	5	Very high

4.7.8 Land use/land cover factors

In the present study, the land use/land cover data were extracted from a series of Landsat imagery such as TM^{+}, ETM, and OLI. The land use/land cover map of the present study was classified based on the first level of image classification and reclassified and rated based on flood hazard generating capacity. The classification of LULC was based on the susceptibility of flood hazard as shown in Table 4. **15**.

Table 4. 15 Land use/land cover suitability for Flood Hazard Zonation.

LULC	Ranking	Classification
Forest	1	Very Low
Agriculture	3	Moderate
Built-Up	4	High
Water	5	Very High

Source: (Morea and Samanta, 2020)

4.8 Flood Hazard Zoning

Flood hazard zoning is the process of determining the degree of susceptibility of a given place to flooding and is indicated by the resultant values of pixels (Dejene, Boja, and Meseret, 2017). In the present study, the flood hazard zone was produced by the flood causative factors such elevation, slope, drainage density, TWI, rainfall, land use, surface runoff, and soil type for the three-land use scenario such as 1988 land use, 2003 land use, and 2018 land use.

The flood hazard map, as well as the flood risk maps, have been developed for different land-use scenarios such as for the LULC of 1988, 2003, and 2018 by integrating different causative factors of flood hazard and risk in the Akaki Watershed. The flood hazard maps of the present study in Figure 4. 13 shows that 29.68, 274.53,961.25, 513.16, 8.92 km^2 of the Akaki Watershed were subjected to Very low flood hazard, low flood hazard, moderate flood, high flood, and very high flood respectively in the land use/land cover of 1988. The percentage of the flooded area in the Akaki Watershed of the 1988 land use/land cover is 1.66 %,15.36 %,53.77%,28.71 %, 0.50 % were subjected to very low flood hazard, low flood hazard, moderate flood hazard, high flood hazard, and very high flood hazard respectively. in the LULC of 2003, the flood hazard was also estimated to 124.83,274.81, 915.62, 562.63, 9.65 km^2 which is subjected to very low flood hazard, low flood hazard, moderate flood hazard, high flood hazard, and very high flood hazard respectively. in addition to the LULC of 1988 and 2003, the LULC of 2018 was estimated to 17.12, 233.28, 698.21, 827.38, 11.56 $km^2$of the watershed which is subjected to very low, low, moderate, high, and very high flood hazard respectively. As the result obtained from the present study the change in land use/land cover such as rapid urbanization, and deforestation are the main cause of the increase in flood hazard in the Akaki Watershed. As the analysis of flood hazard indicates the high and very high flood hazard was estimated to 513.16, 8.92 km^2 in the land use of 1988, and 562.63, 9.65 km^2 in the land use of 2003, and also 827.38, 11.56 km^2 in the land use of 2018.

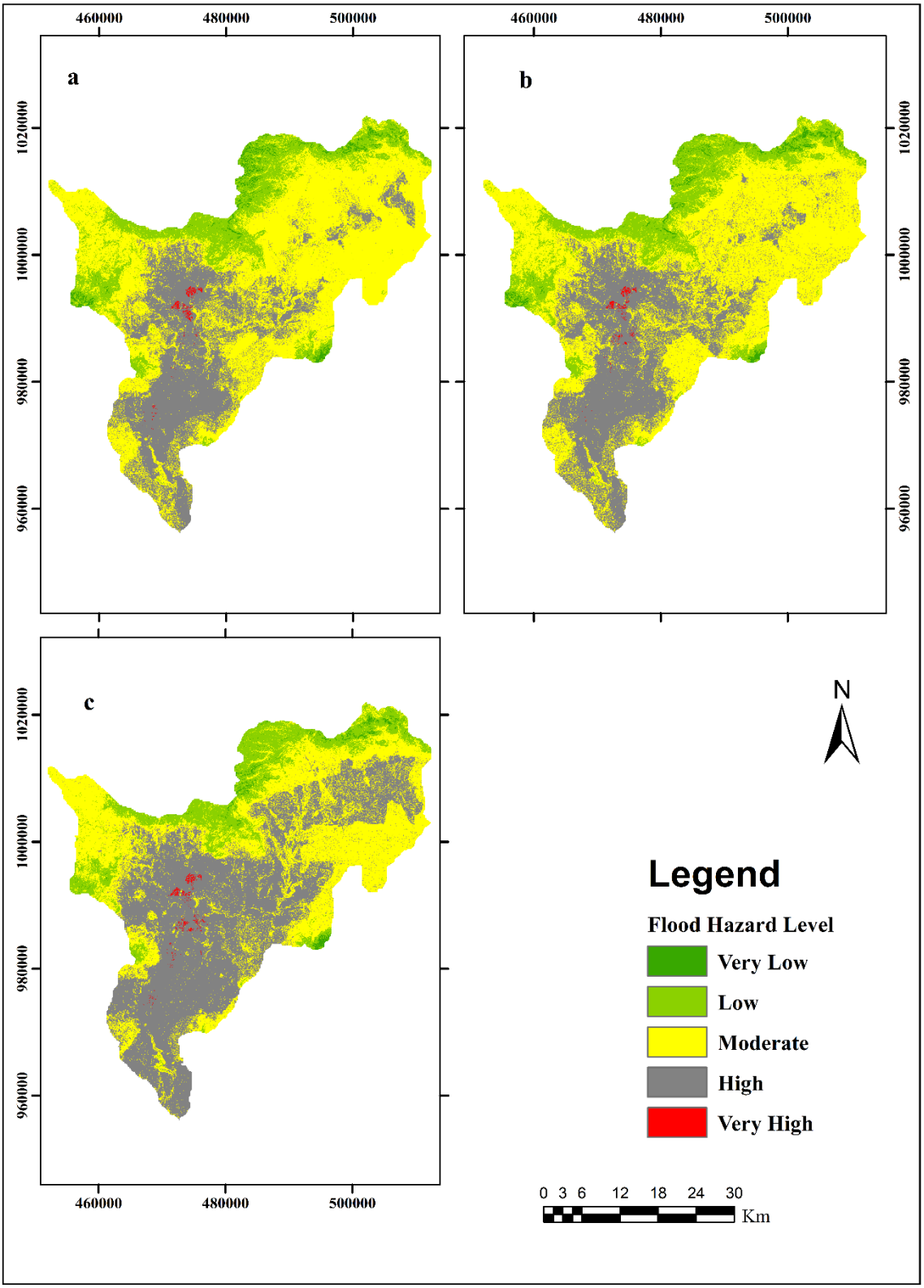

Figure 4. 13 Flood hazard estimation of LULC 1988(a), LULC 2003 (b), and LULC 2018(C).

Table 4. 16 Area coverage of flood hazard in different years

Flood hazard group	1988	2003	2018
Very low	29.68	24.83	17.12
Low	274.53	274.81	233.28
Moderate	961.25	915.62	698.21
High	513.16	562.63	827.38
Very high	8.92	9.65	11.56

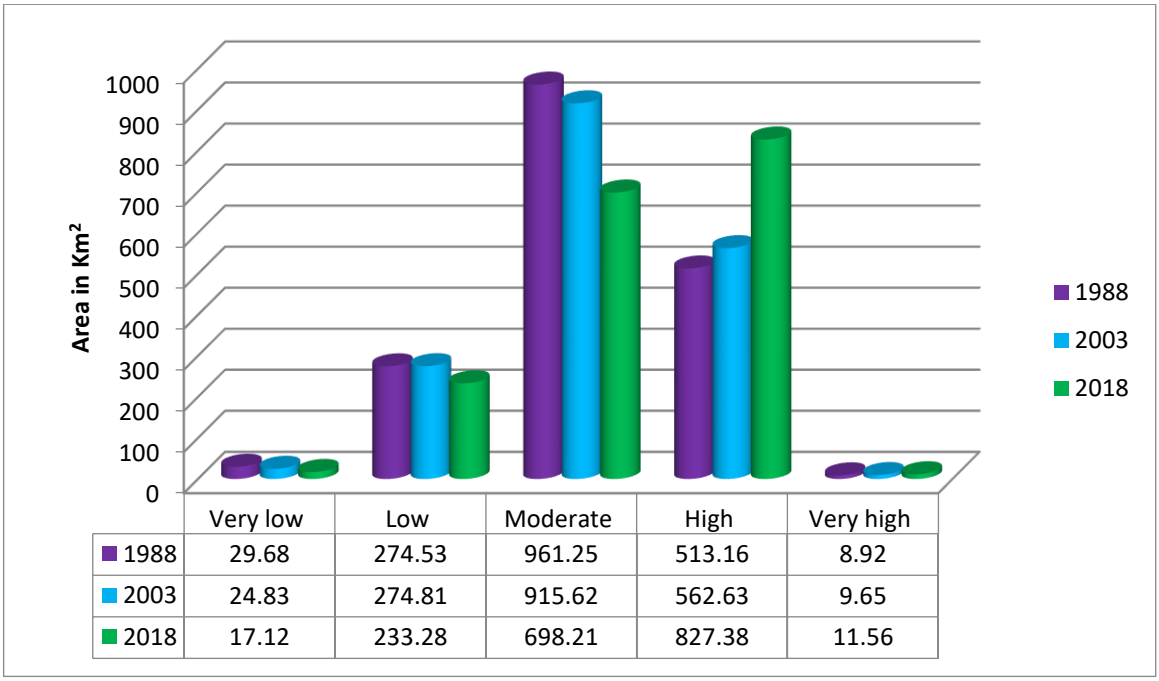

Figure 4. 14 Flood hazard level in different years.

The change in land use/land cover affects the flood hazard, due to rapid urbanization. The loss of forest cover also contributed significantly to increased flood hazards (Rijal, Rimal, and Sloan, 2018). Urbanization is the main cause of changes in hydrologic and hydraulic processes, loss of existing drainage capacity, and flooding in urban areas. It increases the total runoff volume and peak discharge of storm runoff events (Zope, Eldho, and Jothiprakash, 2016). The result of the present study is similar to many studies considering LULC changes and their impact on flooding hazard and runoff formation such as (Zope, Eldho and Jothiprakash, 2015, 2016, 2016; Brevante, 2017; Rijal, Rimal, and Sloan, 2018; Szwagrzyk *et al.*, 2018).

4.9 Flood Vulnerability Analysis

4.9.1 Population Density

The population density had been considered as one of the social factors in flood risk analysis. It was computed based on the projected value of CSA 2018 in the woreda level of the watershed. Further, the population density was reclassified into five sub-factors. the reclassified population density was rated and ranked based on the level of risk. The denser the population the more vulnerable to flooding and the lesser the density the lower the vulnerability to flooding.

4.9.2 Distance from river

The distance from the river is one of the factors of flood risk assessment; it was computed using multiple ring buffer analysis. The buffering had been computed at a distance of 1000m, 1500m, 3000m, 6000m, and 1500m. These values were further rated and classified into five classes such as Very high (1000m), high (1000-1500m), moderate (1500-3000), low (3000 -6000m), and Very low (6000-1500m). The more the nearest to the river have more chance to flood risk.

4.9.3 Road density

The road density was computed from the major road network of the Akaki Watershed using a line density module in spatial analyst. Line Density Calculates a magnitude-per-unit area from polyline features that fall within a radius around each cell. The computed road density was further reclassified into five subgroups using standard classification schemes. Also, level as the higher the density will be expected to more vulnerable to flooding, and the lower the density will be expected to low vulnerable to flooding.

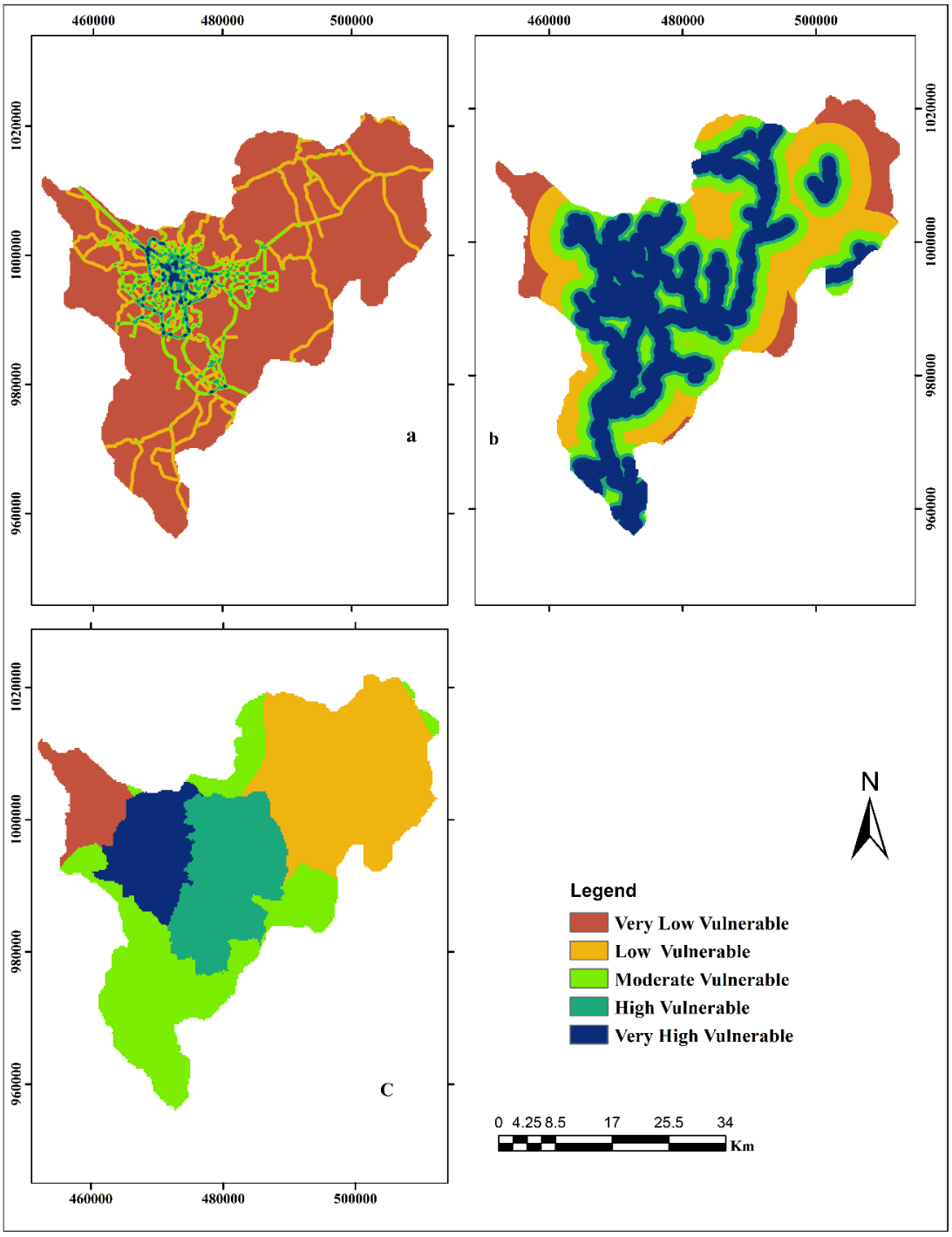

Figure 4. 15 Infrastructure (Road) vulnerability (a), distance to river (b) vulnerability and population vulnerability (c)

4.9.4 Total Vulnerability of flood risk

The total Vulnerability index of flood risk mapping had been computed with the help of multicriteria decision-making techniques using different causative factors such as distance to a river, population density, road density, and land use/land cover by forming a pairwise comparison.

Table 4. 17 Pairwise comparisons matrix for total Vulnerability index

Factors	Distance to River	Population	Road density	Land use
Distance to River	1.00	2.00	3.00	4.00
Population	0.50	1.00	2.00	3.00
Road density	0.33	0.50	1.00	3.00
Land use	0.25	0.33	0.33	1.00
Sum	2.08	3.83	6.33	11.00

Table 4. 18 Standard Normalized Matrix

Factors	Distance to River	Population	Road density	Land use	Weight
Distance to River	0.48	0.52	0.47	0.36	0.46
Population	0.24	0.26	0.32	0.27	0.27
Road density	0.16	0.13	0.16	0.27	0.18
Land use	0.12	0.09	0.05	0.09	0.09
Total					1.00

Table 4. 19 CI and CR computation

Factors	Distance River	Population	road density	Land use	Sum	Sum/Weight
Distance: River	0.46	0.54	0.54	0.35	1.90	4.12
Population	0.23	0.27	0.36	0.26	1.13	4.13
Road density	0.15	0.14	0.18	0.26	0.73	4.06
Land use	0.11	0.09	0.06	0.09	0.35	4.03

After forming the pairwise comparison matrix, the weight of each flood vulnerability causative factor was computed and the consistency of the matrix was computed using equation (25). As the result revealed that, the consistency index (CI) and consistency ratio (CR) is 0.029 and 0.033 respectively.

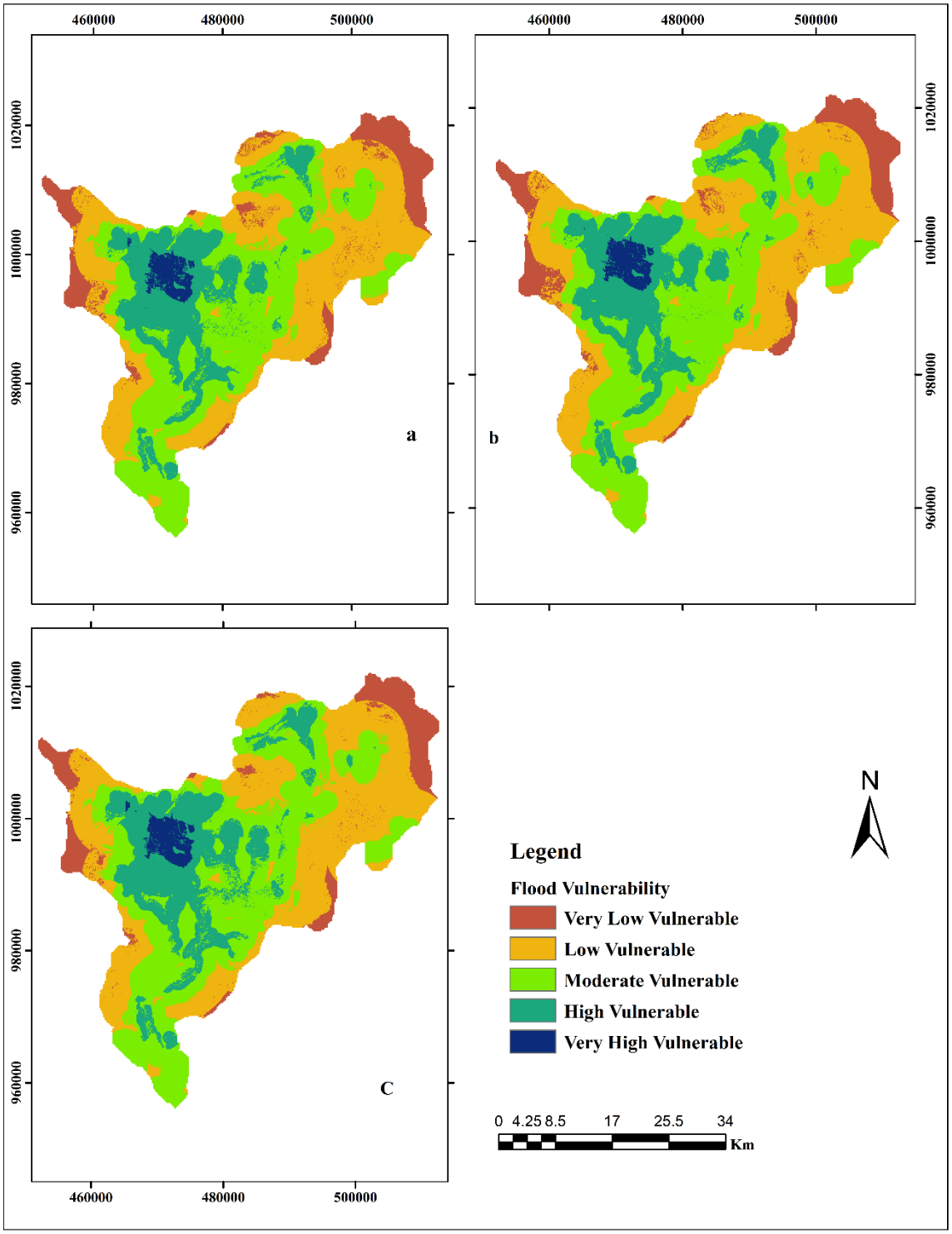

Figure 4. 16 Total Vulnerability of flood risk in different LULC 1988 LULC (a), 2003LULC, 2018 LULC (C).

In the present study, the flood vulnerability prone area had been computed with the help of pairwise comparison using four vulnerability index such as road density as infrastructure Vulnerability, population density as asocial vulnerability, distance from the river as ecological vulnerability, and the land use/land cover as economical vulnerability.

The flood vulnerability index had been developed for different land-use scenarios such as for the LULC of 1988, 2003, and 2018. The analysis of total flood vulnerability shown in Figure 4. 16 revealed that, 169.50, 607.27, 660.49, 313.13, and 37.10km^2, which is subjected to very low vulnerability, low vulnerability, moderate vulnerability, high vulnerability, and very high vulnerability respectively in the land use of 1988. In the LULC of 2003, the flood vulnerability prone area was also estimated to 165.56, 612.38, 654.7338, 316.72, and 38.11km^2 which is subjected to very low, low, moderate, high, and very high flood vulnerability respectively. In the third land-use scenario, the flood vulnerability results as shown in Figure 4. 16(c) revealed that 153.21, 607.07, 648.20, 338.78, and 38.82km^2 which is subjected to very low, low, moderate, high, and very high flood vulnerability respectively. Within 1km of the riverside, high road density and highly populated near riverside areas of the Akaki Watershed had been highly vulnerable to flooding.

The very low and low vulnerability levels of flood occupy the eastern part and western part of the Akaki Watershed. Whereas the moderate, high and very high vulnerability of flood occupies the central part of the Akaki Watershed. As the analysis of flood vulnerability result revealed the vulnerability increased through the three-land use scenario, which is due to the rapid urbanization, distance from the river, road density, and population density.

4.10 Flood Risk Prone Area

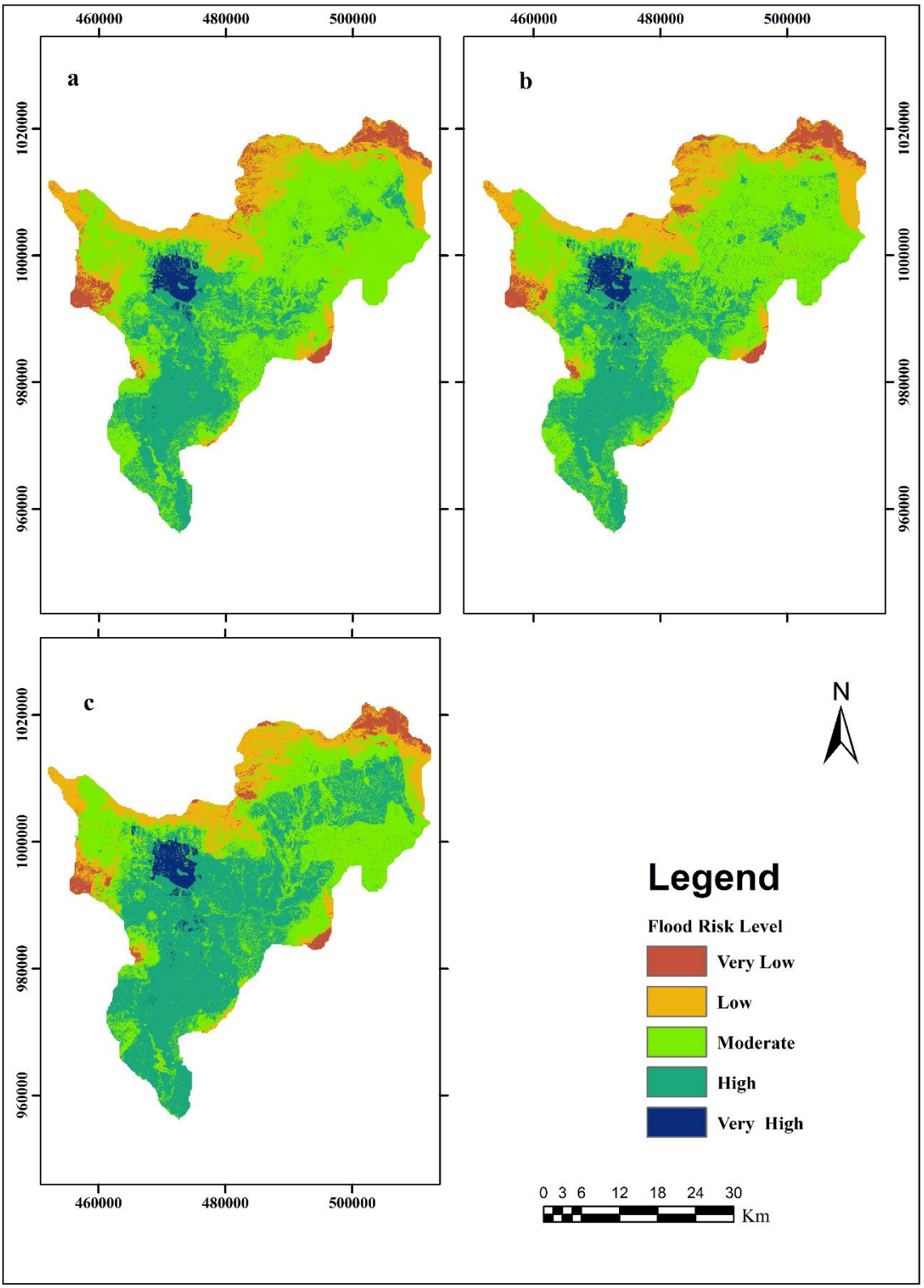

Figure 4. 17 Flood-prone area for (a) 1988, (b) 2003, (C) 2018 LULC

Table 4. 20 Flood Risk Level area coverage of each year

Flood Risk Level	1988	2003	2018
Very low	88.82	86.77	69.46
Low	298.56	297.79	255.04
Moderate	879.20	829.30	632.34
High	481.68	532.81	786.83
Very high	39.30	40.87	43.87

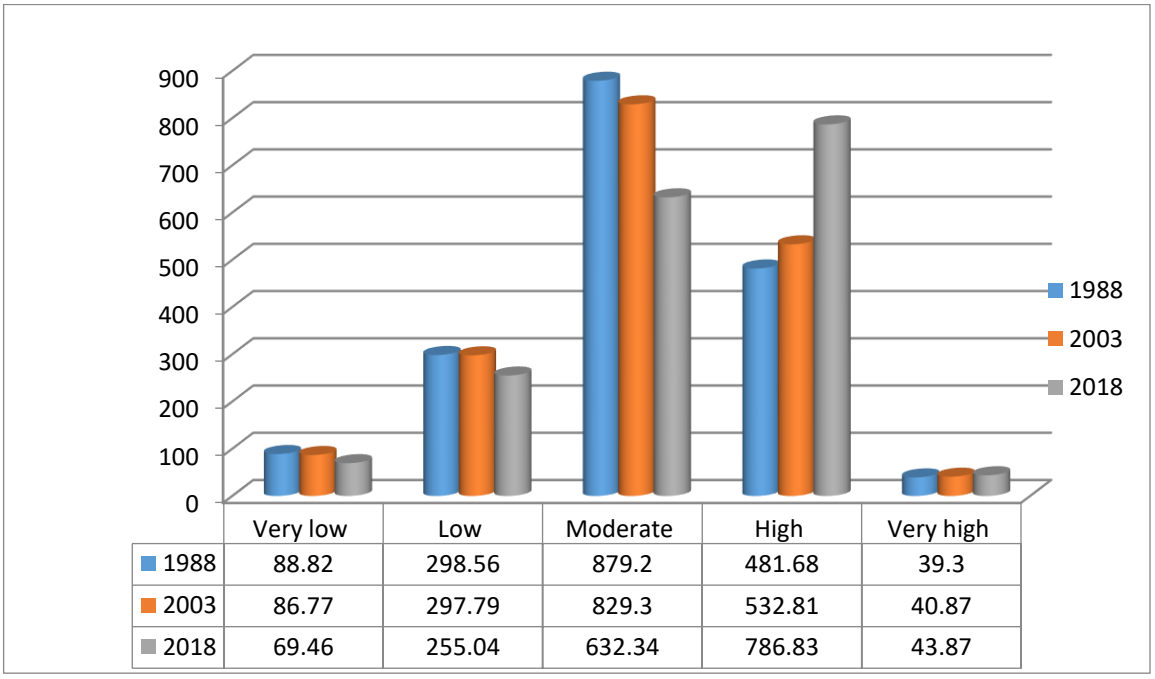

Figure 4. 18 area coverage of flood risk level in each year

The flood risk maps of the present study in Figure 4. 17 shows the level of risks such as Very low flood risk, low flood risk, Moderate flood risk, High flood risk, and Very High flood with the area coverage of 88.82, 298.56, 879.20, 481.68, 39.30 km^2 from the total area in the LULC of 1988 respectively. Consequently, in the land use of 2003 the percent coverage of the flood risk was estimated to 86.77, 297.79, 829.30, 532.81, 40.87 km^2 and in the land use of 2018 the area 69.46, 255.04, 632.34, 786.83, 43.87 km^2 which are attribute to very low, low, moderate, high and very high respectively. The high and very high flood risk levels occupy the area of highly populated, low-lying, high-density road density, and near to riverside of the Akaki Watershed.

Based on the three-land use scenario result, the high and very high flood risk increased from the first land-use scenario to the last scenario, which is, 481.68 km^2, and 39.30 km^2 of the watershed were in the land use of 1988, later it changes to 532.81 and 40.87 km^2 of

the watersheds in the land use of 2003. Although, in the land use of 2018 the high and very high-risk level changes to 786.83, 43.87 km^2 respectively. In the present study, the areas under very low, low, and medium risk of flooding are characterized by high slope, forest land, low population density, and low road density of the Akaki Watershed. In the study conducted by (Hounkpè *et al.*, 2019), the change in LULC significantly affects the degree and occurrence of flood risk.

A similar study was conducted by different authors and in the different study area, the study conducted in fogera by considering the population density, land use, and the level of flood hazard the result indicates agricultural land and highly populated land were faced to under high to Very high flood risk(Alemu, 2008). The study conducted in Cote d'Ivoire shows five levels of flood risk, ranging from very low to very high. Areas under very low, low, and medium risk of flooding cover 5.23 %, 24.37 %, and 36.31 % of Abidjan respectively. The areas under very low, low, and medium risk of flooding are characterized by high slope, vegetation(cropland areas), and low population density(Danumah *et al.*, 2016). The present study completely agrees with the study conducted by different authors.

CHAPTER 5 : CONCLUSIONS AND RECOMMENDATIONS

5.1 Conclusions

The result of the land use /land cover dynamics in the Akaki Watershed confirms there is rapid urban growth or rapid urbanization and causing environmental deterioration. The built-up areas significantly increased from 112.54 to 209.60 km^2 between 1988 and 2003, which is due to the rapid increase of population in the watershed. Between 2003 and 2018, the built environment increased from 209.60 to 461.34 km^2. The water bodies and forest covers are slightly increased from 1988 to 2003 in the area. Although; waterbodies, Agricultural, and forest cover are reducing in between 2003 and 2018. Which is due to the increased urbanization and population growth. The change in land use/land cover could affect peak runoff and flooding. In the present study, surface runoff was computed in three different land-use scenarios, which are the LULC of 1988, 2003, and 2018, as the result revealed that the runoff increased from 261.03 mm to 278.27 mm between 1988 and 2003, which indicates there is a change in the built environment. Consequently, the runoff changes from 2003 to 2018 from 278.27 to 303.12mm. Generally, the runoff increases as the built environment rapidly increase and the forest cover decrease.

The change in land use/land cover affects flooding in the Akaki Watershed, Flood hazard and risk of the Akaki Watershed was computed based on the three-land use scenario and integrated with other causative factors such as elevation, slope, drainage density, rainfall, TWI, and runoff. Based on the Capacity of flood generating factors were selected for the delineation of flood hazard using multicriteria evaluation techniques in GIS. All the selected factors had not an equal contribution to the delineation of the flood hazard zone, due to these reasons the factors were rated and ranked in the Analytical hierarchical process (AHP) using the pairwise comparison matrix for the final spatial weighted overlay analysis of all factors to generate the final flood hazard map of the present study. The flood hazard result indicates that the agricultural, built-up, and downstream or low-lying areas were mainly flooded, which ranges from high to very high.

The major causes of flooding in the present study are the excess amount of rainfall during the rainy season of (June to September), the rapid expansion of the built environment, deforestation, and the topography of the watershed. The flood risk in the present study was

also generating using the product of flood hazard and vulnerability. The flood risk assessment indicates that in terms of risk level highly populated areas, higher road density, and population live near to riverside were faced with high to very high flood risk

5.2 Recommendations

- ✓ The finding of the present study revealed that the spatiotemporal variation of the change in land use /land cover was observed from 1988 to 2018 in different land-use scenarios, the built-up areas significantly increased throughout the study period. This is due to rapid urbanization and unplanned construction of the built environment. So, the stakeholders, environmentalists, and the concerned bodies could prevent unplanned construction and deforestation. The change in land use/land cover change may alter surface runoff since 1988, This is due to the rapid urbanization and the decline of forest land. The present study will help the environmentalists such as Addis Ababa city environmental protection authority (AAEPA) will help them as an input to have an overview of the spatial location of the change in land use/land cover and its impact on surface runoff. This study recommends the use of the multicriteria evaluation technique; the same method should be applied in another study area by considering different causative factor for better result and the hazard of place model for flood risk analysis but feature research may consider the population vulnerability in terms of sex, age, and also may consider built environment in terms of housing type for better result and also Future research will use CHIRPS satellite rainfall estimation data for ground station data-scarce environment.

REFERENCES

Abuzied, S. M. and Mansour, B. M. H. (2018) "Geospatial hazard modeling for the delineation of flash flood-prone zones in Wadi Dahab basin, Egypt," *Journal of Hydroinformatics*, (October), pp. 1–29. DOI: 10.2166/hydro.2018.043.

Alaghmand, S. *et al.* (2010) "GIS-based river flood hazard mapping in urban area (a case study in Kayu Ara river basin, Malaysia)," *International Journal of Engineering and Technology*, 2(6), pp. 488–500.

Alemu, W. G. (2008) "FLOOD HAZARD AND RISK ASSESSMENT IN FOGERA WOREDA USING GIS & REMOTE SENSING," in.

Ali, K., Bajracharyar, R. M. and Raut, N. (2017) "Advances and Challenges in Flash Flood Risk Assessment: A Review," *Journal of Geography & Natural Disasters*, 07(02). doi: 10.4172/2167-0587.1000195.

Askar, M. K. (2014) "Rainfall-runoff model using the SCS-CN method and geographic information systems : a case study of Gomal River watershed," 178, pp. 159–170.

Assefa, T. H. (2011) "Flood Risk Assessment in Ethiopia," 10(1)(6), pp. 35–40. doi: 10.1007/s002670010258.

Assefa, T. H. (2018) "Flood Risk Assessment in Ethiopia," *civil and environmental Research*, 10(1), pp. 35–40.

Atta-Ur-Rahman and Shaw, R. (2015) "Hazard, Vulnerability and Risk: The Pakistan Context," pp. 31–52. doi: 10.1007/978-4-431-55369-4_2.

Ayehu, G. T. *et al.* (2018) "Validation of new satellite rainfall products over the Upper Blue Nile Basin , Ethiopia," pp. 1921–1936.

Baky, M. A. Al, Islam, M. and Paul, S. (2020) "Flood Hazard, Vulnerability and Risk Assessment for Different Land Use Classes Using a Flow Model," *Earth Systems and Environment*, 4(1), pp. 225–244. doi: 10.1007/s41748-019-00141-w.

Balica, S. F., Wright, N. G. and van der Meulen, F. (2012) *A flood vulnerability index for coastal cities and its use in assessing climate change impacts*, *Natural Hazards*. doi: 10.1007/s11069-012-0234-1.

Bank, W. (2016) *Methods in Flood Hazard and Risk Management*.

Berhanu, Y. M. (2018) *Impact of Land Use and Land Cover Change on the River Flow in the Lake Tana Basin, North Western Ethiopia*. doi: 10.1109/robot.1994.350900.

Betru, T. *et al.* (2019) "Trends and drivers of land use/land cover change in Western Ethiopia," *Applied Geography*, 104(December 2017), pp. 83–93. doi: 10.1016/j.apgeog.2019.02.007.

Bhuiyan, M. J. A. N. and Dutta, D. (2012) "Analysis of flood vulnerability and assessment of the impacts in coastal zones of Bangladesh due to potential sea-level rise," *Natural Hazards*, 61(2), pp. 729–743. DOI: 10.1007/s11069-011-0059-3.

Birhanu, D. *et al.* (2016) "Flood Risk and Vulnerability of Addis Ababa City Due to Climate Change and Urbanization," *Procedia Engineering*, 154, pp. 696–702. DOI:

10.1016/j.proeng.2016.07.571.

Bishaw, K. (2012) "Application of GIS and Remote Sensing Techniques for Flood Hazard and Risk Assessment," in *the 2012 Berlin Conference on the Human Dimensions of Global Environmental Change Abstract*, pp. 1–17. Available at: http://www.diss.fu-berlin.de/docs/receive/FUDOCS_document_000000016509.

Bracken, L. J. *et al.* (2016) "Flood risk management, an approach to managing cross-border hazards," *Natural Hazards*, 82(2), pp. 217–240. doi: 10.1007/s11069-016-2284-2.

Brevante, B. M. (2017) *Analyzing the Effects of Land Cover / Land Use Changes on Flashflood: A Case Study of Marikina River Basin (MRB), Philippines (M. Sc. Thesis)*. Available at: https://webapps.itc.utwente.nl/librarywww/papers_2017/msc/aes/brebante.pdf.

Buldakova, E. V., Zaikanov, V. G. and Minakova, T. B. (2016) "Assessing area vulnerability to natural hazards: Case study of floods," *Water Resources*, 43(7), pp. 998–1003. doi: 10.1134/S0097807816070022.

Chakraborty, S. and Mukhopadhyay, S. (2019) "Assessing flood risk using analytical hierarchy process (AHP) and geographical information system (GIS): application in Coochbehar district of West Bengal, India," *Natural Hazards*, 99(1), pp. 247–274. doi: 10.1007/s11069-019-03737-7.

Climate Hazard Center (2019) "CHIRPS: Rainfall Estimates from Rain Gauge and Satellite Observations | Climate Hazards Center - UC Santa Barbara." Available at: https://www.chc.ucsb.edu/data/chirps/ (Accessed: June 3, 2020).

Dandapat, K. and Panda, G. K. (2017) "Flood vulnerability analysis and risk assessment using analytical hierarchy process," *Modeling Earth Systems and Environment*, 3(4), pp. 1627–1646. DOI: 10.1007/s40808-017-0388-7.

Danumah, J. H. *et al.* (2016) "Flood risk assessment and mapping in Abidjan district using multi-criteria analysis (AHP) model and geoinformation techniques, (cote d ' Ivoire)," *Geoenvironmental Disasters*. DOI: 10.1186/s40677-016-0044-y.

Darabi, H. *et al.* (2019) "Urban flood risk mapping using the GARP and QUEST models: A comparative study of machine learning techniques," *Journal of Hydrology*, 569(December 2018), pp. 142–154. DOI: 10.1016/j.jhydrol.2018.12.002.

Dejene, T., Boja, M. and Meseret, B. (2017) "assessment of Adama city flood risk using the multicriteria approach," *Ethiopian Journal of Science and Sustainable Development*, (January), pp. 6–23.

Demir, V. and Kisi, O. (2016) "Flood Hazard Mapping by Using Geographic Information System and Hydraulic Model: Mert River, Samsun, Turkey," *Advances in Meteorology*, 2016. DOI: 10.1155/2016/4891015.

Department of the Interior U.S. Geological Survey USGS, "Landsat 8 Science Data Users Handbook (2016).

Desta, H. and Fetene, A. (2020) "Land Use Policy Land-use and land-cover change in Lake Ziway watershed of the Ethiopian Central Rift Valley Region and its environmental impacts," *Land Use Policy*, 96(March), p. 104682. DOI: 10.1016/j.landusepol.2020.104682.

Desta, Y., Goitom, H. and Aregay, G. (2019) "Journal of African Earth Sciences Investigation of runoff response to land use/land cover change on the case of Aynalem catchment, North of Ethiopia," *Journal of African Earth Sciences*, 153(February), pp. 130–143. DOI: 10.1016/j.jafrearsci.2019.02.025.

Dewan, A. M., and Corner, R. J. (2014) "Dhaka megacity: Geospatial perspectives on urbanization, environment, and health," *Springer Science*, pp. 1–405. DOI: 10.1007/978-94-007-6735-5.

Ejenma, and E.Sunday, and O. (2014) "Mapping Flood Vulnerability arising from Land use/Land covers Change along River Kaduna, Kaduna State, Nigeria," *IOSR Journal of Humanities and Social Science*, 19(7), pp. 155–160. DOI: 10.9790/0837-1974155160.

Ellis, E. (2007) "Land use and land cover change and Climate change."

Fang, J., Li, M. and Shi, P. (2015) *Mapping Flood Risk of the World*. DOI: 10.1007/978-3-662-45430-5_5.

Gashaw, W. and Legesse, D. (2011a) "Flood Hazard and Risk Assessment Using GIS and Remote Sensing in Fogera Woreda, Northwest Ethiopia," *Nile River Basin*, 6(9), pp. 179–206. DOI: 10.1007/978-94-007-0689-7_9.

Gashaw, W. and Legesse, D. (2011b) "Flood Hazard and Risk Assessment Using GIS and Remote Sensing in Fogera Woreda, Northwest Ethiopia," *Nile River Basin*, (July 2007), pp. 179–206. DOI: 10.1007/978-94-007-0689-7_9.

Gebre SL, G. Y. (2015) "Flood Hazard Assessment and Mapping of Flood Inundation Area of the Awash River Basin in Ethiopia using GIS and HEC-GeoRAS / HEC-RAS Model," *Journal of Civil & Environmental Engineering*, 5(4). DOI: 10.4172/2165-784X.1000179.

Gebresamuel, G., Singh, B. A. L. R. A. M. and Dick, Ø. Y. (2010) "Land-use changes and their impacts on soil degradation and surface runoff of two catchments of Northern Ethiopia." doi: 10.1080/09064710902821741.

Gessesse, B. and Bewket, W. (2014) "Drivers and Implications of Land Use and Land Cover Change in the Central Highlands of Ethiopia: Evidence from Remote Sensing and Socio-demographic Data Integration," *Ethiopian Journal of the Social Sciences and Humanities*, 10(2), pp. 1-23–23.

Ghosh, A. and Kar, S. K. (2018) "Application of analytical hierarchy process (AHP) for flood risk assessment: a case study in Malda district of West Bengal, India," *Natural Hazards*, 94(1), pp. 349–368. DOI: 10.1007/s11069-018-3392-y.

Githui, F., Mutua, F. and Bauwens, W. (2009) "Estimating the impacts of land-cover change on runoff using the soil and water assessment tool (SWAT): Case study of Nzoia catchment, Kenya," *Hydrological Sciences Journal*, 54(5), pp. 899–908. DOI: 10.1623/hysj.54.5.899.

Guzha, A. C. (2018) "Impacts of land use and land cover change on surface runoff, discharge, and low flows : Evidence from East Africa," *Journal of Hydrology:*, 15(November 2017), pp. 49–67. DOI: 10.1016/j.ejrh.2017.11.005.

Guzha, A. C. *et al.* (2018) "Impacts of land use and land cover change on surface runoff, discharge, and low flows: Evidence from East Africa," *Journal of Hydrology: Regional*

Studies, 15(December 2017), pp. 49–67. DOI: 10.1016/j.ejrh.2017.11.005.

Hillier, F. *et al.* (2012) *76-Models, Methods, Concepts & Applications of the Analytic Hierarchy Process Second Edition*.

Hoang, T. T., Nasahara, K. N. and Katagi, J. (2018) "Advances and Applications in Geospatial Technology and Earth Resources," *Advances and Applications in Geospatial Technology and Earth Resources*, 1. doi: 10.1007/978-3-319-68240-2.

Hounkpè, J. *et al.* (2019) "Land use change increases flood hazard: a multi-modeling approach to assess change in flood characteristics driven by socio-economic land-use change scenarios," *Natural Hazards*, 98(3), pp. 1021–1050. DOI: 10.1007/s11069-018-3557-8.

Hu, S. *et al.* (2017) "GIS-based flood risk assessment in suburban areas: a case study of the Fangshan District, Beijing," *Natural Hazards*, 87(3), pp. 1525–1543. doi: 10.1007/s11069-017-2828-0.

Hu, S., Fan, Y. and Zhang, T. (2020) "Assessing the E ff ect of Land Use Change on Surface Runoff in a Rapidly Urbanized City : A Case Study of," *Land*.

Hu, Y. *et al.* (2019) "Assessment of Land-Use and Land-Cover Change in Guangxi, China," *Scientific Reports*, 9(1), pp. 1–13. DOI: 10.1038/s41598-019-38487-w.

Humagain, K. (2012) *Examining land use/Land cover change and potential causal factors in the context of climate change in Sagarmatha National Park, Nepal*, *Masters Theses & Projects*. Available at: http://digitalcommons.wku.edu/cgi/viewcontent.cgi?article=2221&context=theses.

Jae, K., Sun, S. and Shik, Y. (2018) "Improvement and Application of the ArcGIS-based Model to Estimate Direct Runoff," *Journal of the Korean Society of Agricultural Engineers*, 60(6), pp. 65–71. DOI: 10.5389/KSAE.2018.60.6.065.

Jog, S. and Dixit, M. (2016) "Supervised classification of satellite images," in *Conference on Advances in Signal Processing, CASP 2016*, pp. 93–98. DOI: 10.1109/CASP.2016.7746144.

Jokar Arsanjani, J. (2012) "Dynamic land use/cover change modeling," *springer*. DOI: 10.1007/978-3-642-23705-8.

Joseph Asen, J., Godwin Nnaemeka, N. and Ashetu, A. (2020) "Modelling of Urban Growth With Land Change Modeler in Otukpo Metropolis of Benue State, Nigeria," *International Journal of Engineering Applied Sciences and Technology*, 04(09), pp. 26–40. DOI: 10.33564/ijeast.2020.v04i09.004.

Kannan, S. S. S. V. R. (2017) "Rainfall-runoff estimation using SCS – CN and GIS approach in the Pappiredipatti watershed of the Vaniyar sub-basin, South India," *Modeling Earth Systems and Environment*, 3(1), pp. 1–8. DOI: 10.1007/s40808-017-0301-4.

Khanna, R. *et al.* (2017) "On-field radiometric calibration for multispectral cameras," in *Proceedings - IEEE International Conference on Robotics and Automation*, pp. 6503–6509. DOI: 10.1109/ICRA.2017.7989768.

Khare, D. *et al.* (2017) "Impact of land use/land cover change on run-off in the catchment of a hydropower project," *Applied Water Science*, 7(2), pp. 787–800. DOI:

10.1007/s13201-015-0292-0.

Kindu, M. *et al.* (2015) "Drivers of land use/land cover changes in Munessa-Shashemene landscape of the south-central highlands of Ethiopia," *Environmental Monitoring and Assessment*, 187(7). DOI: 10.1007/s10661-015-4671-7.

Klijn, F. *et al.* (2015) "Adaptive flood risk management planning based on a comprehensive flood risk conceptualization," *Mitigation and Adaptation Strategies for Global Change*, 20(6), pp. 845–864. DOI: 10.1007/s11027-015-9638-z.

Koch, A. *et al.* (2016) "Evaluation of Flow Speed in Urbanized Areas and Flood Hazard Mapping in Flood Risk Prevention Schemes," pp. 47–58. DOI: 10.1007/978-981-287-615-7_4.

Kumar, P. S. *et al.* (2010) "Analysis of the Runoff for Watershed Using SCS-CN Method and Geographic Information Systems," *International Journal of Engineering Science and Technology*, 2(8), pp. 3947–3954.

Lam, N. S. N. (2008) "Methodologies for mapping land cover/land use and its change," *Advances in Land Remote Sensing: System, Modeling, Inversion and Application*, pp. 341–367. DOI: 10.1007/978-1-4020-6450-0_13.

Laura, M. I., Keri, A. A. and Rusu, T. (2011) "Soil Conservation Service Curve Number Method for Surface Runoff Estimation Using GIS Techniques, in Ro ş ia Poieni Mining Area (Romania)," 4, pp. 240–246.

Lian, J. *et al.* (2017) "Flash flood vulnerability assessment for small catchments with a material flow approach," *Natural Hazards*, 88(2), pp. 699–719. DOI: 10.1007/s11069-017-2887-2.

Liu, X. and Zhang, Z. (2010) "Extracting Drainage Network from High-Resolution DEM in Toowoomba , Queensland," in *SSSI Queensland*. Available at: http://eprints.usq.edu.au/18258/1/Liu_Zhang_QSSC_2010_PV.pdf.

Lollino, G. *et al.* (2015) "Engineering geology for society and territory – volume 5: Urban geology, sustainable planning and landscape exploitation," *Engineering Geology for Society and Territory - Volume 5: Urban Geology, Sustainable Planning and Landscape Exploitation*, 5, pp. 1–1400. doi: 10.1007/978-3-319-09048-1.

López-Valencia, A. P. (2019) "Vulnerability assessment in urban areas exposed to flood risk: methodology to explore green infrastructure benefits in a simulation scenario involving the Cañaveralejo River in Cali, Colombia," *Natural Hazards*, 99(1), pp. 217–245. doi: 10.1007/s11069-019-03736-8.

Maiti and Bidinger (1981) *Assessing the accuracy of remotely sensed data principles and practices, Journal of Chemical Information and Modeling*.

Mather, P. and Tso, B. (2010) *Classification methods for remotely sensed datMather, P., & Tso, B. (2010). Classification methods for remotely sensed data. Vasa.a, Taylor& farncis group*.

Mattivi, P. *et al.* (2019) "TWI computation: a comparison of different open source GISs," *springer*, 4(1). doi: 10.1186/s40965-019-0066-y.

Michael, B. K. W. (2017) "Cellular Automata Model Based Urban Sprawl Mapping: a

Case of Mekelle City, Ethiopia."

Mishra, S. K. and Singh, V. P. (2006) "A relook at NEH-4 curve number data and antecedent," 2768(May 2005), pp. 2755–2768. doi: 10.1002/hyp.6066.

Morea, H. and Samanta, S. (2020) "Multi-criteria decision approach to identify flood vulnerability zones using geospatial technology in the Kemp-Welch Catchment, Central Province, Papua New Guinea," *Applied Geomatics*. doi: 10.1007/s12518-020-00315-6.

Nagarajan, N. and Poongothai, S. (2012) "Spatial Mapping of Runoff from a Watershed Using SCS-CN Method with Remote Sensing and GIS," 17(November), pp. 1268–1277. doi: 10.1061/(ASCE)HE.1943-5584.0000520.

National Disaster Risk Management Commission, E. W. and E. R. D. F. A. # 3 (2018) *National Disaster Risk Management Commission , Early Warning and Emergency Response Directorate Flood Alert # 3*.

nicole molders (2012) *Land-Use and Land-Cover Changes Impact on Climate and Air Quality*.

Ningaraju, H. J., B, G. K. S. and Surendra, H. J. (2016) "Estimation of Runoff Using SCS-CN and GIS method in ungauged watershed : A case study of Kharadya mill watershed , India," (5), pp. 36–42.

Ogato, G. S. *et al.* (2020) "Geographic information system (GIS)-Based multicriteria analysis of flooding hazard and risk in Ambo Town and its watershed, West shoa zone, oromia regional State, Ethiopia," *Journal of Hydrology: Regional Studies*, 27(December 2019), p. 100659. doi: 10.1016/j.ejrh.2019.100659.

De Oliveira Duarte, D. C. *et al.* (2016) "Comparison of supervised classification methods of Maximum Likelihood image, Minimum Distance, Parallelepiped and Neural Network in images of Unmanned Air Vehicle (UAV) in Viçosa-MG," *Proceedings of the Brazilian Symposium on GeoInformatics*, 2016-November(2004), pp. 12–21.

Ouma, Y. O. and Tateishi, R. (2014) "Urban flood vulnerability and risk mapping using integrated multi-parametric AHP and GIS: Methodological overview and case study assessment," *Water (Switzerland)*, 6(6), pp. 1515–1545. doi: 10.3390/w6061515.

Panahi, A., Alijani, B. and Mohammadi, H. (2010) "The Effect of the Land Use/Cover Changes on the Floods of the Madarsu Basin of Northeastern Iran," *Journal of Water Resource and Protection*, 02(04), pp. 373–379. doi: 10.4236/jwarp.2010.24043.

Pani, S. and Chakrabarty, A. (2017) "Runoff Depth Estimation using SCS-CN Method in Jhargram Community Development Block - A Remote Sensing and Geographic Information System Approach," *international journal of advanced remote sensing and GIS*, 6(1), pp. 2306–2324.

Prasad, G. and Ramesh, M. V. (2019) "Spatio-Temporal Analysis of Land Use/Land Cover Changes in an Ecologically Fragile Area—Alappuzha District, Southern Kerala, India," *Natural Resources Research*, 28(s1), pp. 31–42. doi: 10.1007/s11053-018-9419-y.

R. Viji, P. Rajesh Prasanna, R. I. (2015) "EARTH SCIENCES GIS Based SCS - CN Method For Estimating Runoff In Kundahpalam Watershed , Nilgries District , Tamilnadu," *EARTH SCIENCES RESEARCH JOURNAL*, 19(1), pp. 59–64.

Rajbanshi, J. (2016) "Estimation of Runoff Depth and Volume Using NRCS-CN Method in Konar Catchment (Jharkhand, India)," *Journal of Civil & Environmental Engineering*, 6(4), pp. 4–9. doi: 10.4172/2165-784X.1000236.

Rijal, S., Rimal, B. and Sloan, S. (2018) "Flood Hazard Mapping of a Rapidly Urbanizing City in the Foothills (Birendranagar, Surkhet) of Nepal," *Land*, 7(2), p. 60. doi: 10.3390/land7020060.

De Risi, R. *et al.* (2020) "From flood risk mapping toward reducing vulnerability: the case of Addis Ababa," *Natural Hazards*, 100(1), pp. 387–415. doi: 10.1007/s11069-019-03817-8.

Rosser, J. F., Leibovici, D. G. and Jackson, M. J. (2017) "Rapid flood inundation mapping using social media, remote sensing and topographic data," *Natural Hazards*, 87(1), pp. 103–120. doi: 10.1007/s11069-017-2755-0.

Rwanga, S. S. and Ndambuki, J. M. (2017) "Accuracy Assessment of Land Use/Land Cover Classification Using Remote Sensing and GIS," *International Journal of Geosciences*, 08(04), pp. 611–622. doi: 10.4236/ijg.2017.84033.

Saaty, T. L. (2001) *Fundamentals of the Analytic Hierarchy Process*. doi: 10.1007/978-94-015-9799-9_2.

Schneiderbauer, S. and Ehrlich, D. (2004) "Risk, hazard and people's vulnerability to natural hazards: A review of definitions, concepts and data," *European Commission Joint Research Centre. EUR, 21410*, 40(January).

Shafizadeh-Moghadam, H. *et al.* (2018) "Novel forecasting approaches using combination of machine learning and statistical models for flood susceptibility mapping," *Journal of Environmental Management*, 217, pp. 1–11. doi: 10.1016/j.jenvman.2018.03.089.

Shawul, A. A. and Chakma, S. (2019) "Spatiotemporal detection of land use/land cover change in the large basin using integrated approaches of remote sensing and GIS in the Upper Awash basin, Ethiopia," *Environmental Earth Sciences*, 78(5), p. 0. doi: 10.1007/s12665-019-8154-y.

Szwagrzyk, M. *et al.* (2018) "Impact of forecasted land use changes on flood risk in the Polish Carpathians," *Natural Hazards*, 94(1), pp. 227–240. doi: 10.1007/s11069-018-3384-y.

Talisay, B. A. M., Puno, G. R. and Amper, R. A. L. (2019) "Flood hazard mapping in an urban area using combined hydrologic-hydraulic models and geospatial technologies," *Global Journanal of Environment and Science*, 5(2), pp. 139–154. doi: 10.22034/gjesm.2019.02.000.

Thapa, R. B. and Murayama, Y. (2011) *Accuracy of Land Use and Land Cover Mapping Methods*. doi: 10.1007/978-94-007-0671-2_9.

Tilahun, A. (2015) "Accuracy Assessment of Land Use Land Cover Classification using Google Earth," *American Journal of Environmental Protection*, 4(4), p. 193. doi: 10.11648/j.ajep.20150404.14.

USGS (2011) "Landsat 7 Science Data Users Handbook Landsat 7 Science Data Users Handbook," *National Aeronautics and Space Administration*, p. 186.

USGS (2018) "Using the USGS Landsat Level-1 Data Product," in, pp. 1–5. Available at: https://landsat.usgs.gov/using-usgs-landsat-8-product.

V, S. S. S. *et al.* (2017) "Flood risk assessment using multi-criteria analysis : a case study from Kopili River Basin , Assam , India," *Geomatics, Natural Hazards and Risk*, 5705(January 2018). doi: 10.1080/19475705.2017.1408705.

Vishwanath, V. H. and Tomaszewski, B. (2018) "Flood Hazard , Vulnerability and Risk Assessments for Uttarakhand State in," (June 2013), pp. 10–11.

Werren, G. *et al.* (2016) "Flood hazard assessment and mapping in semi-arid piedmont areas: a case study in Beni Mellal, Morocco," *Natural Hazards*, 81(1), pp. 481–511. doi: 10.1007/s11069-015-2092-0.

Williams, J. R. *et al.* (2012) "Evolution of the scs runoff curve number method and its application to continuous runoff simulation," *Journal of Hydrologic Engineering*, 17(11), pp. 1221–1229. doi: 10.1061/(ASCE)HE.1943-5584.0000529.

Wisner, B. *et al.* (2014) *At risk: natural hazards, peoples vulnerability and disasters*. doi: 10.4324/9780203714775.

Worako, A. W. (2016) "Land Use / Land Cover Change Detection in Swarnamukhi River Basin Using Remote Sensing and GIS Techniquies," (1), pp. 9380–9387.

World Weather Information Service (no date). Available at: https://worldweather.wmo.int/en/city.html?cityId=162 (Accessed: September 23, 2020).

Wu, Y. *et al.* (2015) "Integrated flood risk assessment and zonation method: A case study in Huaihe River basin, China," *Natural Hazards*, 78(1), pp. 635–651. doi: 10.1007/s11069-015-1737-3.

Yesuph, A. Y. and Dagnew, A. B. (2019) "Land use/cover spatiotemporal dynamics, driving forces and implications at the Beshillo catchment of the Blue Nile Basin, North Eastern Highlands of Ethiopia," *Environmental Systems Research*, 8(1). doi: 10.1186/s40068-019-0148-y.

Yin, J. *et al.* (2017) "Effects of land use / land cover and climate changes on surface runoff in a semi-humid and semi-arid transition zone in northwest China," *Hydrology and Earth System Sciences*, 183, pp. 183–196. doi: 10.5194/hess-21-183-2017.

Younis, S.M.Z., Ammar, A. . E. (2017) "The Egyptian Journal of Remote Sensing and Space Sciences Quantification of impact of changes in land use-land cover on hydrology in the upper Indus Basin , Pakistan," *The Egyptian Journal of Remote Sensing and Space Sciences*, 11, pp. 1–9. doi: 10.1016/j.ejrs.2017.11.001.

Zeberie, W. (2019) "Modelling of Rainfall-Runoff Relationship in Big-Akaki Watershed , Upper Awash Basin ," 27(October), pp. 108–120.

Zhang, H., Ma, W. C. and Wang, X. R. (2008) "Rapid urbanization and implications for flood risk management in hinterland of the Pearl River Delta, China: The Foshan study," *Sensors*, 8(4), pp. 2223–2239. doi: 10.3390/s8042223.

Zope, P. E., Eldho, T. I. and Jothiprakash, V. (2015) "Impacts of urbanization on flooding of a coastal urban catchment: a case study of Mumbai City, India," *Natural Hazards*, 75(1), pp. 887–908. doi: 10.1007/s11069-014-1356-4.

Zope, P. E., Eldho, T. I. and Jothiprakash, V. (2016) "Impacts of land use-land cover change and urbanization on flooding: A case study of Oshiwara River Basin in Mumbai, India," *Catena*, 145, pp. 142–154. doi: 10.1016/j.catena.2016.06.009.

APPENDIX A

Appendix A. 1 Rain Gage Station used to Validate the accuracy of CHIRPS

	Station Name	Longitude	Latitude	Elevation	Year
1	Abyssinia School	38.723333	9.0447220	2501	2003-2018
2	Addis Ababa Bole	38.79871	8.9810810	2354	1986-2018
3	Addis Ababa Bole Eng.	38.78577	8.9852800	2330	2009-2018
4	Addis Ababa Obs.	38.7475	9.0189100	2386	1986-2018
5	Akaki	38.7862	8.8698000	2057	1986-2018
6	Asko	38.75	9.0500000		1999-2003
7	Ayertena	38.696389	8.9830560	2325	2003-2018
8	Kotebe	38.839167	9.0591670	2755	1997-2018
9	Dire Gidib	38.943	9.1578300	2560	2000-2018
10	Enttoto	38.72133	9.0836670	2903	1988-2018
11	Kality	38.766833	8.9333300	2186	2007 -2016
12	Kolfe Keranio School	38.702139	9.0153610	2382	2010-2018
13	Kotebe TTC	38.83667	9.0418000	2462	2005-2018
14	Medhanalem/School	38.723	9.0553330	2539	2010-2018
15	Sendafa (Add)	39.0215	9.1521670	2569	1986-2016
16	Yekatit 23 School	38.725	9.0335000	2456	1998-2018
17	Zequala	38.866667	8.8666700	3050	1986-2018

Appendix A. 2 Population and Population Density of the Study Area

REGION NAME	WOREDANAME	Population	Area(km2)	Pop density
Addis Ababa	Addis Ketema	320053	7.385317	43336.39301
Addis Ababa	Arada	265141	9.498728	27913.31639
Addis Ababa	Lideta	252842	10.992014	23002.33606
Addis Ababa	Kirkos	277346	14.646766	18935.64764
Addis Ababa	Gulele	335434	31.846055	10532.98438
Addis Ababa	Kolfe – Keranio	537561	65.466417	8211.248219
Addis Ababa	Nefas Silk	396486	58.317578	6798.739138
Addis Ababa	Yeka	434599	86.196375	5041.963772
Addis Ababa	Bole	387355	127.63752	3034.805126
Addis Ababa	Akaki – Kality	227182	127.065904	1787.906849
Oromia	Alem Gena	250400	916.494554	273.214935
Oromia	Aleltu	69254	414.824803	166.9475873
Oromia	Sululta	169257	1052.17798	160.8634693
Oromia	Akaki	101271	684.031504	148.0501986
Oromia	Bereh	122616	844.255112	145.2357211
Oromia	Walmara	107762	777.65085	138.5737571

Appendix A. 3 Samples of the computed surface runoff using SCS CN methods

Date	Rainfall	AMC Condition	CN	S(mm)	Q(mm)	Q(Volume)
6/1/1988	21.1788	1	79.71574	64.63218	0.9343	27176.59
6/2/1988	21.1788	1	79.71574	64.63218	0.9344	27176.59
6/3/1988	0	1	79.71574	64.63218	0	0
6/4/1988	21.1788	1	79.71574	64.63218	0.9343	27176.59
6/5/1988	0	1	79.71574	64.63218	0	0
6/6/1988	0	3	95.45318	12.09905	0	0
6/7/1988	0	2	89.96404	28.33502	0	0
6/8/1988	0	1	79.71574	64.63218	0	0
6/9/1988	0	1	79.71574	64.63218	0	0
6/10/1988	0	1	79.71574	64.63218	0	0
6/11/1988	0	1	79.71574	64.63218	0	0
6/12/1988	0	1	79.71574	64.63218	0	0
6/13/1988	5.03571	1	79.71574	64.63218	0	0
6/14/1988	0	1	79.71574	64.63218	0	0
6/15/1988	14.2696	1	79.71574	64.63218	0.0273	795.3351
6/16/1988	0	1	79.71574	64.63218	0	0
6/17/1988	10.4218	1	79.71574	64.63218	0	0
6/18/1988	0	1	79.71574	64.63218	0	0
6/19/1988	0	1	79.71574	64.63218	0	0
6/20/1988	0	1	79.71574	64.63218	0	0
6/21/1988	0	1	79.71574	64.63218	0	0
6/22/1988	0	1	79.71574	64.63218	0	0
6/23/1988	0	1	79.71574	64.63218	0	0
6/24/1988	23.0076	1	79.71574	64.63218	1.3602	39563.69
6/25/1988	0	1	79.71574	64.63218	0	0
6/26/1988	6.53368	1	79.71574	64.63218	0	0
6/27/1988	0	1	79.71574	64.63218	0	0
6/28/1988	12.4007	1	79.71574	64.63218	0	0
6/29/1988	8.53378	2	89.96404	28.33502	0.2633	7660.931
6/30/1988	15.7342	1	79.71574	64.63218	0.1169	3399.99
7/1/1988	0	2	89.96404	28.33502	0	0
7/2/1988	15.6419	2	89.96404	28.33502	2.5972	75540.37
7/3/1988	11.878	2	89.96404	28.33502	1.1166	32478.66
7/4/1988	15.935	2	89.96404	28.33502	2.7311	79437.16
7/5/1988	7.82095	3	95.45318	12.09905	1.6669	48484.34
7/6/1988	0	2	89.96404	28.33502	0	0
7/7/1988	12.1526	2	89.96404	28.33502	1.2079	35134.75
7/8/1988	6.62448	2	89.96404	28.33502	0.0312	910.2761
7/9/1988	12.1526	2	89.96404	28.33502	1.2079	35134.75
7/10/1988	23.2089	2	89.96404	28.33502	6.7074	195088.8
7/11/1988	24.7936	3	95.45318	12.09905	14.521	422353
7/12/1988	0	3	95.45318	12.09905	0	0

7/13/1988	0	3	95.45318	12.09905	0	0
7/14/1988	7.23148	3	95.45318	12.09905	1.3690	39820.15
7/15/1988	25.4817	3	95.45318	12.09905	15.126	439949.5
7/16/1988	10.5148	3	95.45318	12.09905	3.2449	94380.62
7/17/1988	6.26868	2	89.96404	28.33502	0.0125	363.8733
7/18/1988	5.94721	2	89.96404	28.33502	0.0027	79.8053
7/19/1988	4.70151	3	95.45318	12.09905	0.3620	10529.52
7/20/1988	3.46921	2	89.96404	28.33502	0	0
7/21/1988	0	1	79.71574	64.63218	0	0
7/22/1988	0	1	79.71574	64.63218	0	0
7/23/1988	0	1	79.71574	64.63218	0	0
7/24/1988	15.3047	1	79.71574	64.63218	0.0844	2454.999
7/25/1988	11.1617	1	79.71574	64.63218	0	0
7/26/1988	5.76	1	79.71574	64.63218	0	0
7/27/1988	0	1	79.71574	64.63218	0	0
7/28/1988	0	1	79.71574	64.63218	0	0
7/29/1988	10.08	1	79.71574	64.63218	0	0
7/30/1988	0	1	79.71574	64.63218	0	0
7/31/1988	17.28	1	79.71574	64.63218	0.2747	7991.055

Table 4. 21 Confusion matrix table of LULC 1988

LULC Class	Built up	forest	Agriculture	Water	Total	Producer Accuracy (%)	User Accuracy (%)
Built up	52	0	1	1	54	96	96
Forest	0	50	2	9	61	98	81
Agriculture	2	1	47	26	76	94	61
Water	0	0	0	71	71	66	100
Total	54	51	50	107	262		

Kappa = 78.5 % and overall accuracy = 83.9 %

Table 4. 22 Confusion matrix table of LULC 2003

LULC Class	Built up	forest	Agriculture	Water	Total	Producer Accuracy (%)	User Accuracy (%)
Built up	123	4	15	0	142	93.2	86.6
Forest	5	96	0	4	105	91.4	91.4
Agriculture	4	5	95	5	109	86.4	87.15
Water	0	0	0	66	66	88	100
Total	132	105	110	75	422		

kappa coefficient =86.5 %, and overall accuracy 90.04%

Table 4. 23 Confusion matrix table of LULC 2018

LULC Class	Built up	forest	Agriculture	Water	Total	Producer Accuracy (%)	User Accuracy (%)
Built up	156	3	11	1	171	93.4	91.23
Forest	9	91	1	5	106	91.0	85.85
Agriculture	2	6	149	16	173	92.5	86.13
Water	0	0	0	90	90	80.3	100

Total	167	100	161	112	540

Kapp coefficient =86.4% and overall accuracy = 90%

Table 1 Transition matrix between the land use of 2003 and 2018.

Classification (2003)	Reference (1988)				
	1	2	3	4	Total
1	92.82	10.02	9.58	0.11	112.54
2	27.44	174.58	113.01	0.66	315.70
3	95.80	160.52	1088.03	2.38	1346.75
4	0.0018	0.32	0.31	11.88	12.52
Total	216.07	345.45	1210.94	15.05	1787.53

Table 2 Transition matrix between the land use of 1988 and 2003.

Classification (2018)	Reference (2003)				
	1	2	3	4	Total
1	179.11	8.18	28.20	0.00	215.51
2	56.73	136.41	151.50	0.16	344.60
3	225.67	43.70	943.58	0.14	1213.11
4	0.01	1.04	2.17	11.07	14.31
Total	461.53	189.34	1125.47	11.39	1787.53

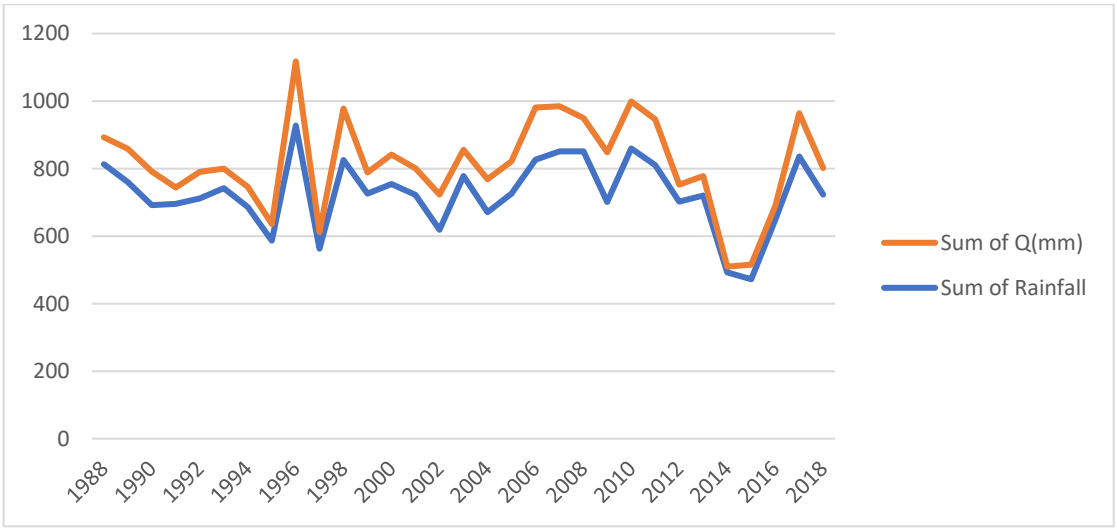

Appendix Figure 1. 1 Time series rainfall runoff

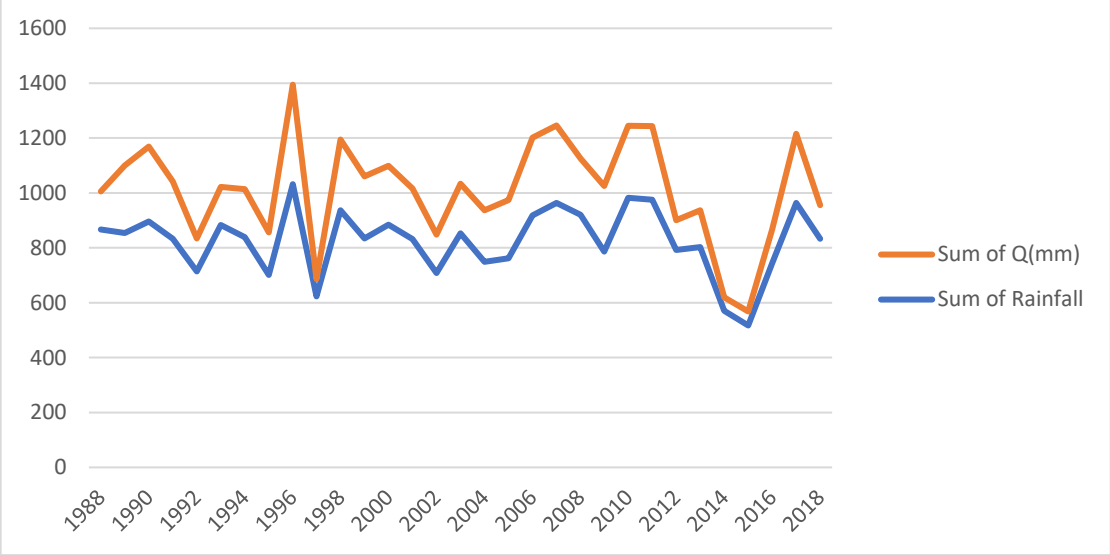

Appendix Figure 1. 2 Time series rainfall Vs Runoff at Addis Ababa Engineering.

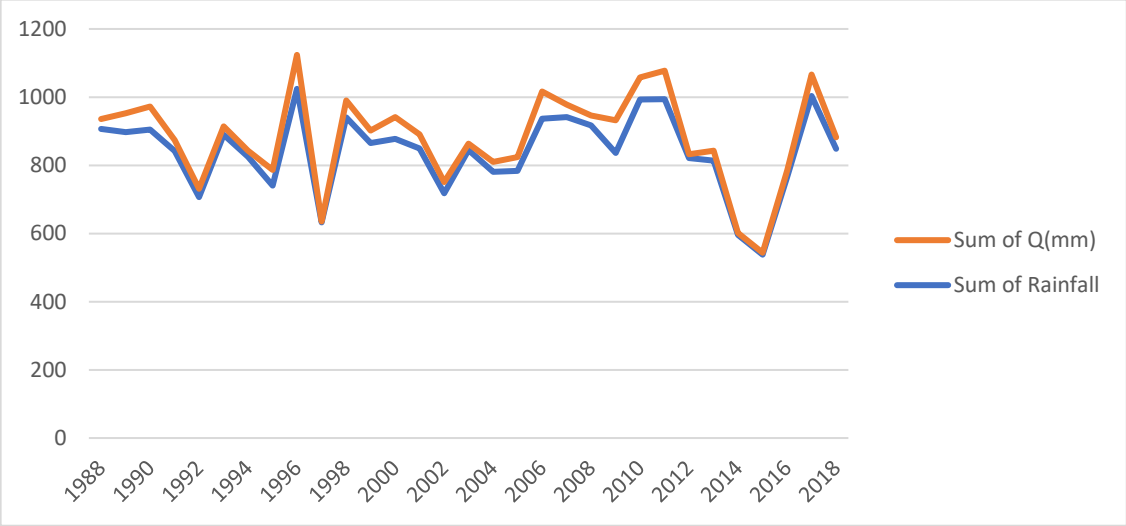

Appendix Figure 1. 3 Time series rainfall Vs Runoff at Ayertena

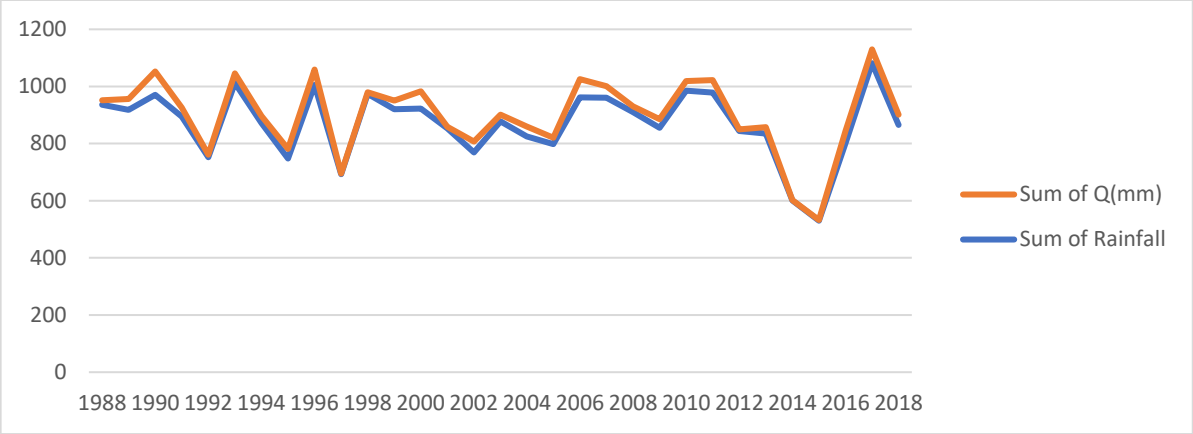

Appendix Figure 1. 4 Time series rainfall Vs Runoff at Asko,

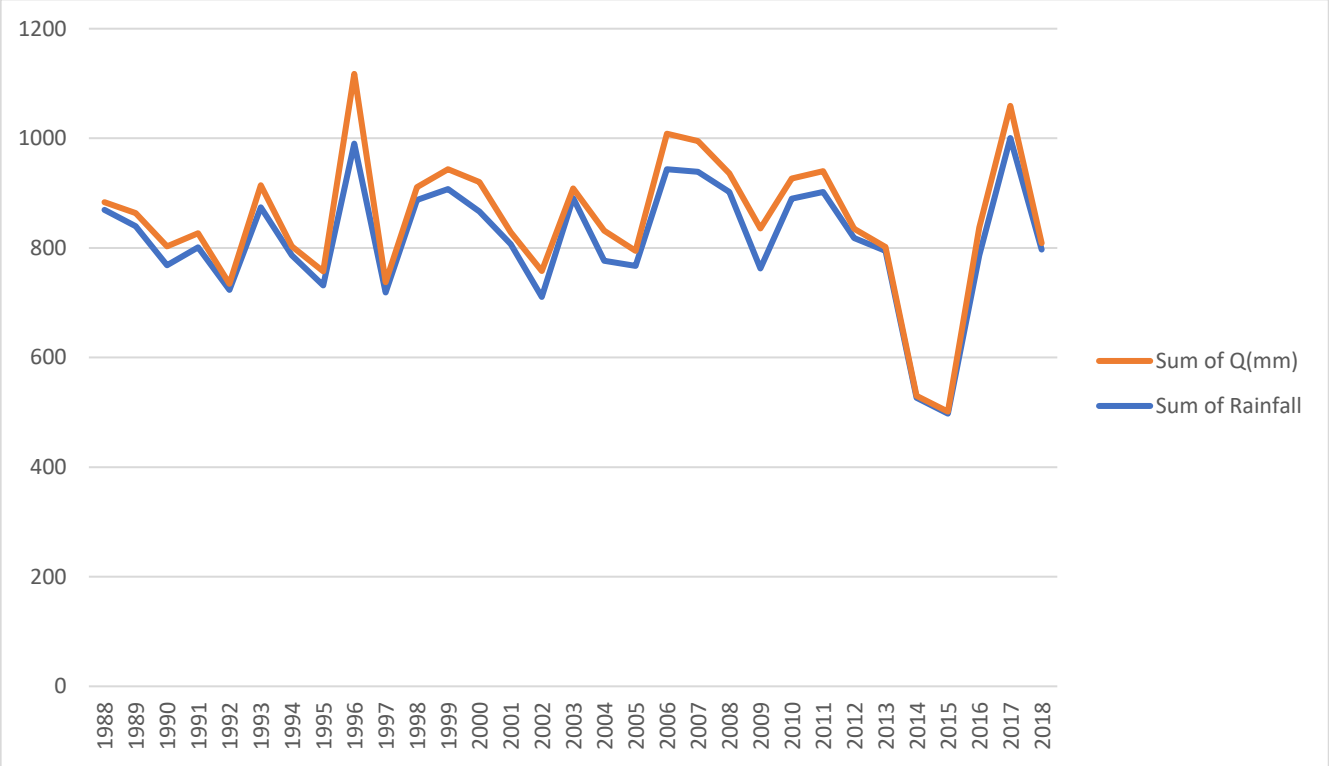

Appendix Figure 1. 5 Time series rainfall runoff at diregidib.

Appendix A. 4 Floods in different part of addis ababa city

Source http://storymaps.arcgis.com/

Table of Appendix A. 1 Flood Hazard and Risk part of Addis Ababa

ክ/ከተማ	ወረዳ	ልዩ ቦታ	የአደጋው አይነት	ብዛት	የመንሰኤ አይነቶች
ቂርቆስ	5	ቄራ ፍርድ ቤት ጀርባ	የጐርፍ አደጋ	1	ከባድ ዝናብ
ቂርቆስ	2	አሎምፒያ አካባቢ	የጐርፍ አደጋ	1	ከባድ ዝናብ
ቂርቆስ	2	ጀሞ 2 መስኪድ አካባቢ	የጐርፍ አደጋ	1	ከባድ ዝናብ
ልደታ	8	ኮንዶሚኒየም በግ ተራ አካባቢ	የጐርፍ አደጋ	1	ከባድ ዝናብ
አቃቂ	8	በሰቃ ት/ቤት አጠገብ	የጐርፍ አደጋ	1	የወንዝ ሙላት
ቦሌ	7	ጉርድ ሾላ ቴሌ	የጐርፍ አደጋ	1	የተደፈነ ቱቦ መፈንዳት
ቦሌ	6	እግዚአብሔርአብ ቤ/ክ መግቢያ	የጐርፍ አደጋ	1	ከመንገድ ላይ የገባ ጐርፍ
ቦሌ	13	ገርጂ ኤምባሲ ጋራዥ	የጐርፍ አደጋ	1	ከባድ ዝናብ
ኮ/ቀ	7	ወረዳ 7 ጽ/ቤት ጀርባ	የጐርፍ አደጋ	1	ከባድ ዝናብ
ልደታ	2	ኪዳኔ ህንፃ ፊት ለፊት	የጐርፍ አደጋ	1	ከባድ ዝናብ
ቂርቆስ	7	ስታድየም አካባቢ	የጎርፍ አደጋ	1	የትቦ መደፈን
ኮልፌ	7	ወረዳ 7 ጽ/ቤት አካባቢ	የጎርፍ	1	ከባድ ዝናብ
ኮ/ቀ	12	ኮልፌ ጤ/ጣቢያ አካባቢ	የጐርፍ አደጋ	1	ከፍተኛ ዝናብ መዝነቡ
ልደታ	10	ምርታማነት ማሻሻያ ጀርባ	የጎርፍ አደጋ	1	ከባድ ዝናብ
ኮ/ቀራኒዮ	6	ወረዳ 6 ጽ/ቤት ውስጥ	የጎርፍ አደጋ	1	ከባድ ዝናብ
አራዳ	9	አራት ኪሎ ኢህአዴግ ጽ/ቤት ግቢ ውስጥ	የጎርፍ አደጋ	1	ከባድ ዝናብ
አቃቂ	3	ቀጠና 01 ባቡር ጣብያ አካባቢ	የጎርፍ አደጋ	1	የቱቦ መዘጋት
አቃቂ	3	ባቡር ጣብያ አካባቢ	የጎርፍ አደጋ	1	ከባድ ዝናብ
ኮ/ቀራኒዮ	9	18 ማዞርያ መብራት ሀይል አካባቢ	የጎርፍ አደጋ	1	የቱቦ መዘጋት

ንሰልክ	12	አርሴማ ቤ/ክ ጸበል አካባቢ	የጎርፍ አደጋ	1	ከባድ ዝናብ
ኦሮሚያ	ከታ ለኩ	ከታ ለኩ	የጎርፍ መጥለቅለቅ	1	ዝናብ
ኦሮሚያ	ሰበታ	ፉሪ ኖክ ማደያ አካባቢ	የጎርፍ አደጋ	1	ከባድ ዚናብ
ኦሮሚያ	ከታ ለኩ	ከታ ለኩ	የጎርፍ መጥለቅለቅ	1	ዝናብ
ቦሌ	3	ደሳለኝ ሆቴል አካባቢ	የጎርፍ መጥለቅለቅ	1	ዝናብ
ጉለሌ	3	ሸገር መናፈሻ አካባቢ	የጎርፍ መጥለቅለቅ	1	ትቦ መደፈን
ኮልፌ	4	ኮልፌ ኪዳነምህረት አካባቢ	የጎርፍ መጥለቅለቅ	1	ዝናብ
ቦሌ	13	ገርጅ ሰላም ሰፈር	የጎርፍ መጥለቅለቅ	1	የትቦ መደፈን
ኮልፌ	15	ካአጂጂ አካባባ	የጎርፍ መጥለቅለቅ	1	ዝናብ
የካ	9	ጉርድ ሾላ ንግድ ባንክ ጀርባ	የጎርፍ መጥለቅለቅ	1	ዝናብ
ኮልፌ	15	ካአጂጂ አካባባ	የጎርፍ መጥለቅለቅ	1	ዝናብ
ኦሮሚያ	ሰበታ	ፉሪ ኖክ ማደያ አካባቢ	የጎርፍ አደጋ	1	ከባድ ዚናብ
አ/ከተማ	9	ፍቃዱ የጥርስ ህክምና አካባቢ	የጎርፍ አደጋ	1	የቱቦ መደፍን
ኮ/ቀራኒዮ	7	ሀና ካፌ አካባቢ	የጎርፍ አደጋ	1	ከባድ ዚናብ
ቦሌ	17	ቦሌ 17 ጤ/ጣ አካባቢ	የጐርፍ አደጋ	1	ከባድ ዝናብ
አ/ከ	9	ፍቃዱ ጥርስ ክሊኒክ አካባቢ	የጐርፍ አደጋ	1	የቱቦ መደፈን
አ/ከ	9	ኳስ ሜዳ አካባቢ	የጐርፍ አደጋ	1	ከመንገድ የመጣ ውሃ
አራዳ	3	እሪ በከንቱ መንታ መንገድ ሃግቤስ ፊትለፊት	የጐርፍ አደጋ	1	
ቂርቆስ	7	ጊዮን ከነማ መድኃኒት ቤት አካባቢ	የጐርፍ አደጋ	1	ከባድ ዝናብ
ንሰ	4	ጠመንጃ ያዥ ሜሪ ስቶስ አጠገብ	የጐርፍ አደጋ	1	ከባድ ዝናብ
ኮ/ቀ	4	አየር ጤና ኪዳነ ምህረት መቃብር	የጐርፍ አደጋ	1	ከባድ ዝናብ
ቦሌ	3	ቦሌ ሩዋንዳ ጅቡቲ ኤምባሲ አካባቢ	የጐርፍ አደጋ	1	ከባድ ዝናብ
ቂርቆስ	5	ቄራ ፍ/ቤት ጀርባ	የጐርፍ አደጋ	1	ከባድ ዝናብ
ንሰ	6	ቂራ ከሰል ተራ አካባቢ	የጐርፍ አደጋ	1	ከባድ ዝናብ
ኮ/ቀ	4	አለም ባንክ ኪዳነ ምህረት አካባቢ	የጐርፍ አደጋ	1	ከባድ ዝናብ
ንሰ	11	ፊውቸር ት/ቤት አካባቢ	የጐርፍ አደጋ	1	ከባድ ዝናብ
ኮ/ቀ	7	ቤተል ፊርማ ሆቴል አጠገብ	የጐርፍ አደጋ	1	ከባድ ዝናብ
ኮ/ቀ	4	አለም ባንክ አካባቢ	የጐርፍ አደጋ	1	ከባድ ዝናብ
አ/ከ	9	ፍቃዱ ጥርስ ክሊኒክ አካባቢ	የጐርፍ አደጋ	1	የቱቦ መደፈን
ኮ/ቀ	4	ኪዳነ ምህረት ቤ/ክ አካባቢ	የጐርፍ አደጋ	1	ከባድ ዝናብ
አ/ከተማ	19	ኳስ ሜዳ አካባቢ	የጎርፍ አደጋ	1	የቱቦ መዘጋት
አ/ከተማ	9	አበበ በቂላ ስታድየም ጀርባ	የጎርፍ አደጋ	1	የቱቦ መዘጋት
ጉለሌ	9	ጌታየ ብረታ ብረት ጀርባ	የጎርፍ አደጋ	1	ከባድ ዝናብ
አ/ከተማ	9	እሸቱ ት/ቤት አካባቢ	የጎርፍ አደጋ		የቱቦ መዘጋት
አ/ከተማ	9	መብራት ሀይል ገነት ቸርች አካባቢ	የጎርፍ አደጋ	1	የቱቦ መዘጋት

ቦሌ	12	ቦሌ ኮንዶምንየም አካባቢ	የጎርፍ አደጋ	1	ከባድ ዝናብ
ን/ስልክ	2	ጀሞ ሚካኤል አካባቢ	የጎርፍ አደጋ	1	ከባድ ዝናብ
ቦሌ	9	ወለጋ ሰፈር አካባቢ	የጎርፍ አደጋ	1	ከባድ ዝናብ
ቦሌ	5	ወረዳ 05 ጽ/ቤት አከባቢ	የጎርፍ አደጋ	1	ከባድ ዝናብ
ኮልፌ	9	18 ማዞርያ መብራት ሀይል አካባቢ	የጎርፍ አደጋ	1	የቱቦ መዘጋት
አ/ከ	9	ፍቃዱ የጥርስ ህክምና ፊት ለፊት	የጎርፍ አደጋ	1	የቱቦ መዘጋት
ቦሌ	3	ጂቡቲ ኢንባሲ አካባቢ	የጎርፍ አደጋ	1	ከባድ ዝናብ
አቃቂ	3	ወረዳ 03 ቄራ አካባቢ	የጎርፍ አደጋ	1	ከባድ ዝናብ
ን/ስልክ	10	ብሔረ ጽጌ ማርያም ቄስ ሰፈር አካባቢ	የጎርፍ አደጋ	1	ከባድ ዝናብ
ኮልፌ	7	ሃና ካፌ አካባቢ	የጎርፍ አደጋ	1	ከባድ ዝናብ
ቦሌ	11	ኮተቤ መደይ በጎ አድራጎትማህበር	የጎርፍ አደጋ	1	ከ/ዝናብ
የካ	9	ጉርድ ሾላ አትሌቲክስ ፌደሬሽን ህንፃ ላይ	የጎርፍ አደጋ	1	ከ/ዝናብ
የካ	9	ጉርድ ሾላ አትሌቲክስ ፌደሬሽን ህንፃ ላይ	የጎርፍ አደጋ	1	ከ/ዝናብ
ልደታ	10	ምርታማነት ማሻሻያ ጀርባ	የጎርፍ አደጋ	1	ከባድ ዝናብ
ኮ/ቀራኒዮ	6	ወረዳ 6 ጽ/ቤት ውስጥ	የጎርፍ አደጋ	1	ከባድ ዝናብ
አራዳ	9	አራት ኪሎ ኢህአዴግ ጽ/ቤት ግቢ ውስጥ	የጎርፍ አደጋ	1	0
አቃቂ	3	ቀጠና 01 ባቡር ጣብያ አካባቢ	የጎርፍ አደጋ	1	የቱቦ መዘጋት
አቃቂ	3	ባቡር ጣብያ አካባቢ	የጎርፍ አደጋ	1	ከባድ ዝናብ
ኮ/ቀራኒዮ	9	18 ማዞርያ መብራት ሀይል አካባቢ	የጎርፍ አደጋ	1	የቱቦ መዘጋት
ን/ስልክ	12	አርሴማ ቤ/ክ ጸበል አካባቢ	የጎርፍ አደጋ	1	ከባድ ዝናብ
አሮሚያ	ከታ ለኩ	ከታ ለኩ	የጎርፍ መጥለቅለቅ	1	ዝናብ
ቦሌ	3	ደሳለኝ ሆቴል አካባቢ	የጎርፍ መጥለቅለቅ	1	ዝናብ
ጉለሌ	3	ሸገር መናፈሻ አካባቢ	የጎርፍ መጥለቅለቅ	1	ትቦ መደፈን
ኮልፌ	4	ኮልፌ ኪዳነምህረት አካባቢ	የጎርፍ መጥለቅለቅ	1	ዝናብ
ቦሌ	13	ገርጅ ሰላም ሰፈር	የጎርፍ መጥለቅለቅ	1	የትቦ መደፈን
ኮልፌ	15	ካአጀጄ አካባባ	የጎርፍ መጥለቅለቅ	1	ዝናብ
የካ	9	ጉርድ ሾላ ንግድ ባንክ ጀርባ	የጎርፍ መጥለቅለቅ	1	ዝናብ
ኮልፌ	15	ካአጀጄ አካባባ	የጎርፍ መጥለቅለቅ	1	ዝናብ
አሮሚያ	ሰበታ	ፉሪ ኖክ ማደያ አካባቢ	የጎርፍ አደጋ	1	ከባድ ዚናብ
አ/ከተማ	9	ፍቃዱ የጥርስ ህክምና አካባቢ	የጎርፍ አደጋ	1	የቱቦ መደፍን
ኮ/ቀራኒዮ	7	ሀና ካፌ አካባቢ	የጎርፍ አደጋ	1	ከባድ ዚናብ
ቦሌ	17	ቦሌ 17 ጤ/ጣ አካባቢ	የጐርፍ አደጋ	1	ከባድ ዝናብ
አ/ከ	9	ፍቃዱ ጥርስ ክሊኒክ አካባቢ	የጐርፍ አደጋ	1	የቱቦ መደፈን
አ/ከ	9	ኳስ ሜዳ አካባቢ	የጐርፍ አደጋ	1	ከመንገድ የመጣ ውሃ
አራዳ	3	አሪ በከንቱ መንታ መንገድ ሃግቤስ ፊትለፊት	የጐርፍ አደጋ	1	

ቂርቆስ	7	ጊዮን ክነማ መድኃኒት ቤት አካባቢ	የጐርፍ አደጋ	1	ከባድ ዝናብ
ን/ስ	4	ጠመንጃ ያዥ ሜሪ ስቶስ አጠገብ	የጐርፍ አደጋ	1	ከባድ ዝናብ
ኮ/ቀ	4	አየር ጤና ኪዳነ ምህረት መቃብር	የጐርፍ አደጋ	1	ከባድ ዝናብ
ቦሌ	3	ቦሌ ሩዋንዳ ጅቡቲ ኤምባሲ አካባቢ	የጐርፍ አደጋ	1	ከባድ ዝናብ
ቂርቆስ	5	ቄራ ፍ/ቤት ጀርባ	የጐርፍ አደጋ	1	ከባድ ዝናብ
ን/ስ	6	ቂራ ከሰል ተራ አካባቢ	የጐርፍ አደጋ	1	ከባድ ዝናብ
ኮ/ቀ	4	አለም ባንክ ኪዳነ ምህረት አካባቢ	የጐርፍ አደጋ	1	ከባድ ዝናብ
ን/ስ	11	ፊውቸር ት/ቤት አካባቢ	የጐርፍ አደጋ	1	ከባድ ዝናብ
ኮ/ቀ	7	ቤተል ፊርማ ሆቴል አጠገብ	የጐርፍ አደጋ	1	ከባድ ዝናብ
ኮ/ቀ	4	አለም ባንክ አካባቢ	የጐርፍ አደጋ	1	ከባድ ዝናብ
አ/ከ	9	ፍቃዱ ጥርስ ክሊኒክ አካባቢ	የጐርፍ አደጋ	1	የቱቦ መደፈን
ኮ/ቀ	4	ኪዳነ ምህረት ቤ/ክ አካባቢ	የጐርፍ አደጋ	1	ከባድ ዝናብ
አ/ከተማ	19	ኳስ ሜዳ አካባቢ	የጎርፍ አደጋ	1	የቱቦ መዘጋት
አ/ከተማ	9	አበበ በቂላ ስታድየም ጀርባ	የጎርፍ አደጋ	1	የቱቦ መዘጋት
ጉለሌ	9	ጌታየ ብረታ ብረት ጀርባ	የጎርፍ አደጋ	1	ከባድ ዝናብ
አ/ከተማ	9	እሸቱ ት/ቤት አካባቢ	የጎርፍ አደጋ		የቱቦ መዘጋት
አ/ከተማ	9	መብራት ሀይል ገነት ቸርች አካባቢ	የጎርፍ አደጋ	1	የቱቦ መዘጋት
ቦሌ	12	ቦሌ ኮንዶምንየም አካባቢ	የጎርፍ አደጋ	1	ከባድ ዝናብ
ን/ስልክ	2	ጀሞ ሚካኤል አካባቢ	የጎርፍ አደጋ	1	ከባድ ዝናብ
ቦሌ	9	ወሊጋ ሰፈር አካባቢ	የጎርፍ አደጋ	1	ከባድ ዝናብ
ቦሌ	5	ወረዳ 05 ጽ/ቤት አካባቢ	የጎርፍ አደጋ	1	ከባድ ዝናብ
ኮልፌ	9	18 ማዞርያ መብራት ሀይል አካባቢ	የጎርፍ አደጋ	1	የቱቦ መዘጋት
አ/ከ	9	ፍቃዱ የጥርስ ህክምና ፊት ለፊት	የጎርፍ አደጋ	1	የቱቦ መዘጋት
ቦሌ	3	ጂቡቲ ኢንባሲ አካባቢ	የጎርፍ አደጋ	1	ከባድ ዝናብ
አቃቂ	3	ወረዳ 03 ቄራ አካባቢ	የጎርፍ አደጋ	1	ከባድ ዝናብ
ን/ስልክ	10	ብሔረ ጽጌ ማርያም ቄስ ሰፈር አካባቢ	የጎርፍ አደጋ	1	ከባድ ዝናብ
ኮልፌ	7	ሃና ካፌ አካባቢ	የጎርፍ አደጋ	1	ከባድ ዝናብ
አ/ከ	9	አበበ ቢቂላ ስታዲየም አካባቢ	የጐርፍ አደጋ	1	ዝናብ
ቦሌ	11	ኮተቤ መደይ በጎ አድራጎትማህበር	የጎርፍ አደጋ	1	ከ/ዝናብ
የካ	9	ጉርድ ሾላ አትሌቲክስ ፌደሬሽን ህንፃ ላይ	የጎርፍ አደጋ	1	ከ/ዝናብ
የካ	9	ጉርድ ሾላ አትሌቲክስ ፌደሬሽን ህንፃ ላይ	የጎርፍ አደጋ	1	ከ/ዝናብ
ኦሮሚያ	ከታ ለኩ	ከታ ለኩ	የጎርፍ መጥለቅለቅ	1	ዝናብ
ቦሌ	3	ደሳለኝ ሆቴል አካባቢ	የጎርፍ መጥለቅለቅ	1	ዝናብ
ጉለሌ	3	ሸገር መናፈሻ አካባቢ	የጎርፍ መጥለቅለቅ	1	ትቦ መደፈን
ኮልፌ	4	ኮልፌ ኪዳነምህረት አካባቢ	የጎርፍ መጥለቅለቅ	1	ዝናብ

ቦሌ	13	ገርጅ ሰላም ሰፈር	የጎርፍ መጥለቅለቅ	1	የትቦ መደፈን
ኮልፌ	15	ካአጂፂ አካባባ	የጎርፍ መጥለቅለቅ	1	ዝናብ
የካ	9	ጉርድ ሾላ ንግድ ባንክ ጀርባ	የጎርፍ መጥለቅለቅ	1	ዝናብ
ኮልፌ	15	ካአጂፂ አካባባ	የጎርፍ መጥለቅለቅ	1	ዝናብ
ቂርቆስ	5	ቡልጋሪያ ናስ ኬክ ቤት	የጎርፍ አደጋ	1	ከባድ ዝናብ
አቃቂ ቃሊቲ	2	አቃቂ ብሔራዊ እድር ቤት አካባቢ	የጎርፍ አደጋ	1	ከባድ ዝናብ ወንዝ መገልበጥ
አዲስ ከተማ	9	ኳስ ሜዳ አካባቢ	የጎርፍ አደጋ	1	የትቦ መዘጋት
ንፋስ ስልክ	1	ሃይሌ ጋርመንት ኮ/ሚንየም	የጎርፍ አደጋ	1	በከባድ ዝናብ የትቦ መዘገት
ንፋስ ስልክ	2	ዮሃንስ መናፈሻ ግቢ ውስጥ	የጎርፍ አደጋ	1	የከባድ ዝናብ
የካ	9	ቶፕ ቴን ሆቴል ውስጥ	የጎርፍ አደጋ	1	የቱቦ መፈንዳት
ቦሌ	5	24 ወሊጋ ሠፈር	የጎርፍ አደጋ	1	ከባድ ዝናብ
አቃቂ	8	ወረዳ 8 ጀርባ	የጎርፍ አደጋ	1	ከባድ ዝናብ
አቃቂ	3	ዶሮ ተራ ቂራ ደርባ	የጎርፍ አደጋ	1	ከባድ ዝናብ
አቃቂ	3	ወረዳ3 ሸማች ብሔራዊ እድር ቤት ጋር	የጎርፍ አደጋ	1	ከባድ ዝናብ
አቃቂ	8	ወረዳ 8 ሠርጢ ማሪያም	የጎርፍ አደጋ	1	ከባድ ዝናብ
ቦሌ	13	ሰላም ሰፈር	የጎርፍ አደጋ	1	ከባድ ዝናብ
አቃቂ	8	አቃቂ መሻለኪያ ድልድይ	የጎርፍ አደጋ	1	አይታወቅም
አቃቂ	3	ሰላም ፍሬ ጤና ጣቢያ አካባቢ	የጎርፍ አደጋ	1	ከባድ ዝናብ
አቃቂ	8	ከላን ኮንደምኒየም	የጎርፍ አደጋ	1	ከባድ ዝናብ
አራዳ	10	ጊዮርጊስ ቤ/ክ ግቢ ውስጥ	የጎርፍ አደጋ	1	በዝናብ ምክንያት
አራዳ	1	ካቴድራል ት/ቤት አጠገብ	የጎርፍ አደጋ	1	ከባድ ዝናብ
ቂርቆስ	5	ቄራ መስኪድ ጀርባ	የጎርፍ አደጋ	1	ከባድ ዝናብ
የካ	2	ፊረንሳይ ለጋሲዮን መጋዘን አካባቢ	የጎርፍ አደጋ	1	ከባድ ዝናብ
ቦሌ	5	ዘርፈሸዋል ት/ቤት አካባቢ	የጎርፍ አደጋ	1	የትቦ መዘጋት
ጉለሌ	9	ፅዮን ሆቴል አካባቢ	የጎርፍ አደጋ	1	ከባድ ዝናብ
አ/ከተማ	9	ኳስ ሜዳ ጮራ አካባቢ	የጎርፍ አደጋ	1	አይታወቅም
ኮልፌ	3	ስልጤ ሰፈር	የጎርፍ አደጋ	1	ከባድ ዝናብ
ቦሌ	13	ቦሌ ኤርፓርት አካባቢ F.B,I ቸርች	የጎርፍ አደጋ	1	ከባድ ዝናብ
ቂርቆስ	5	ቡልጋሪያ ናስ ኬክ ቤት	የጎርፍ አደጋ	1	ከባድ ዝናብ
አቃቂ ቃሊቲ	2	አቃቂ ብሔራዊ እድር ቤት አካባቢ	የጎርፍ አደጋ	1	ከባድ ዝናብ ወንዝ መገልበጥ
አዲስ ከተማ	9	ኳስ ሜዳ አካባቢ	የጎርፍ አደጋ	1	የትቦ መዘጋት
ንፋስ ስልክ	1	ሃይሌ ጋርመንት ኮ/ሚንየም	የጎርፍ አደጋ	1	በከባድ ዝናብ የትቦ መዘገት
ንፋስ ስልክ	2	ዮሃንስ መናፈሻ ግቢ ውስጥ	የጎርፍ አደጋ	1	የከባድ ዝናብ
የካ	9	ቶፕ ቴን ሆቴል ውስጥ	የጎርፍ አደጋ	1	የቱቦ መፈንዳት
ቦሌ	5	24 ወሊጋ ሠፈር	የጎርፍ አደጋ	1	ከባድ ዝናብ
አቃቂ	8	ወረዳ 8 ጀርባ	የጎርፍ አደጋ	1	ከባድ ዝናብ
አቃቂ	3	ዶሮ ተራ ቂራ ደርባ	የጎርፍ አደጋ	1	ከባድ ዝናብ

ኢቃቂ	3	ወረዳ3 ሸማቾ ብሔራዊ እድር ቤት ጋር	የጎርፍ አደጋ	1	ከባድ ዝናብ
ኢቃቂ	8	ወረዳ 8 ሠርጢ ማሪያም	የጎርፍ አደጋ	1	ከባድ ዝናብ
ቦሌ	13	ሰላም ሰፈር	የጎርፍ አደጋ	1	ከባድ ዝናብ
ኢቃቂ	8	ኢቃቂ መሻለኪያ ድልድይ	የጎርፍ አደጋ	1	አይታወቅም
ኢቃቂ	3	ሰላም ፍሬ ጤና ጣቢያ አካባቢ	የጎርፍ አደጋ	1	ከባድ ዝናብ
ኢቃቂ	8	ከላን ኮንደምኒየም	የጎርፍ አደጋ	1	ከባድ ዝናብ
የካ	8	ሾላ ገበያ ቅጠል ተራ	የጎርፍ አደጋ	1	የቱቦ መዘጋት
ቦሌ	17	ቤሌ ሚካኤል ቤ/ክርስቲያን ጆኒ ባር አካባቢ	የጎርፍ አደጋ	1	በዝናብ የመጣ
ኮ/ቀ	4	አለም ባንክ አካባቢ	የጎርፍ አደጋ	1	በዝናብ የነሳ
ኮ/ቀ	4	አለም ባንክ አካባቢ	የጎርፍ አደጋ	1	የቱቦ መዘጋት
ኮ/ቀ	4	አለም ባንክ አካባቢ	የጎርፍ አደጋ	1	ከባድ ዝናብ
አራዳ	10	ጊዮርጊስ ቤ/ክ ግቢ ውስጥ	የጎርፍ አደጋ	1	በዝናብ ምክንያት
አራዳ	1	ካቴድራል ት/ቤት አጠገብ	የጎርፍ አደጋ	1	ከባድ ዝናብ
ቂርቆስ	5	ቄራ መስኪድ ጀርባ	የጎርፍ አደጋ	1	ከባድ ዝናብ
የካ	2	ፊረንሳይ ለጋሲዮን መጋዘን አካባቢ	የጎርፍ አደጋ	1	ከባድ ዝናብ
ቦሌ	5	ዘርፈሸዋል ት/ቤት አካባቢ	የጎርፍ አደጋ	1	የትቦ መዘጋት
ጉለሌ	9	ፅዮን ሆቴል አካባቢ	የጎርፍ አደጋ	1	ከባድ ዝናብ
አ/ከተማ	9	ኳስ ሜዳ ጮራ አካባቢ	የጎርፍ አደጋ	1	አይታወቅም
ኮልፌ	3	ስልጤ ሰፈር	የጎርፍ አደጋ	1	ከባድ ዝናብ
ቦሌ	13	ቦሌ ኤርፓርት አካባቢ F.B,I ቸርች	የጎርፍ አደጋ	1	ከባድ ዝናብ
1	1	ከባድ ዝናብ በመጣል	0	0	0
1	1	ከባድ ዝናብ በመጣል	0	0	0
ኮልፌ	7	ጥቁር አባይ አካባቢ	የጎርፍ አደጋ	1	ከባድ ዝናብ በመጣል
ኮልፌ	13	ጊዬን በረኪና ጀርባ	የጎርፍ አደጋ	1	ከባድ ዝናብ በመጣል
ኮልፌ	4	አየር ጤና ኪዳነ ምህረት አካባቢ	የጎርፍ አደጋ	1	ከባድ ዝናብ በመጣል
አራዳ	2	አቤት ሆስፒታል ጀርባ	የጎርፍ አደጋ	1	ከባድ ዝናብ በመጣል
አራዳ	5	ሶራአምባ ሆቴል አካባቢ	የጎርፍ አደጋ	1	ከባድ ዝናብ በመጣል
ቂርቆስ	5	ቄራ መስኪድ ጀርባ	የጎርፍ አደጋ	1	ከባድ ዝናብ በመጣል
ንፋስ ስልክ	6	ጎፋ ካምፕ አካባቢ	የጎርፍ አደጋ	1	ከባድ ዝናብ በመጣል
ንፋስ ስልክ	6	ጎፋ ካምፕ ኮንደሚንየም አካባቢ	የጎርፍ አደጋ	1	ከባድ ዝናብ በመጣል
ቦሌ	6	አምቼ ጀርባ	የጎርፍ አደጋ	1	የትቦ መዘጋት
ቦሌ	7	ጃክሮስ አደባባይ	የጎርፍ አደጋ	1	ወንዝ የጣሰ ዉሃ
ቦሌ	13	ኤርፓርት ጀርባ	የጎርፍ አደጋ	1	የትቦ መዘጋት
ቦሌ	5	ኒያላ ሞተር አካባቢ	የጎርፍ አደጋ	1	ከባድ ዝናብ
ቦሌ	13	ገርጂ መስኪድ ወጣት ማእከል	የጎርፍ አደጋ	1	ከባድ ዝናብ
የካ	13	መሪ ፖሊስ ጣቢያ ገርባ	የጎርፍ አደጋ	1	ከፍተ ዝናብ
ቦሌ	3	ጃፓን ኢንባሲ	የጎርፍ	1	የመንገድ ትቦ መዘጋት

አ/ከተማ	9	ልካንዳ ወጣት ማዕከል አጠገብ	የጎርፍ	1	ዝናብ
ኮ/ቀ	4	አ/ም ቤ /ክ አካባቢ	የጎርፍ	1	ከባድ ዝናብ
አ/ከተማ	7	አማኑኤል ቤ/ክ ፋት ለፋት	የጎርፍ	1	ከፍተኛ ዝናብ
ቦሌ	13	ቦሎ ኤርፖርት ጀርባ	የጎርፍ አደጋ	1	ዝናብ
ጉለሌ	9	መድሃኒያለም ት/ቤተ የውሃ ጋን አካባቢ	የጎርፍ አደጋ	1	ከባድ ዝናብ
ኮ/ቀ	7	ቤተል ፊርማ ሆቴል አጠገብ	የጎርፍ አደጋ	1	ከባድ ዝናብ
ኮ/ቀ	7	ወረዳ 7 አጠገብ	የጎርፍ አደጋ	1	ከባድ ዝናብ
ቂርቆስ	9	ፍላሚንጎ ማርክ አካባቢ	የጎርፍ አደጋ	1	የትቦ መዘጋት
ኮ/ቀ	15	ሳንሱሲ 19 ቁጥረ ማዞሪያ	የጎርፍ አደጋ	1	ከባድ ዝናብ
ቂርቆስ	5	አጎና ሲኒማ ጀርባ	የጎርፍ አደጋ	1	ከባድ ዝናብ
ን/ስልክ	6	ጎፋ ካምፕ አካባቢ	የጎርፍ አደጋ	1	ከባድ ዝናብ በመጣል
ን/ስልክ	6	ጎፋ ካምፕ ኮንደሚንየም አካባቢ	የጎርፍ አደጋ	1	ከባድ ዝናብ በመጣል

Source: Addis Ababa Fire and Emergency Prevention and Rescue Agency